

POLITECNICO DI TORINO

Corso di Laurea Magistrale
in Automotive Engineering

Tesi di Laurea Magistrale

Consideration of car secondary energy demand
sensitivity for different drivetrain concepts through
thermodynamic modelling



Relatore
prof. Andrea Tonoli

Candidato
Stefano Givone

Anno Accademico 2017/2018

Abstract

Cars are responsible for around 12% of total EU emissions of carbon dioxide (CO₂), the main greenhouse gas. For this reason the growing concern about environmental pollution, climate change and global warming is shifting the attention of the transportation sector towards the development of technologies less dependent on fossil fuels. In particular, for passenger cars, BEVs (Battery Electric Vehicles) and HEVs (Hybrid Electric Vehicles) are expected to gain a greater importance on the market in the upcoming years, especially in the European Union where new regulations will be phased in from 2020. Thus, the increasing interest towards electrification raised a number of rather new problems, which were usually negligible in vehicles powered by an internal combustion engine. These issues consist mainly in the increase in energy consumption, and the consequent decrease in the available electric range, due to the use of constant and variable secondary users, which include all those systems not used to move the car but necessary for increasing the comfort of driver and passengers and increasing safety. The most energy consuming between all the secondary users is the so-called HVAC system (Heating Ventilation and Air Conditioning system), which is strictly related to the external environment conditions, and can, therefore, have a big impact on the decrease in the available range for BEVs, according to the considered geographical region. For what concerns HEVs, the main problem is the decrease in the electric energy available for traction, thus reducing the advantage given by the hybridization.

The work carried out for this thesis was to investigate the effects of different ambient temperatures on the consumption of BEVs and PHEVs (Plug-In Hybrid Electric Vehicles), of which the P2-configuration was considered, in comparison with ICEVs (Internal Combustion Engine Vehicles), through a simulative data-driven approach, with the aim of having quantitative and qualitative results for the problems just mentioned. In particular, a secondary users consumption model was developed and integrated in an already present primary consumption model in order to estimate vehicle's energy demand based on real world driving profiles and weather data.

The results show that especially in the case of the BEV and PHEV, the trip distance and the ambient temperature are a first-order influencing factor on the total vehicle energy demand, with a consumption increase up to 22.7 % for full electric vehicles during the worst operating condition considered, against a maximum deviation of 5.5 % for conventional vehicles. Therefore, it is not sufficient to evaluate new vehicle concepts solely on one-dimensional driving cycles to assess their energy demand. Instead, the external conditions must be taken into account for a proper assessment of the vehicle's real world consumption.

Keywords: vehicle secondary users, thermodynamic modelling, sensitivity study, drivetrain concepts, real-life consumptions

Table of Contents

| | |
|--|-----------|
| ABSTRACT | 1 |
| TABLE OF CONTENTS | 2 |
| LIST OF FIGURES | 4 |
| LIST OF TABLES | 6 |
| LIST OF ABBREVIATIONS | 7 |
| LIST OF SYMBOLS | 8 |
| 1 INTRODUCTION | 10 |
| 1.1 LITERATURE REVIEW | 11 |
| 1.2 SELECTION OF ESSENTIAL COMFORT USERS..... | 13 |
| 1.3 WORK PHASES..... | 14 |
| 2 BASICS | 16 |
| 3 STATE OF THE ART – HEATING AND COOLING ELEMENTS | 18 |
| 3.1 HEATING SYSTEMS | 19 |
| 3.1.1 <i>Waste heat from Internal Combustion Engine</i> | 19 |
| 3.1.2 <i>PTC – Positive Temperature Coefficient</i> | 22 |
| 3.2 COOLING SYSTEMS..... | 25 |
| 3.2.1 <i>Air-Conditioning system</i> | 25 |
| 3.3 ADDITIONAL POSSIBILITIES | 26 |
| 3.3.1 <i>Heat Pump</i> | 27 |
| 3.3.2 <i>Preconditioning</i> | 28 |
| 3.3.3 <i>Direct heating</i> | 29 |
| 3.3.4 <i>New technologies</i> | 29 |
| 4 CONSTRUCTION OF THE SIMULATION MODEL | 31 |
| 4.1 PARAMETERS | 31 |
| 4.2 CABIN THERMODYNAMIC MODEL | 33 |
| 4.2.1 <i>Inputs and Outputs of the function</i> | 36 |
| 4.2.2 <i>Operation</i> | 37 |
| 4.3 PI CONTROLLER | 37 |
| 4.4 OVERALL SIMULATION | 39 |
| 4.4.1 <i>Driving cycles</i> | 40 |
| 4.4.2 <i>Time optimization study</i> | 43 |
| 4.4.3 <i>Results</i> | 45 |
| 4.4.3.1 <i>WLTP</i> | 46 |



| | | |
|----------|--|-----------|
| 4.4.3.2 | NEDC..... | 59 |
| 4.4.3.3 | ECE-15..... | 60 |
| 4.4.3.4 | FTP-75..... | 61 |
| 5 | INTEGRATION IN THE OPTIMIZATION ENVIRONMENT..... | 62 |
| 5.1 | DESCRIPTION OF THE OPTIMIZATION ENVIRONMENT..... | 62 |
| 5.2 | DRIVING CYCLES FOR THE EVALUATION OF VEHICLE’S CONSUMPTION | 65 |
| 5.3 | RESULTS | 68 |
| 5.3.1 | <i>Internal Combustion Engine Vehicle</i> | <i>69</i> |
| 5.3.2 | <i>Battery Electric Vehicle</i> | <i>69</i> |
| 5.3.3 | <i>Plug-In Hybrid Electric Vehicle</i> | <i>70</i> |
| 6 | CONCLUSIONS AND FUTURE DEVELOPMENTS..... | 73 |
| 7 | ACKNOWLEDGEMENTS | 74 |
| | APPENDIX – MATLAB CODE..... | 75 |
| | REFERENCES..... | 88 |

List of Figures

| | |
|--|----|
| Figure 1. Energy consumption per kilometer vs. Ambient temperature [2]. | 11 |
| Figure 2. Nissan Leaf energy consumption per mile versus ambient temperature [4]. | 12 |
| Figure 3. Energy consumption per mile averaged across the fleet over a full year [4]. | 12 |
| Figure 4. Weighted range 45% UDDS / 55% HWFET2X [6]. | 13 |
| Figure 5. Example of engine map. In blue the operating points of the NEDC cycle. | 20 |
| Figure 6. Energy subdivision in an ICE. | 20 |
| Figure 7. Schematic of an ICE cooling system. In the upper part it is possible to see the cabin heater. | 21 |
| Figure 8. PTC heating element [Source: BorgWarner]. | 22 |
| Figure 9. Draw of a PTC and detail of the heating element. | 22 |
| Figure 10. Electrical resistance characteristics of the different stages of a 4-stage PTC element [8]. | 23 |
| Figure 11. Voltage-current characteristics of the different stages of a 4-stage PTC element [8]. | 24 |
| Figure 12. Example of air heating system with a PTC heater [8]. | 24 |
| Figure 13. A simple stylized diagram of the refrigeration cycle [Source: Wikipedia]. | 25 |
| Figure 14. Schematic of an A/C system used in vehicles. | 26 |
| Figure 15. Architecture of a heat pump in an ICEV [Source: ClearMechanic.com]. | 27 |
| Figure 16. A simple stylized diagram of a heat pump's vapor-compression refrigeration cycle [Source: Wikipedia]. | 28 |
| Figure 17. Range gain and energy requirement of a PTC heater at a target air temperature of 22 °C [11]. | 29 |
| Figure 18. Average relative humidity over one year in Frankfurt, Germany [17]. | 31 |
| Figure 19. Cabin thermodynamic model. | 36 |
| Figure 20. Example of application of the PID controller. | 38 |
| Figure 21. Velocity vs Time, WLTP cycle. | 41 |
| Figure 22. Velocity vs Time, NEDC cycle. | 41 |
| Figure 23: Velocity vs Time, ECE-15 cycle. | 42 |
| Figure 24. Velocity vs Time, FTP-75 cycle. | 42 |
| Figure 25. Profile summary – first attempt. | 44 |
| Figure 26. Profile summary – final results. | 45 |
| Figure 27. Cabin air temperature trends in case of a BEV in the WLTP cycle. | 46 |
| Figure 28. Dashboard temperature trends in case of a BEV in the WLTP cycle. | 47 |
| Figure 29. Doors temperature trends in case of a BEV in the WLTP cycle. | 48 |
| Figure 30. Interiors temperature trends in case of a BEV in the WLTP cycle. | 49 |
| Figure 31. Roof temperature trends in case of a BEV in the WLTP cycle. | 50 |
| Figure 32. Heat fluxes along time in case of a BEV in the WLTP cycle. | 51 |
| Figure 33. Secondary users electrical power demand for cooling, versus time in case of a BEV in the WLTP cycle. | 52 |
| Figure 34. Secondary users electrical power demand for heating, versus time in case of a BEV in the WLTP cycle. | 53 |
| Figure 35. Water mass fraction trends in case of a BEV in the WLTP cycle. | 54 |

| | |
|---|-----------|
| <i>Figure 36. Water mass trends in case of a BEV in the WLTP cycle.</i> | 55 |
| <i>Figure 37. Energy consumption for only secondary users in case of a BEV in the WLTP cycle.</i> | 56 |
| <i>Figure 38. Energy consumption for only secondary users in case of an ICEV in the WLTP cycle.</i> | 57 |
| <i>Figure 39. Secondary users electrical power demand versus time in case of an ICEV in the WLTP cycle. ...</i> | 58 |
| <i>Figure 40. Energy consumption for only secondary users in case of BEV and ICEV in the NEDC cycle.</i> | 59 |
| <i>Figure 41. Energy consumption for only secondary users in case of BEV and ICEV in the ECE-15 cycle. ..</i> | 60 |
| <i>Figure 42. Energy consumption for only secondary users in case of BEV and ICEV in the FTP-75 cycle. ...</i> | 61 |
| <i>Figure 43. Exemplary outputs of the primary consumption model for the PHEV on a representative driving cycle with a trip distance of 100 km.</i> | 64 |
| <i>Figure 44. Distribution of the daily mean ambient temperatures measured in Darmstadt by “Deutscher Wetterdienst” during the period from January 2013 until January 2017.</i> | 65 |
| <i>Figure 45. Database of driving data used for this study.</i> | 66 |
| <i>Figure 46. On the right, the best cycles and corresponding errors for each trip distance are displayed. On the left, the error distributions of synthesized cycles are shown.</i> | 68 |
| <i>Figure 47. Fuel consumption in dependency of ambient temperature and trip distance for an ICEV.</i> | 69 |
| <i>Figure 48. Electricity consumption in dependency of ambient temperature and trip distance for a BEV.</i> | 70 |
| <i>Figure 49. Electricity consumption as a function of ambient temperature and trip distance for the PHEV. .</i> | 72 |
| <i>Figure 50. Fuel consumption as a function of ambient temperature and trip distance for the PHEV.</i> | 72 |

List of Tables

| | |
|---|-----------|
| <i>Table 1. Power consumption of constant loads.</i> | 14 |
| <i>Table 2. HVAC technology depending on vehicle concepts where checks in brackets (✓) are not considered within this work.</i> | 19 |
| <i>Table 3. Maximum thermal power considered for heating and cooling elements</i> | 32 |
| <i>Table 4. Main features of the type-approval cycles considered.</i> | 43 |
| <i>Table 5. Main parameters of the defined vehicle drivetrain concepts.</i> | 63 |
| <i>Table 6. Exemplary calculation of the overall error of the best synthesized cycle at a trip distance of 80 km for all single criteria θ_i and the criteria set θ.</i> | 67 |

List of Abbreviations

| | |
|-------|--|
| A/C | Air Conditioning |
| BEV | Battery Electric Vehicle |
| BSFC | Brake Specific Fuel Consumption |
| COP | Coefficient Of Performance |
| ECE | Economic Commission for Europe |
| ECMS | Equivalent Consumption Minimization Strategy |
| EM | Electric Machine |
| EPA | Environmental Protection Agency |
| EUDC | Extra Urban Driving Cycle |
| FTP | Federal Test Procedure |
| HEV | Hybrid Electric Vehicle |
| HP | Heat Pump |
| HVAC | Heating Ventilation Air Conditioning |
| HWFET | Highway Fuel Economy Test |
| ICE | Internal Combustion Engine |
| ICEV | Internal Combustion Engine Vehicle |
| MIMO | Multi Input Multi Output |
| NEDC | New European Driving Cycle |
| OEM | Original Equipment Manufacturer |
| PHEV | Plug-in Hybrid Electric Vehicle |
| PI | Proportional-Integral |
| PID | Proportional-Integral-Derivative |
| PTC | Positive Temperature Coefficient |
| SOC | State Of Charge |
| UDC | Urban Driving Cycle |
| UDDS | Urban Dynamometer Driving Schedule |
| USA | United States of America |
| WLTC | Worldwide harmonized Light vehicles Test Cycle |
| WLTP | Worldwide harmonized Light vehicles Test Procedure |

List of Symbols

| | |
|------------------|------------------------------------|
| U | Overall heat transfer coefficient |
| A | Area |
| T | Temperature |
| Q | Heat |
| H | Enthalpy |
| E | Total energy |
| P | Mechanical power |
| m | Mass |
| c_p | Specific heat at constant pressure |
| \dot{Q} | Thermal power (Heat flux) |
| I | Solar radiation |
| γ | Absorbance |
| τ | Transmittance |
| ε | Emissivity coefficient |
| σ | Stefan-Boltzmann constant |
| α | Convective coefficient |
| φ | Human metabolic rate |
| n | Number of passengers |
| \dot{m} | Mass flow rate |
| $\Delta h_{v,0}$ | Enthalpy of vaporization of water |
| β | Dehumidification factor |
| h | Convection coefficient |
| λ | Conduction coefficient |
| t | Thickness |
| v | Velocity |
| L | Characteristic length |
| μ | Dynamic viscosity |
| ρ | Density |
| w | Velocity |

| | |
|-----------|----------------------|
| g | Gravity acceleration |
| z | Height |
| Nu | Nusselt number |
| Pr | Prandtl number |
| Re | Reynolds number |
| U_{int} | Internal energy |

1 Introduction

Cars are responsible for around 12% of total EU emissions of carbon dioxide (CO₂), the main greenhouse gas [1]. For this reason the growing concern about environmental pollution, climate change and global warming is shifting the attention of the transportation sector towards the development of technologies not dependent, or less dependent, on fossil fuels. In particular, for passenger cars, BEVs (Battery Electric Vehicles) and HEVs (Hybrid Electric Vehicles) are expected to gain a greater importance on the market in the upcoming years, especially in the European Union where new regulations will be phased in from 2020, decreasing the emission limit of the main greenhouse gas, carbon dioxide, from 130 gCO₂/km to 95 gCO₂/km for the fleet average of car manufacturers [1]. Thus, the increasing interest towards a sustainable mobility, mainly referred to BEVs and HEVs, raised a number of rather new problems, which were usually negligible in vehicles powered by an internal combustion engine. These issues consist mainly in the increase in energy consumption, and the consequent decrease in the available electric range, due to the use of constant and variable secondary users, which include all those systems not used to move the car but necessary for increasing the comfort of driver and passengers and increasing safety. This problem can generate also an increase in range anxiety for BEV drivers or potential customers, further decreasing the spread of electric mobility solutions. The most energy consuming between all the secondary users is the so-called HVAC system (Heating Ventilation and Air Conditioning system), which is strictly related to the external environment conditions, and can, therefore, have a big impact on the decrease in the available range for BEVs, according to the considered geographical region. For what concerns HEVs, the main problem is the decrease in the electric energy available for traction, thus reducing the advantage given by the hybridization. For this reason, these aspects must be considered, by OEMs, both for the design phase and for the market selection process in which to introduce new powertrain concepts.

The work carried out for this thesis was to investigate the effects of different ambient temperatures on the consumption of BEVs and PHEVs (Plug-In Hybrid Electric Vehicles), of which the P2-configuration was considered, in comparison with ICEVs (Internal Combustion Engine Vehicles) through a simulative data-driven approach, with the aim of having quantitative and qualitative results for the problems just mentioned. Going more in details, the idea of this study was to create a MATLAB model to compute the increase in total energy consumption in BEVs, ICEVs and PHEVs due to secondary users, mainly heating and cooling systems, taking into account a range of temperatures from -10 °C to +40 °C. In order to fulfill this task, the work was subdivided into three different steps:

- Creation of a cabin thermodynamic model
- Creation of a controller for the HVAC system
- Integration of the model in an already present optimization environment.

The desired value for the air temperature inside the car was decided to be equal to 21 °C, which can be considered, with good approximation, an acceptable temperature for human comfort.

Finally, this work has been carried out in collaboration with the Institute for Mechatronic Systems in Mechanical Engineering at TU Darmstadt, under the supervision of the Ph.D. candidates Philippe Jardin and Arved Eßer.

1.1 Literature review

In recent years, different approaches were carried out in order to address the problem of energy consumption increase related to external environment conditions. Kai Liu et al. (2017) [2] explored the interactive effects of ambient temperature and vehicle auxiliary loads on electric vehicle energy consumption through the monitoring of 68 EVs in Aichi Prefecture, Japan, developing an energy consumption model versus ambient temperature with a minimum in the range of 21.8-25.2 °C, as can be seen in Figure 1. A quite relevant dependency could be found between energy demands and external conditions.

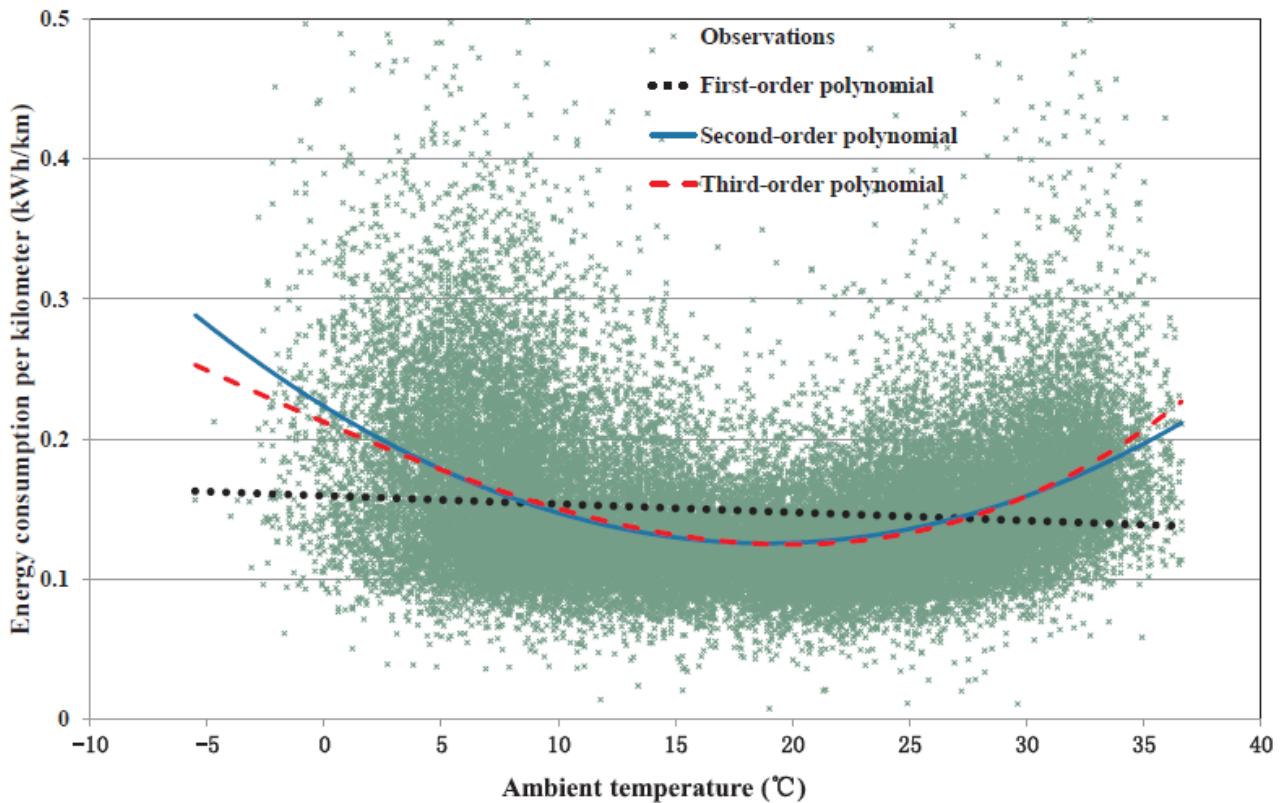


Figure 1. Energy consumption per kilometer vs. Ambient temperature [2].

Chiara Fiori et al. (2016) [3] developed a simple EV energy model computing the instantaneous energy consumption using second-by-second vehicle speed, acceleration and road grade, and also compared different electric vehicles and quantified the impact of auxiliary systems, including air conditioning and heating systems, finding a significant reduction of the travel range, up to 24 % when increasing the auxiliary systems loads. Tugce Yuksel et al. (2015) [4] studied the effect of regional temperature differences on BEV efficiency, range and use-phase power plant CO₂ emissions in the U.S., considering battery efficiency and cabin climate control. In particular, they noticed that the cold temperature effect is generally larger for two main reasons: electric cabin heating consumes more power compared to cooling and batteries have poorer

performance at low temperatures. Furthermore, they found a decrease in range up to 36 % in cold climates. In Figure 2 and Figure 3 it is possible to see the main outcomes of this study.

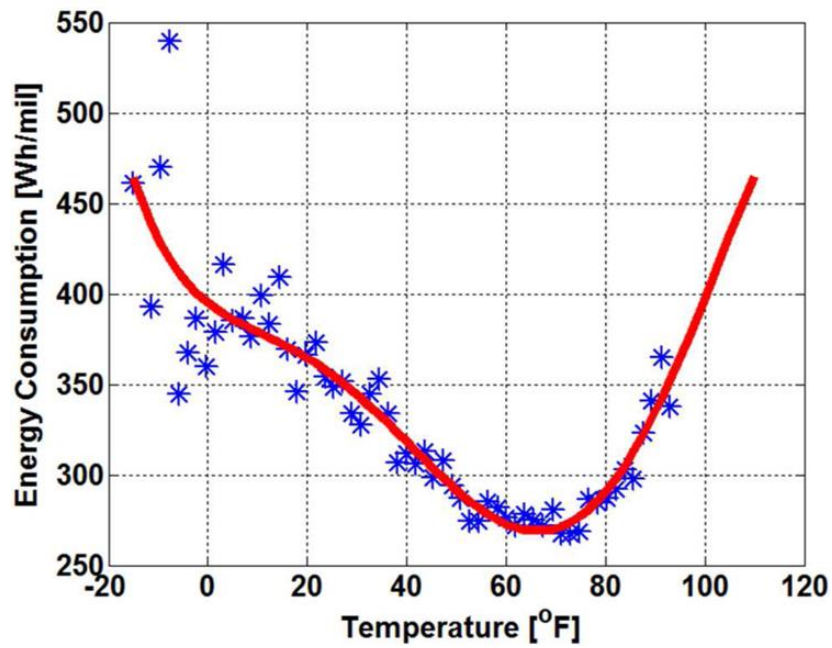


Figure 2. Nissan Leaf energy consumption per mile versus ambient temperature. The blue stars represent the experimental data, while the red curve is the polynomial fit [4].

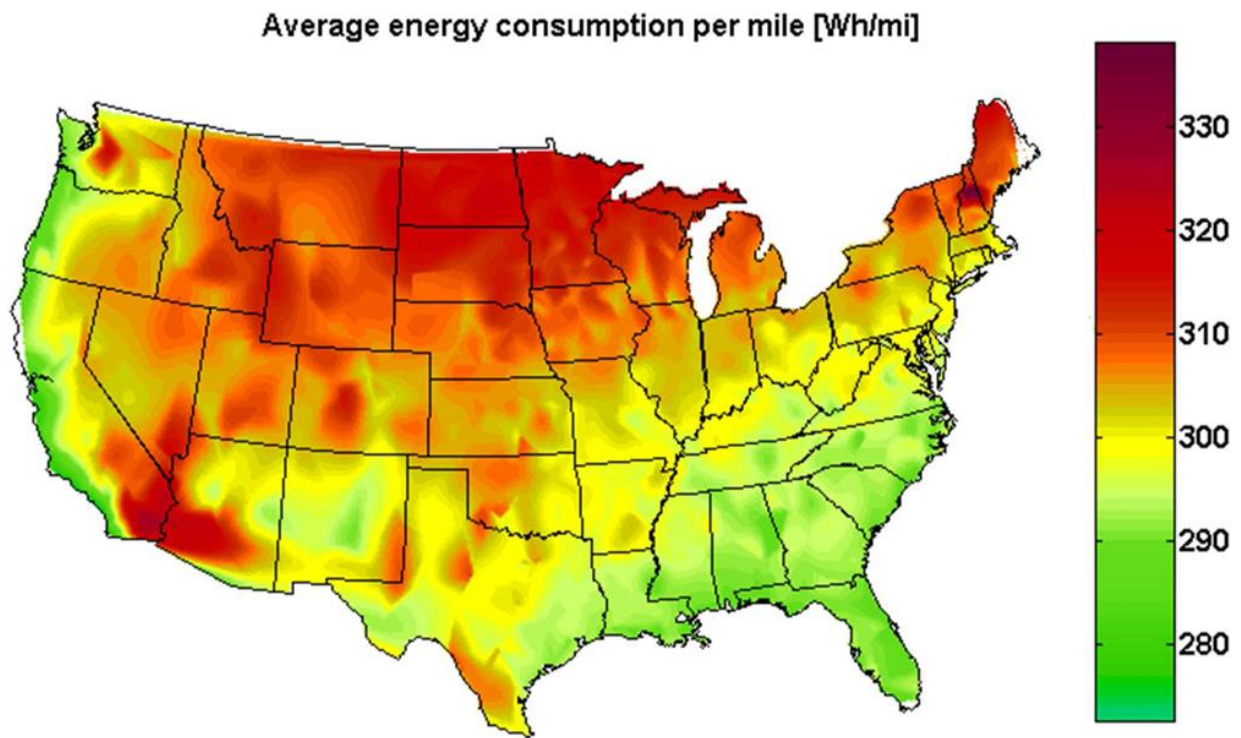


Figure 3. Energy consumption per mile averaged across the fleet over a full year [4].

For what concerns the modeling of vehicle cabin and cabin climate control, Daniel Huang et al. (2007) [5] designed a CAE tool to compute the heat load of a vehicle passenger compartment using a lumped system approach considering solar radiation, conductive/convective heat transfers and passengers' heat and moisture loads. Gene Titov et al. (2017) [6] explored different control strategies and range impacts for EV integrated thermal management systems, considering a range of ambient temperatures between -20 °C and +20 °C, in order to obtain a range improvement over a basic strategy. In Figure 4 the resulting range from 3 different heating configurations is plotted against temperature.

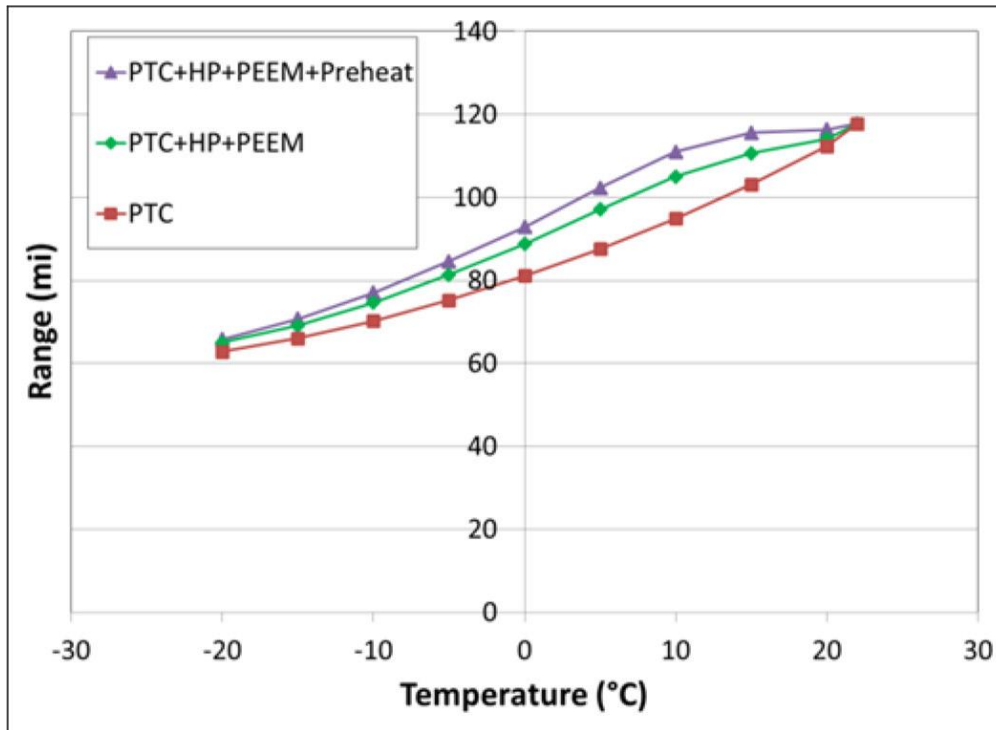


Figure 4. Weighted range 45% UDDS / 55% HWFET2X [6].

Finally, this study is largely based on a previous bachelor thesis work carried out at the TU Darmstadt by Katharina Lange, completed in April 2018 [7], in which a similar topic has been analyzed, computing, in a more simplified way, the energy consumption variation for only electric vehicles due to various ambient temperatures. In particular, with respect to Lange's thesis, the present work covers a wider set of drivetrain concepts, over a higher number of cycles, considering a more detailed cabin thermodynamic model.

1.2 Selection of essential comfort users

Nowadays, in every passenger car it is possible to have a high number of additional systems with the aim of enhancing the comfort of the people inside. Furthermore, some of these secondary users have also the objective of increasing driving safety by, for example, defogging and defrosting the windshield. The most important comfort users, from an energy consumption point of view, analyzed in this work, are divided in two main groups: time-varying users and users constant over time.

The variable loads, as already said in the introduction, are:

- HVAC – Heating Ventilation Air Conditioning system, of which two main technologies are taken into account:
 - PTC – Positive Temperature Coefficient
 - A/C – Air Conditioning system

The constant loads, instead, are:

- Battery thermal management system – considered for BEV and PHEV only
- Headlamps and other lights
- Infotainment system
- Electric power steering
- Interior blower.

The choice of the above constant loads was done considering only the most energy demanding ones present in a vehicle, in order to have an approximated idea of their influence. The reference values of power consumption of these constant loads are reported in Table 1.

Table 1. Power consumption of constant loads.

| | Power [W] |
|-----------------------------------|-----------|
| Battery thermal management system | 500 |
| Lights | 150 |
| Infotainment system | 20 |
| Electric power steering | 500 |
| Interior blower | 200 |

Obviously, the value chosen for battery thermal management system is just an average value in order to get an idea of its influence. A much deeper study is needed to analyze such a complex system, taking into account also the variation in efficiency due to different temperatures.

It should be noted that for the heating phase of vehicles powered by an internal combustion engine, the waste heat produced and recovered was considered, so without additional energy consumptions.

The loads and technologies presented here will be further explained in the following chapters of this thesis.

1.3 Work phases

As already mentioned in the introduction, the work was completely performed using the software MATLAB, release R2017b. In order to create an optimized workspace, both in terms of computational time and ease of use, the final task was subdivided in various *blocks*, namely different scripts were created, each dedicated to

a fundamental part of the study. In the end, all these blocks were merged together, exploiting the possibility of recalling functions and loading different scripts during the same simulation.

In details, the various sections created are:

- Parameters
- Cabin thermodynamic model
- PI controller.

The first block, as the name says, is a script containing just a list of constant and variable parameters necessary to the computation. It was necessary to load this script at the beginning of every simulation in order to have the possibility of using them.

The second block is the core of the project. It is a function with multiple inputs and multiple outputs (MIMO) able to compute the current values of every temperature and of the humidity level inside the vehicle cabin at each simulation step. Calculations are done taking into account all the main heat transfers occurring inside the cabin and between cabin and outside environment.

The last block is basically the one at the highest level. Inside the PI controller script, both the parameters script and the cabin thermodynamic model function are called and, for each different HVAC technology, the required thermal power is computed in order to reach the desired comfort temperature of 21 °C.

2 Basics

In order to estimate the energy consumed by heating and cooling systems, it was obviously necessary to create a thermodynamic model of the passenger compartment of a car, able to describe all the thermal interactions and heat transfers occurring inside the cabin itself and between cabin and external environment.

While the detailed creation of this model will be deeply analyzed in Chapter 4, in this section, the basic thermodynamic processes taken into account are presented. In order to be as complete as possible, all kinds of heat transfers were included in this work: conduction, convection and irradiation. Going more in detail, the basic equations describing the thermal interactions are listed here:

- Conduction

$$Q = \frac{\lambda A \Delta T}{L} \quad (1)$$

- Convection

$$Q = h A \Delta T \quad (2)$$

- Combined convection and conduction

$$Q = U A \Delta T \quad (3)$$

- Irradiation

$$Q = \varepsilon \sigma A (T_2^4 - T_1^4) \quad (4)$$

- Heat absorbed

$$Q = m c_p \Delta T \quad (5)$$

- Enthalpy

$$H = m c_p T \quad (6)$$

- First law of Thermodynamics

$$\frac{dE}{dt} = \dot{Q} + P + \sum_i \dot{m}_i (h_i + \frac{w_i^2}{2} + g z_i) \quad (7)$$

- Law of conservation of mass in a closed system

$$\frac{dm}{dt} = \sum \frac{dm_{in}}{dt} + \sum \frac{dm_{out}}{dt} = 0 \quad (8)$$

Where:

- λ : conduction coefficient
- A : area considered

-
- T : temperature
 - h : convection coefficient
 - L : characteristic length
 - U : global heat transfer
 - ε : emissivity coefficient
 - σ : Stefan-Boltzmann constant
 - m : mass
 - c_p : specific heat at constant pressure
 - Q : heat
 - H : enthalpy
 - E : total energy
 - \dot{Q} : heat flux
 - P : mechanical power
 - \dot{m} : mass flow rate
 - w : velocity
 - g : gravity acceleration
 - z : height.

3 State of the art – Heating and cooling elements

In this section, the systems used for thermal management of the passenger compartment, considered in this analysis, are presented. Additionally, a brief description of other possibilities, not included in this study, is given. The elements investigated here are the most used heating and cooling technologies present on the car market nowadays. However, in order to make a description of the HVAC systems used in modern cars, it is necessary to take into account the differences between various powertrain concepts.

In case of a BEV, since the only energy source are the batteries of the vehicle, the state of the art for HVAC is represented by a PTC element for heating and by a conventional air conditioning system for cooling. A PTC element is, basically, a simple resistor which transforms electric energy directly into heat. In an attempt to offer a better performance, some BEVs are also combined with additional heat pumps. However, heat pumps alone are not capable of heating in harsh conditions at very low temperatures and are therefore an optional equipment. For simplicity, this last layout is not analyzed here.

A different solution is possible to be adopted in the ICEV: due to the abundance of waste heat, there is no need to generate thermal energy through electricity. With the help of a cabin heat exchanger the engine waste heat is enough to provide sufficient heating power for reaching the desired conditions in the cabin. For what concerns the cooling phase, the A/C is used normally. In some cases, premium class vehicles additionally use PTC elements for providing a dynamic heating behavior to further increase passenger comfort and performance, even though this solution increases the electric load of the car, taking electricity from the alternator. However, these additional elements are only present in a minority of vehicles and do only cover a negligible part of the energy demand needed for HVAC. Therefore, these combined systems are not considered within this thesis.

Finally, differently from the previous cases, a PHEV usually needs to be equipped with multiple systems. In fact, in case of a running combustion engine the waste heat can be used through a heat exchanger for heating the passenger cabin, like in a conventional ICEV. In case of purely electric driving an additional PTC element is used to heat the cabin, like in a BEV. For what concerns cooling, instead, again only the air conditioning is used. Thus, the HVAC system in this case is closely related to the operating strategy of the hybrid vehicle considered.

In Table 2 it is possible to find the distribution of HVAC technologies for different vehicle concepts.

Table 2. HVAC technology depending on vehicle concepts where checks in brackets (✓) are not considered within this work.

| | ICEV | BEV | PHEV |
|-----------------------------------|------|-----|------|
| Waste heat <i>heating</i> | ✓ | ✗ | ✓ |
| PTC element <i>heating</i> | (✓) | ✓ | ✓ |
| Heat pump <i>heating</i> | ✗ | (✓) | ✗ |
| Heat pump <i>cooling</i> (A/C) | ✓ | ✓ | ✓ |

3.1 Heating systems

In this section, the above-mentioned heating systems are presented more in detail. Heating is useful not only for increasing the temperature of the passenger compartment in order to reach a good level of comfort for the passengers, but it has also the function of defrosting the windshield in case the car has been many hours at very low temperatures.

3.1.1 Waste heat from Internal Combustion Engine

Vehicles powered by internal combustion engines take advantage of the low efficiency of the engine by exploiting the waste heat generated, through the use of a dedicated cooling system. ICEs, in fact, typically have peak efficiency values in the range of 20-40%, with even lower values in all the remaining parts of the engine operating region.

In Figure 5 an example of engine map is plotted. It is possible to see the Wide Open Throttle (full load) curve of the ICE, the iso-BSFC (Brake Specific Fuel Consumption) lines and the operating points of the NEDC cycle.

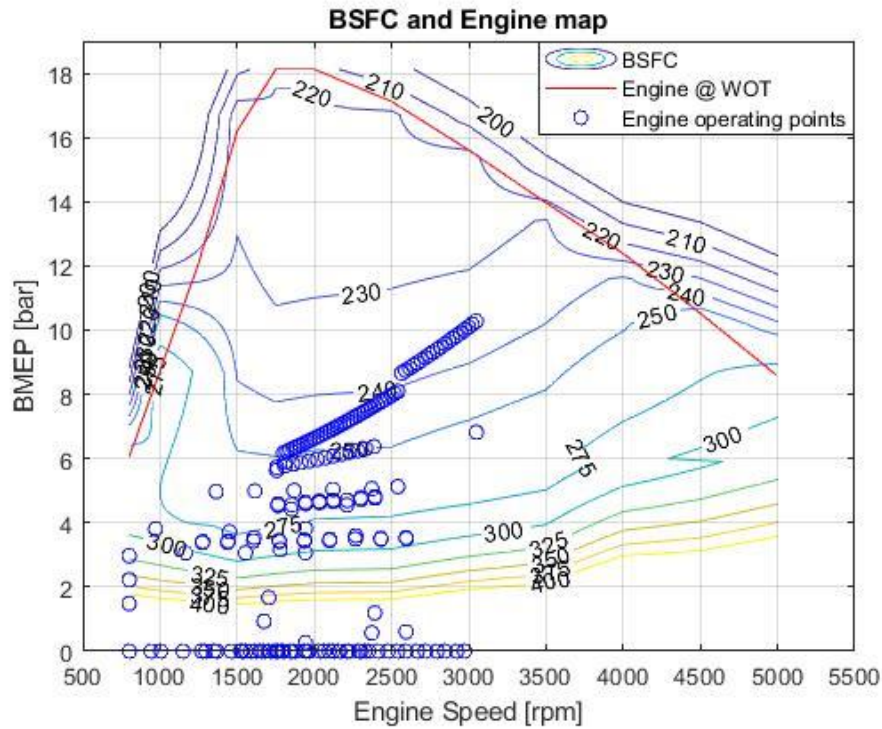


Figure 5. Example of engine map. In blue the operating points of the NEDC cycle.

This means that more than half of the energy generated is wasted. As a matter of fact, it is transformed into heat.

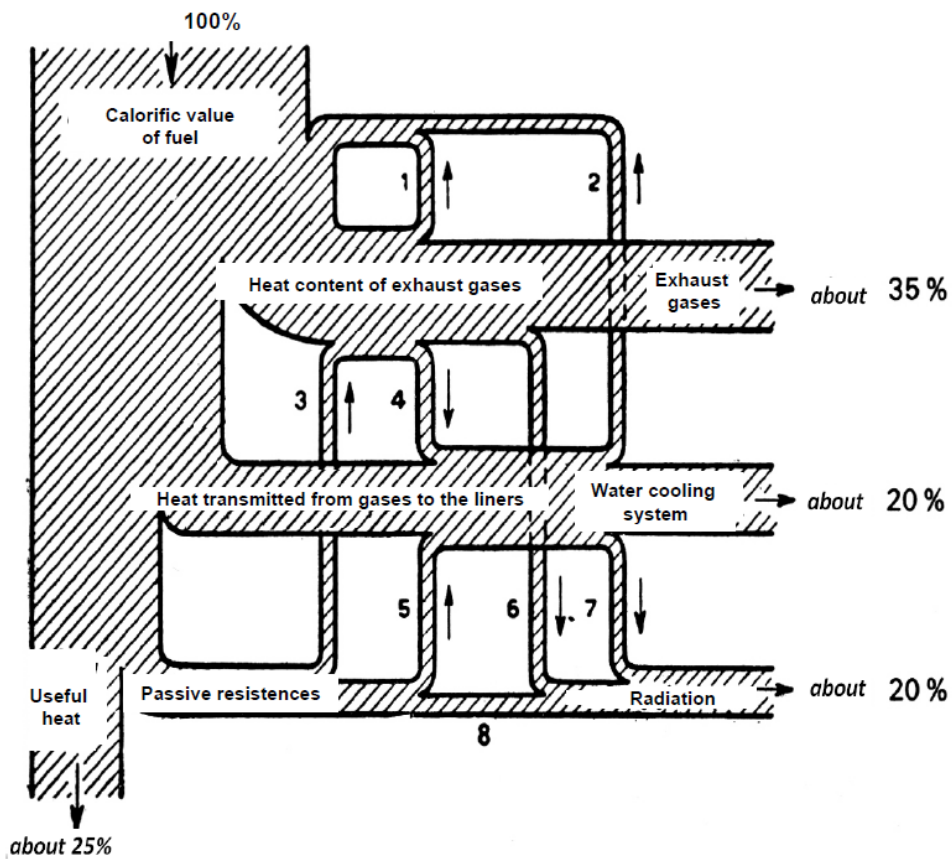


Figure 6. Energy subdivision in an ICE.

This thermal energy is split into various components, as shown in Figure 6: a part of it is exhausted together with hot gases, while another part is transferred to the engine structure through the conduction phenomenon. Finally, the thermal energy in the engine structure is partly irradiated toward the external environment, partly removed by the cooling system. This system uses a mixture of water and glycol to remove the heat in excess from the engine, in order to maintain the right temperature to avoid problems in the materials and to have a high level of efficiency (within the limits typical of an internal combustion engine). This heat is then disposed both in the external environment, through a heat exchanger usually placed in the front part of the car, and in the car cabin, when needed, through a radiator used to increase the enthalpy of the air entering the cabin. This solution permits to have a good thermal comfort for the passengers inside the car, by exploiting the waste energy of the engine with just a minimal cost due to the energy requirement of the cooling system components, such as pumps, fans, etc. It should be noted that both the engine structure and the coolant fluid themselves have certain heat capacities and for this reason they need a certain time to reach an acceptable working temperature. In order to simplify the analysis, this delay time is not considered here, while an already hot engine at steady state condition is taken into account.

From Figure 6, it is also possible to notice that, even though some heat can be recovered somehow, the internal combustion engine still remain a very inefficient machine when compared to an electric one. In addition, in Figure 7, a schematic of a cooling system circuit for an ICE is drawn. From this it can be understood the complexity of such components.

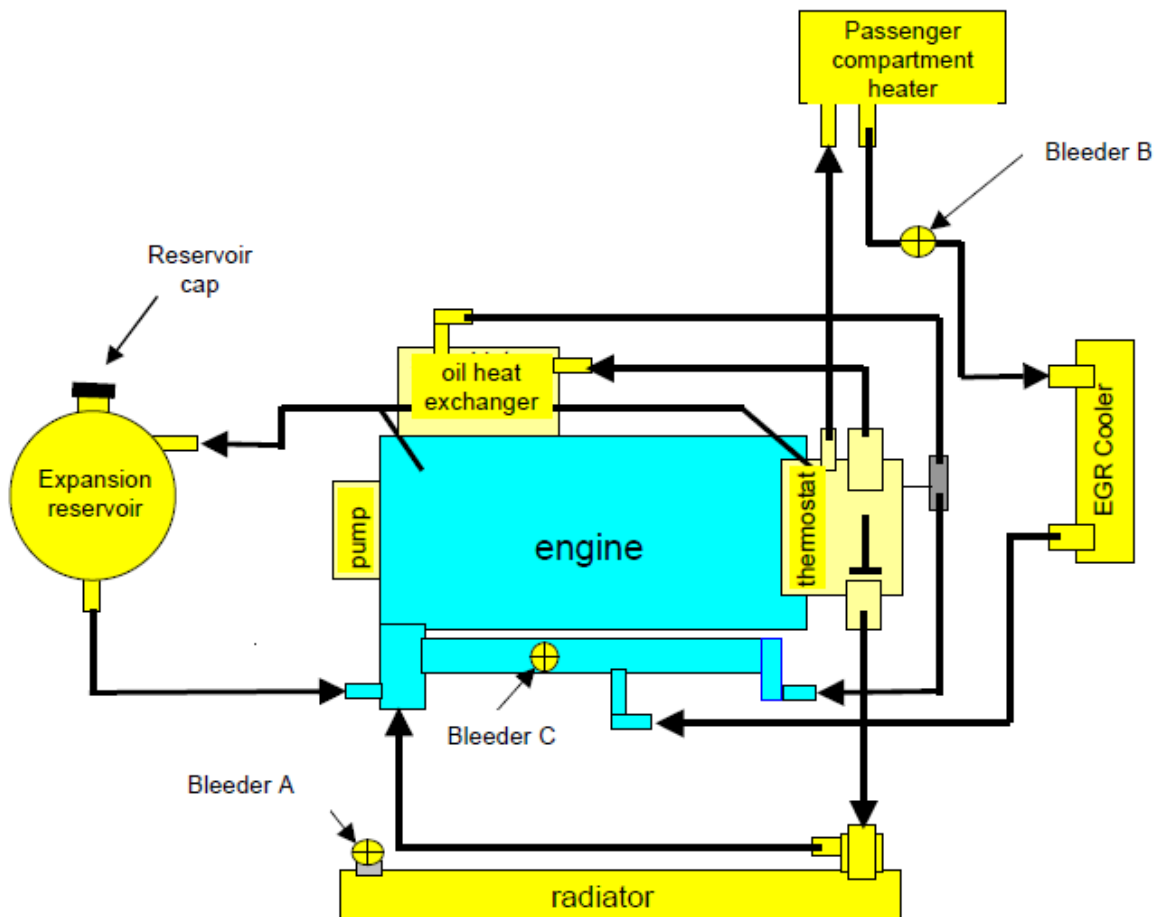


Figure 7. Schematic of an ICE cooling system. In the upper part it is possible to see the cabin heater.

3.1.2 PTC – Positive Temperature Coefficient

Since electric motors have a very high efficiency, often higher than 80 %, it is not possible to exploit the heat generated due its very low value. For this reason BEVs are equipped with other heating elements taking electric energy directly from the battery. The component considered in this work is called PTC, an acronym which stands for Positive Temperature Coefficient. In practical cases, PTC elements are integrated in heat exchangers and contribute to the heating of the air passing through them, as can be seen in Figure 8 and Figure 9.



Figure 8. PTC heating element [Source: BorgWarner].

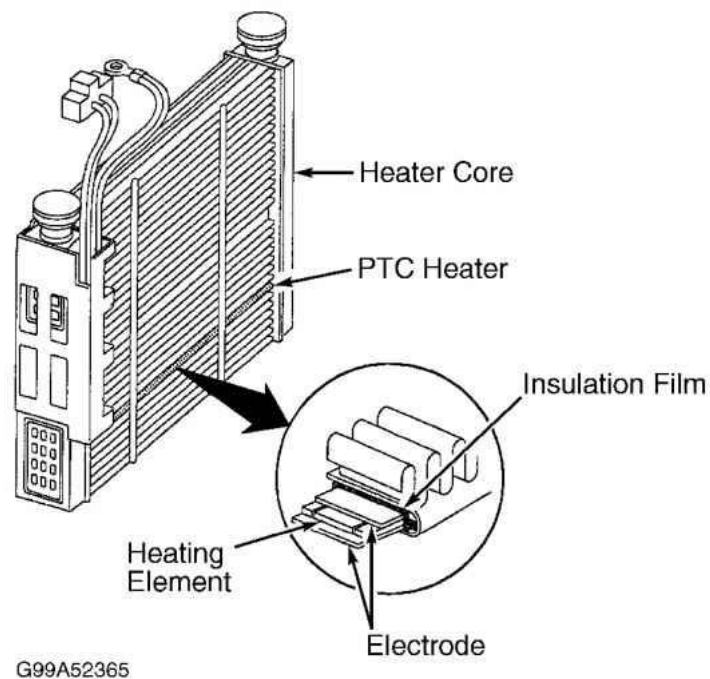


Figure 9. Draw of a PTC and detail of the heating element.

A PTC Element is, thus, a simple resistor which transforms electric energy directly into thermal energy. This heat can then be transferred to the air through a radiator. As the name can suggest, its main characteristic is related to the fact that its resistance rises with its temperature, as shown in the right part of Figure 10. In Figure 11, instead, the voltage-current characteristics are shown and it is possible to see that the electric current drastically decreases after the PTC has reached its working temperature.

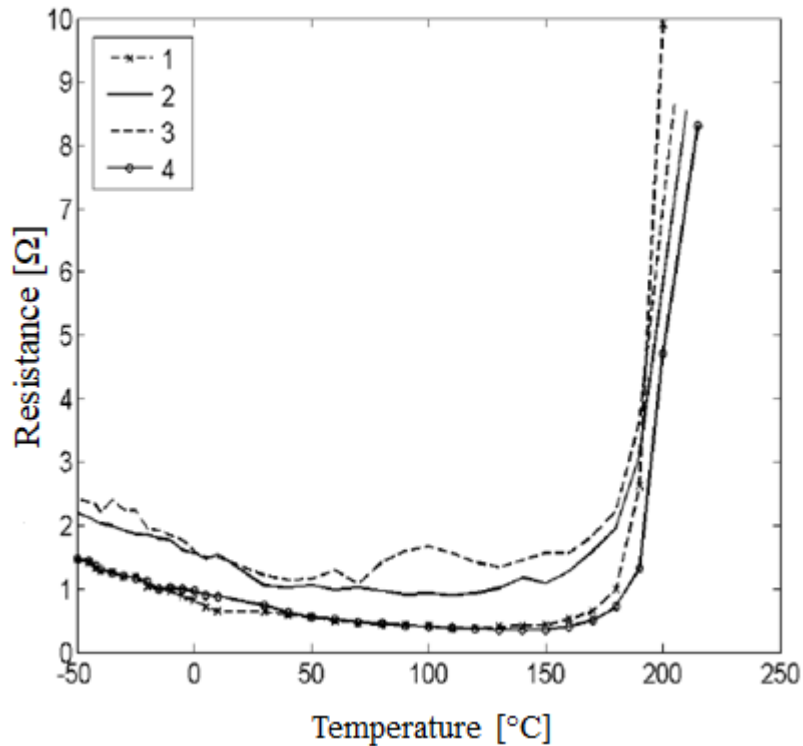


Figure 10. Electrical resistance characteristics of the different stages of a 4-stage PTC element [8].

This allows a self-regulation of the element from the heat generation point of view, so that a fuse against overheating is not needed. Since they transform electrical energy directly into heat through a resistive phenomenon, their efficiency could be assumed equal to 100%. However, some small heat transferred to surrounding components and not directly to the air should be considered, obtaining an efficiency of about 95% [9].

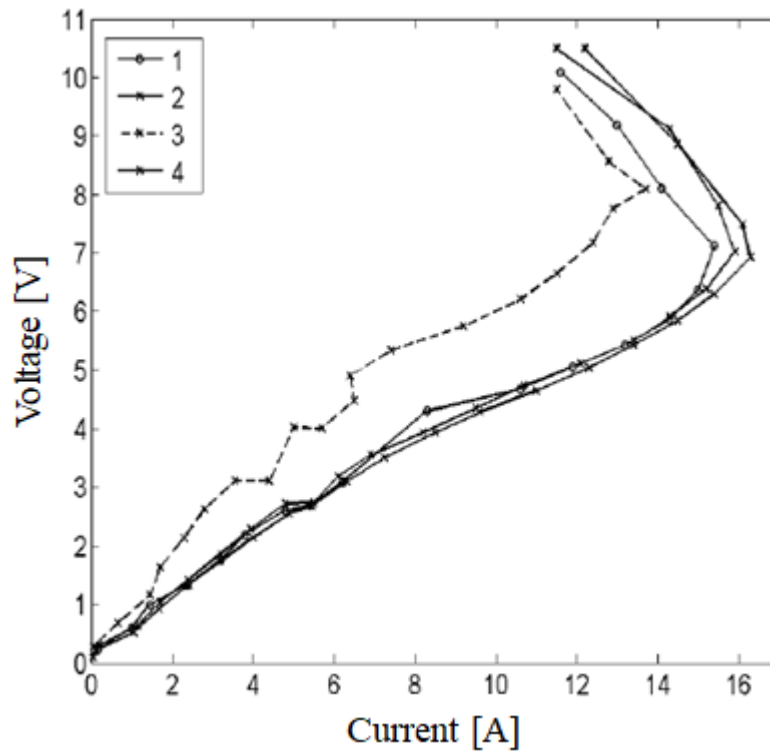


Figure 11. Voltage-current characteristics of the different stages of a 4-stage PTC element [8].

PTC heaters can transmit heat directly to the air passing through the radiators as well as indirectly via PTC water heating, not considered in this work. The latter solution has the advantage of occupying less space, but a big disadvantage is due to the heat capacity of the water, needing more time and energy to increase its temperature compared to the air.

According to [9], the heating power of PTC elements can be 3-5 kW.

Finally, in Figure 12 a simplified example of a possible use of a PTC heater is presented.

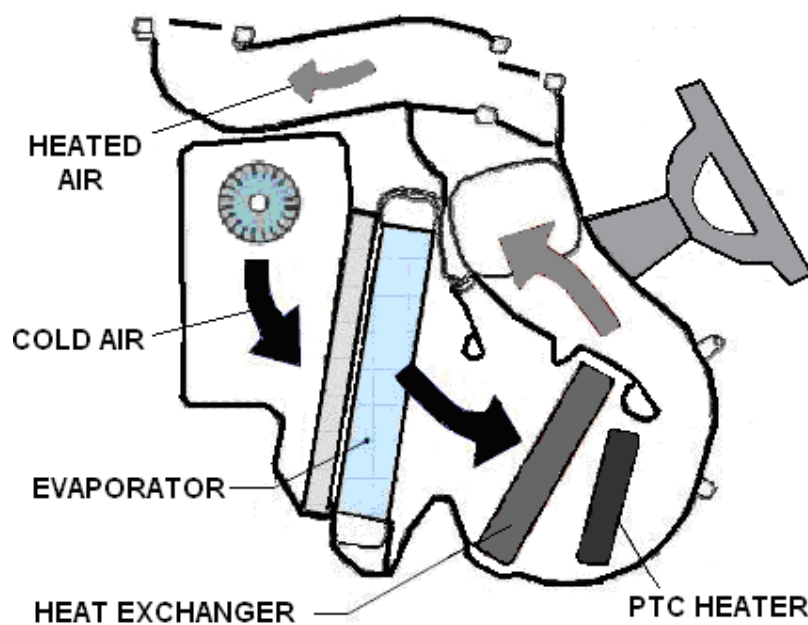


Figure 12. Example of air heating system with a PTC heater [8].

3.2 Cooling systems

For what concerns the cooling phase, practically everywhere an Air-Conditioning system is used. A/C has not only an important role for comfort, removing the heat in the passenger compartment and so reducing the cabin temperature, but it has also a fundamental function related to safety. It has, in fact, an intrinsic possibility of removing also moisture from the air, in addition to heat, favoring the defogging of the windshield, therefore keeping a good visibility condition through the windshield.

3.2.1 Air-Conditioning system

The Air-Conditioning (A/C) is a system able to remove heat from a closed space. In the refrigeration cycle, in fact, heat is transported from a colder location to a hotter area. As heat would naturally flow in the opposite direction, a work is required to achieve this. The heat is then rejected by a condenser located outside of the room to be cooled. While a refrigerant liquid follows this refrigerant cycle, the air is cooled down by a liquid-to-air heat exchanger, called evaporator in this case, before entering the cabin. The most common design of an A/C involves four main components: a condenser, an expansion valve, an evaporator and a compressor, as can be seen in Figure 13.

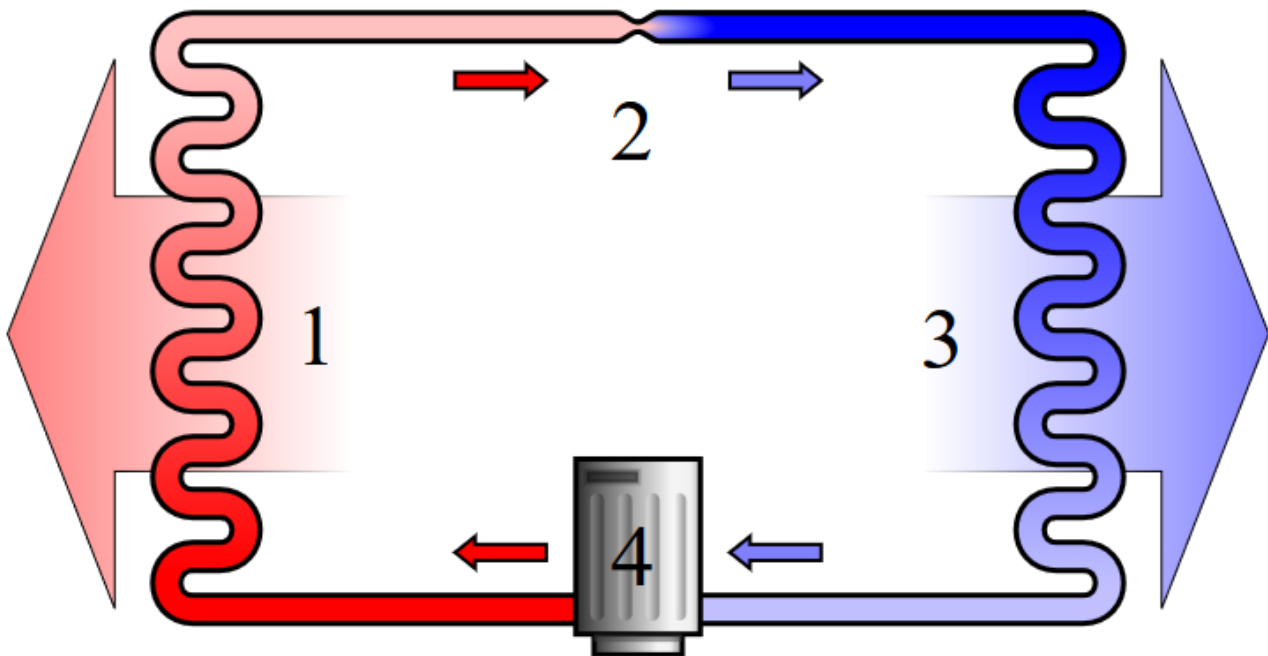


Figure 13. A simple stylized diagram of the refrigeration cycle: 1) condensing coil, 2) expansion valve, 3) evaporator coil, 4) compressor [Source: Wikipedia].

The efficiency of this type of machines is defined by a Coefficient Of Performance (COP), which is the ratio between the useful cooling power provided and the electric power required:

$$COP_{cooling} = \frac{|\dot{Q}_{cooling}|}{P_{electric}}$$

Typical values for the COP of an Air-Conditioning system can vary a lot and usually have values higher than 1. This means that it is possible to consume less electrical energy for the same heating level, or to generate

more heating with the same electrical energy, according to the considered point of view. The specific value chosen for this study is $COP = 3$.

In Figure 14 it is possible to see a schematic of a typical A/C system used in conventional vehicles.

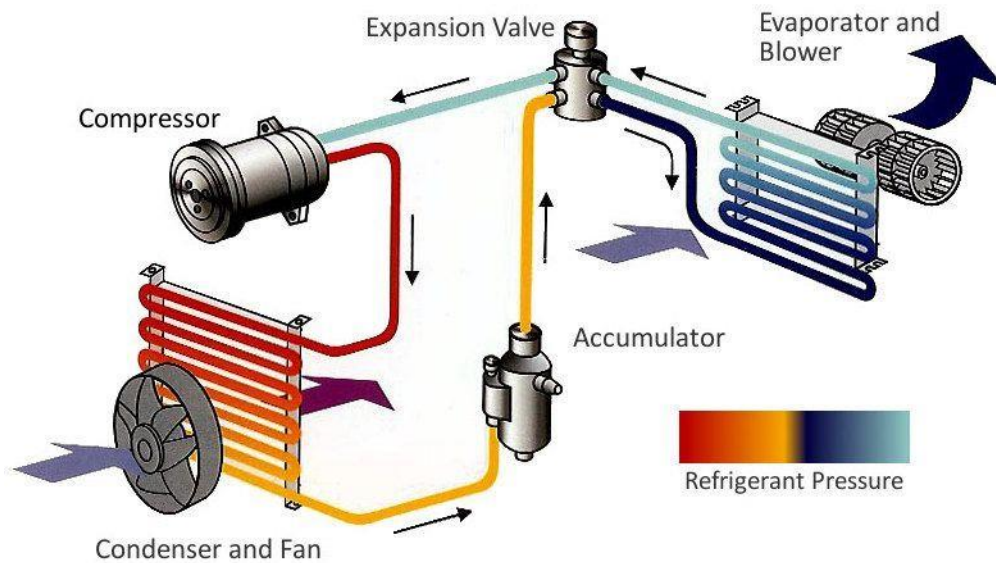


Figure 14. Schematic of an A/C system used in vehicles.

The air-conditioning has a further functionality consisting in reducing the humidity from the processed air entering the cabin, be it the recirculated one or the fresh one coming from outside. This is due to the fact that the air gets in contact with the evaporator, which is at a temperature below the dew point, condensing in this way the water vapour present in the processed air. The water, then, simply drips onto the ground outdoors.

The opportunity to lower the humidity level is very important also from a safety point of view, as already anticipated: as a matter of fact, in this way it is possible to quickly defog the windshield so as to have an acceptable visibility in all conditions. Furthermore, in this study the de-humidification effect was considered active not only during the cooling phase, but also in situations in which the water mass fraction in the air reached the so-called *sultry limit*, equal to $13 \frac{g_{water}}{kg_{dry air}}$, corresponding to a dew point of $16 \text{ }^\circ\text{C}$ [10].

In this work, the implementation of the de-humidification phase was done by acting on the de-humidification factor in Equation (28), presented later in this thesis. This parameter only had two possible values, 0 and 1, and was switched on when needed, activating that portion of equation and lowering the computed amount of water vapour in the air.

3.3 Additional possibilities

The systems analyzed in this study are the most used by car manufacturers, but it is possible to find other technologies that can be implemented on a vehicle, especially in the field of heating systems, since the A/C for cooling is, at present, the only solution used.

Moreover, as already mentioned, a further opportunity is represented by the possibility to combine different technologies in the same vehicle with the aim of obtaining better performance and higher flexibility in

different conditions, but paying the cost of an increased complexity, weight and, in case, also energy consumption. For this reason, this solution is usually implemented only in premium-segment cars.

3.3.1 Heat Pump

Heat pumps for thermal comfort are used very often in hybrid-electric vehicles, due to the presence of an ICE, while only few times in battery-electric vehicles, taking energy from the batteries. Sometimes both PTC elements and heat pumps are used at the same time in order to reduce the global energy consumption at the same heating level. As a matter of fact, heat pumps systems are equal to A/C systems, but they are used to heat up a closed space, instead of cooling it: they are devices which transfer thermal energy from a source of heat to what is called a heat sink. They move thermal energy in the opposite direction of spontaneous heat transfer, by absorbing heat from a cold space and releasing it to a warmer one, by using a small amount of external power to accomplish this work. Their efficiency is described by the same index used for A/C, the Coefficient of Performance, defined in this case as:

$$COP_{heating} = \frac{\dot{Q}_{heating}}{P_{electric}} = \frac{|\dot{Q}_{cooling}| + P_{electric}}{P_{electric}} = COP_{cooling} + 1 \quad (9)$$

One drawback of this heating system, with respect to PTC heaters, is a much more complex arrangement in the vehicle, as can be seen in Figure 15, for which dedicated space and circuits are necessary.

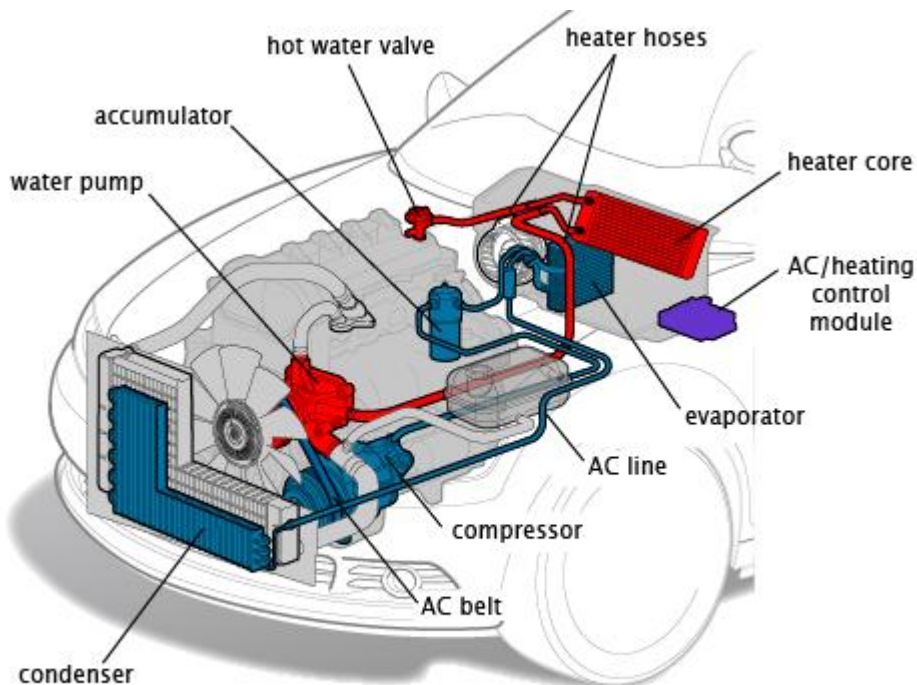


Image courtesy of ClearMechanic.com

Figure 15. Architecture of a heat pump in an ICEV [Source: ClearMechanic.com].

Another problem typical of heat pumps is that, especially in wet and cold weather, icing on the evaporator can become an issue. As this reduces the efficiency of the heat pump, either it is regularly de-iced or its temperature is regulated accordingly.

The main components of a heat pump system are shown in Figure .

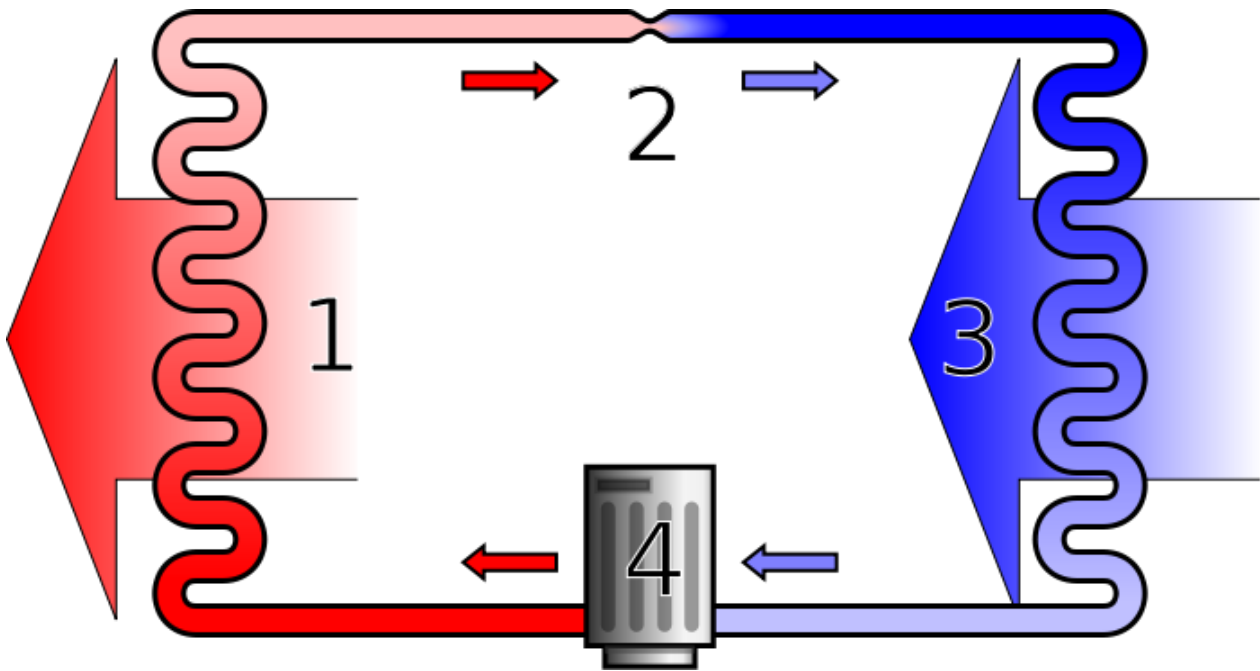


Figure 16. A simple stylized diagram of a heat pump's vapor-compression refrigeration cycle: 1) condenser, 2) expansion valve, 3) evaporator, 4) compressor [Source: Wikipedia].

3.3.2 Preconditioning

This option consists in heating or cooling the passenger compartment before starting a journey by connecting the car to a power grid. In this way, during the subsequent motion, the energy needed by the HVAC system will be lower: just the amount necessary to maintain the cabin temperature around the required one, since all the thermal masses present in the cabin have already reached an optimal temperature, or a close-to-optimal one. As can be seen in Figure 17, from [11], this solution can be worthwhile especially under certain conditions.

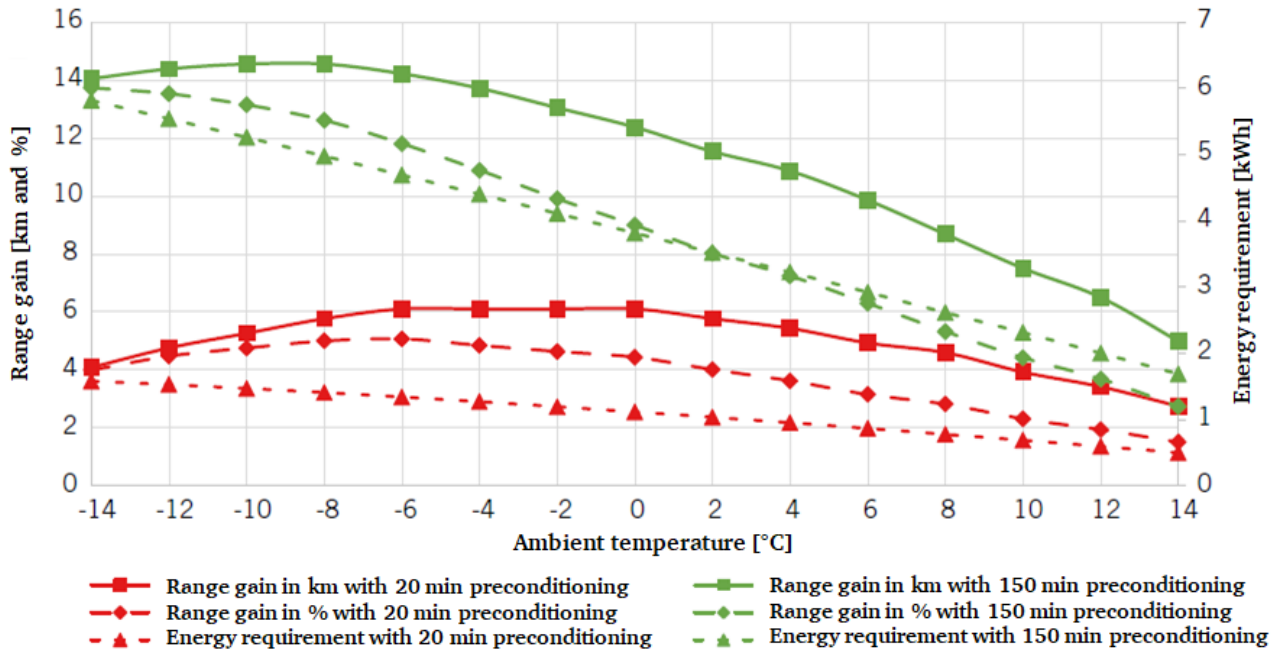


Figure 17. Range gain and energy requirement of a PTC heater at a target air temperature of 22 °C [11].

The energy required for a 2.5 hours preconditioning (green) increases a lot at low temperatures. In contrast, as long as the vehicle has not reached the objective temperature, lower heat losses occur, especially at low temperatures, because of a lower temperature difference between cabin and environment. This unintended energy saving is higher when a vehicle needs more time to heat up depending on its thermal characteristics. Therefore, the range gain in this case decreases at lower temperatures.

3.3.3 Direct heating

Direct heating includes those components which are directly in contact with the body of driver or passengers, without an intermediate medium. These include, for example, seat and steering wheel heating, as they are in contact with about 25% of the occupant's body surface [12]. In particular, it has been proven that seat heating achieves greater thermal comfort, so that the interior temperature can be lowered by up to 7 °C, according to [13]. Moreover, the heating power needed by these heaters can be regarded as constant and equal to about 100-200 W, for a seat. Therefore, this can result in an advantage for energy consumption over pure air heating.

3.3.4 New technologies

High-voltage heaters with layer technology represent another possible solution, in the field of electric vehicles. They are, basically, electrically conductive layers which heat up when current is applied. This technology can be adapted to different geometries and does not require rare earths elements and heavy metals as opposed to PTC. In addition to saving energy, this solution also results in weight savings, which are very relevant in terms of overall consumption due to the power needed for motion [14].

For what concerns infrared heating surfaces, they are similar to direct heating but they can increase the comfort without requiring any contact. This method provides a noiseless alternative and is able to provide a heating effect very quickly [15].

Finally, thermoelectric heating, which works by means of the so-called Peltier effect, can be effectively used for thermal management of the energy accumulator of an electric vehicle: this type of heating is independent of refrigerant circuits and therefore offers advantages especially in the battery air conditioning [16]. It is also conceivable to use this method for heating refrigerants, as is possible with waste heat recovery from conventional vehicles.

4 Construction of the simulation model

In this chapter the various steps to create the final model to compute secondary users' energy consumption are deeply explored one by one. First of all the main constant and variable parameters useful to the calculation are described. Then, the core of the project, which is the MATLAB function able to compute the current temperatures in the cabin, is analyzed in detail. Following this, the PI controller, needed to regulate the heating/cooling power, is presented. Finally, the integration of all these blocks is described, with the aim of having a fully functional, optimized, robust model of the heat transfers occurring inside a car from the energy consumption point of view.

The idea behind the creation of this model is the flexibility, which means to have something which can be adapted to many different cases. It has, in fact, to work with different powertrain and drivetrain architectures, different heating and cooling systems and other technological solutions or even combinations of them as well as to different external conditions just by tuning a certain number of parameters. Furthermore, every cycle should be tested using this model, just by giving in input time and velocity trend. It must be also said that every time step for time and velocity trend can be used, since they will be adapted to the simulation sampling time through the MATLAB function *interp1*, able to perform a 1D interpolation.

4.1 Parameters

As already anticipated, all parameters required for the computations are stored in a single, independent, script. These consist in a set of constants which represent geometry and dimensions of the car under consideration, the external environment conditions, mainly related to air, water vapour and solar radiation, and heating and cooling system technology.

All air and water physical characteristics (e.g. density, etc.), were assumed constant for all the external temperatures range, with values taken at 21 °C. Relative humidity value, instead, was taken according to the average value registered in Frankfurt on an annual basis [17]. In Figure 18 the humidity trend over one year is reported.

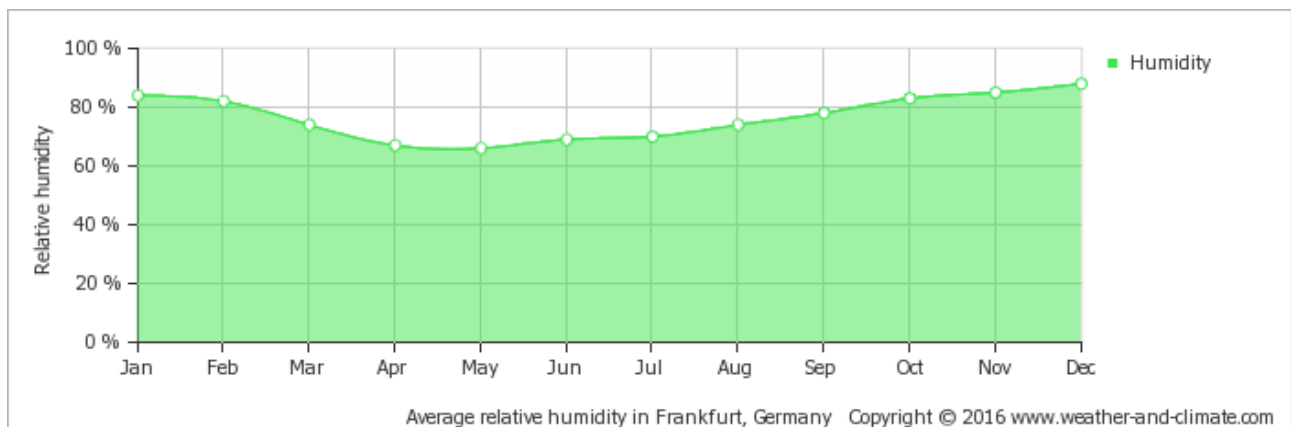


Figure 18. Average relative humidity over one year in Frankfurt, Germany [17].

Parameters and dimensions related to the vehicle considered are the typical values for a C-segment car, such as, for example, a Volkswagen Golf.

Furthermore, a certain number of these parameters can be tuned, as said before, according to the required needs, in order to apply the same model to different conditions, often obtaining a quite important influence on the final results. In the following, the tunable factors are listed, together with some of their default values chosen for the simulation:

- Recirculation factor: a factor between 0 and 1 (0.5 by default) changing the percentage of cabin air to be recirculated by the HVAC system
- Air mass flow rate: $0.08 \frac{kg}{s}$ by default
- Velocity of the air coming from the HVAC system: $2 \frac{m}{s}$ by default
- Car cabin dimensions and characteristics: typical values of a C-segment car were chosen as default, as already mentioned
- Number of passengers (driver always present) and their metabolic rate
- Solar radiation: $200 \frac{W}{m^2}$ by default
- Maximum thermal power for heating the cabin available from the internal combustion engine (Table 3)
- Maximum power consumptions of heating and cooling elements and additional loads (Table 3 and Table 1).

Table 3. Maximum thermal power considered for heating and cooling elements

| | Thermal power [W] |
|-------------------|-------------------|
| PTC | 5000 |
| A/C | -3500 |
| Engine waste heat | 5000 |

The simulation sampling time was decided to be equal to 0.1 s, in order to be as precise as possible in the simulations.

Other quite important parameters are the ones related to the human heat and moisture production: they are the consequence of the metabolic rate of a human being and become quite relevant in a small closed space like the passenger compartment of a car.

Another assumption made to simplify the calculation is related to the initial conditions chosen. As a matter of fact, at the beginning of each simulation, the following equalities apply:

$$T_{cabin} = T_{doors} = T_{roof} = T_{dashboard} = T_{interiors} = T_{external} \quad (10)$$

In the Appendix the complete MATLAB code related to the Parameters is reported.

4.2 Cabin Thermodynamic Model

This section describes the most important part of the work, which is the thermodynamic model of the passenger compartment. The analysis considered heat and enthalpy transfers inside the car, between various components, and with the external environment. It must be said that in the creation of this analytical model able to describe the heat transfers, a certain number of assumptions were made. Every interaction was considered as independent at first, then, subsequently, everything was put together, creating in this way a sort of lumped parameters model of the cabin. Due to the difficulty of taking into account all the thermal energy transfers, being them a quite complicated and interacting phenomenon, only the most important from the point of view of higher heat fluxes involved were considered. These assumptions will for sure bring intrinsic errors to the final results, unavoidable for an equation-based thermal analysis, but acceptable for the purpose of this study, which is understanding the influence of the external environment conditions on the energy consumption of a vehicle.

Therefore, to achieve this task, a MATLAB function was created, considering the interactions described in Chapter 2 applied to the main components of a car cabin:

- Heat transfer through the glasses (windscreen, lateral and rear ones): conduction and convection (internal and external)

$$\begin{aligned} \dot{Q}_{glasses} = & U_{glasses} A_{windshield} (T_{external} - T_{cabin}) + \\ & + U_{glasses} * A_{lateral\ windows} (T_{external} - T_{cabin}) + U_{glasses\ rear} A_{rear\ window} (T_{external} - T_{cabin}) \end{aligned} \quad (11)$$

- Heat transfer through the doors: conduction and convection (internal and external) considering layers of metal-air-metal-air-plastic and irradiation towards the external environment

$$\frac{dT_{doors}}{dt} m_{doors} c_{p,doors} = \dot{Q}_{doors,external} - \dot{Q}_{doors,internal} \quad (12)$$

$$\dot{Q}_{doors\ internal} = U_{doors\ internal} A_{doors} (T_{doors} - T_{cabin}) \quad (13)$$

- Solar radiation on doors, roof and dashboard

$$\begin{aligned} \dot{Q}_{doors\ external} = & 0.5 * I_{solar\ radiation} \gamma_{doors} A_{doors} - \varepsilon_{doors} \sigma T_{doors}^4 + \\ & - \alpha_{external} A_{doors} (T_{doors} - T_{external}) \end{aligned} \quad (14)$$

γ_{doors} : doors absorbance

$$\dot{Q}_{solar\ on\ dashboard} = I_{solar\ radiation} \gamma_{dashboard} \tau_{glass} A_{dashboard} \quad (15)$$

$\gamma_{dashboard}$: dashboard absorbance

τ_{glass} : glass transmittance

$$\begin{aligned} \dot{Q}_{roof\ external} = & I_{solar\ radiation} * \gamma_{roof} * A_{roof} - \varepsilon_{roof} \sigma T_{roof}^4 + \\ & - \alpha_{external} A_{roof} (T_{roof} - T_{external}) \end{aligned} \quad (16)$$

γ_{roof} : roof absorbance

- Heat transfer by convection on dashboard and interiors (mainly the seats)

$$\frac{dT_{dashboard}}{dt} m_{dashboard} c_{p,dashboard} = \dot{Q}_{sun} - \dot{Q}_{dashboard} \quad (17)$$

$$\dot{Q}_{dashboard} = U_{dashboard} A_{dashboard} (T_{dashboard} - T_{cabin}) \quad (18)$$

$$\frac{dT_{interiors}}{dt} m_{interiors} c_{p,interiors} = \dot{Q}_{interiors} \quad (19)$$

$$\dot{Q}_{interiors} = U_{interiors} A_{interiors} (T_{interiors} - T_{cabin}) \quad (20)$$

- Heat transfer through the roof: conduction and convection (internal and external) considering layers of metal-air-plastic and irradiation towards the external environment

$$\frac{dT_{roof}}{dt} m_{roof} c_{p,roof} = \dot{Q}_{roof,external} - \dot{Q}_{roof,internal} \quad (21)$$

$$\dot{Q}_{roof\ internal} = U_{roof\ internal} A_{roof} (T_{roof} - T_{cabin}) \quad (22)$$

- Driver and passengers thermal and moisture loads due to metabolism

$$\dot{Q}_{driver} = \varphi_{human} A_{body} * 1.4 \quad (23)$$

φ_{human} : human metabolic rate

$$\dot{Q}_{passengers} = n_{passengers} \varphi_{human} A_{body} \quad (24)$$

Furthermore, the humidity change in the cabin air was included in the analysis too. In particular, a fixed value of moisture generation for driver and passengers was considered as well as the relative humidity coming from outside air, depending on ambient conditions. Thus for the air entering and exiting the cabin through the HVAC system, the variation of the enthalpy flux was described by the following equations:

- Enthalpy fluxes of air entering and exiting the cabin, with a tunable air recirculation factor

$$\dot{H}_{in} = \dot{m}_{recirculating\ air} (T_{cabin} c_{p,air} + X_{cabin} (c_{p,steam} T_{cabin} + \Delta h_{v,0})) + \dot{m}_{fresh\ air} h_{fresh\ air} + \dot{Q}_{HVAC} \quad (25)$$

$$\dot{H}_{out} = \dot{m}_{air} T_{cabin} (c_{p,air} + X_{cabin} c_{p,steam}) + \dot{m}_{air} X_{cabin} \Delta h_{v,0} \quad (26)$$

- Cabin water mass fraction

$$X_{cabin} = \frac{m_{water}}{m_{air} - m_{water}} \quad (27)$$

- Cabin water mass

$$\frac{dm_{water}}{dt} = (\dot{m}_{recirculating\ air} - \dot{m}_{air}) X_{cabin} + X_{environment} \dot{m}_{fresh\ air} + \dot{m}_{humans} - \beta \dot{m}_{air} X_{cabin} \quad (28)$$

β : dehumidification factor

- Humans' moisture mass flow rate:

$$\dot{m}_{humans} = (n_{passengers} + 1) * 8.3 * 10^{-6} \quad (29)$$

Finally, the considerations made for every heat transfer can be put together in order to find the cabin air temperature variation in time through the first law of thermodynamics, just by equating the following Equations (30) and (31), where U_{int} is the system's internal energy, the only component considered of the total energy present in Equation (7):

$$\frac{dU_{int}}{dt} = \dot{Q}_{dashboard} + \dot{Q}_{glasses} + \dot{Q}_{interiors} + \dot{Q}_{doors} + \dot{Q}_{roof} + \dot{Q}_{driver} + \dot{Q}_{passengers} + \dot{H}_{in} - \dot{H}_{out} \quad (30)$$

$$\frac{dU_{int}}{dt} = \frac{dT_{cabin}}{dt} (m_{air}c_{p,air} + m_{water}c_{p,water}) + \frac{dm_{water}}{dt} (T_{cabin}c_{p,water} + \Delta h_{v,0}) \quad (31)$$

For what concerns the heat transfer coefficients used in these calculations, they all follow the same structure:

$$U_{overall} = \left(\sum \frac{1}{h_{i,convection}} + \sum \frac{t_j}{\lambda_{j,conduction}} \right)^{-1} \quad (32)$$

Where:

- h : convection coefficient
- λ : conduction coefficient
- t : thickness of the considered component.

In particular:

$$h_{convection} = \frac{Nu * \lambda_{air}}{L_{characteristic}} \quad (33)$$

$$Nu = 2 * 0.332 * Re^{\frac{1}{2}} * Pr^{\frac{1}{3}} \quad (34)$$

$$Pr = \frac{c_{p,air} * \mu_{air}}{\lambda_{air}} \quad (35)$$

$$Re = \frac{v_{air} * L_{characteristic} * \rho_{air}}{\mu_{air}} \quad (36)$$

Where:

- Nu : average Nusselt number for laminar flow over a flat plate
- Pr : Prandtl number
- Re : Reynolds number.

As already mentioned, all these thermal interactions were modeled one by one, independently from each other, and then considered as occurring simultaneously.

A draw representing all the cabin heat transfers is presented in Figure 19.

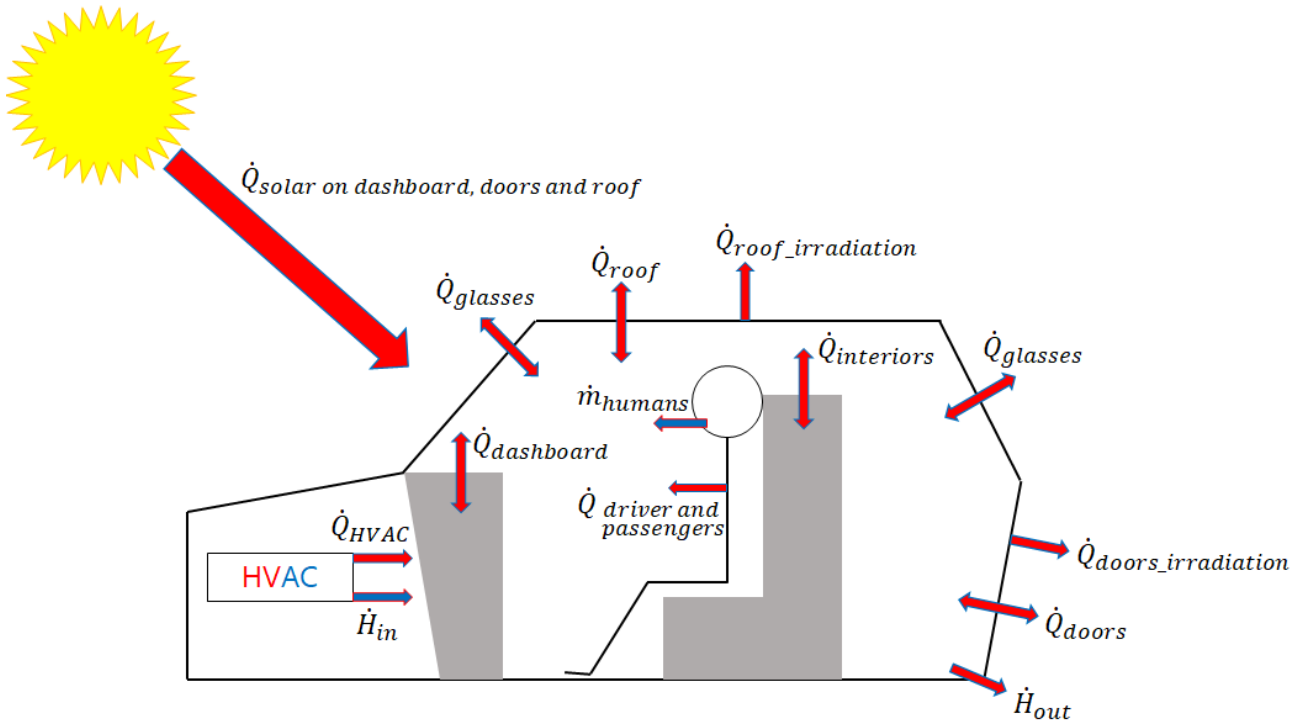


Figure 19. Cabin thermodynamic model

In this way it was possible to simulate the main heat transfers of a car cabin occurring during normal use.

Since the system under consideration is a dynamic one, the evolution of the various temperatures and thermal powers is described by a set of first order differential equations, introduced in Chapter 2. In order to find a solution for them and so to implement them on MATLAB, it has been necessary to transform them into a set of discretized differential equations. This process was possible using the Forward Euler Discretization method:

- First order differential equation:

$$\frac{dy(t)}{dt} = f(y, t) \quad (37)$$

- Discretized differential equation:

$$\dot{y}(k) = \frac{y(k+1) - y(k)}{T} \quad (38)$$

Where T is the sampling time and k is the simulation time step.

The complete MATLAB script of the cabin model is reported in the Appendix, at the end of this thesis.

4.2.1 Inputs and Outputs of the function

The function of the cabin thermodynamic model requires in input a series of variables and parameters related to the current conditions considered, both in terms of simulation steps and of physical characteristics of the system considered:

- i^{th} simulation step

- Air parameters
- Car parameters
- Driver and passengers parameters
- Solar radiation amount and Stefan-Boltzmann constant
- Current water mass in cabin air
- HVAC load (heating or cooling)
- Current temperature values of external environment, cabin air, dashboard, doors (external panel), interiors, roof (external panel)
- Current cabin and environment water mass fractions
- Fresh air specific enthalpy
- Dehumidification factor
- Simulation sampling time

Given all these data, being the function a MIMO type, it is able to give in output:

- Next temperature values for cabin air, dashboard, interiors, doors (external panel), roof (external panel)
- Next value of cabin water mass fraction
- Next value of cabin air specific humidity.

4.2.2 Operation

The functioning of the cabin thermodynamic model is as follows: at every simulation step, thanks to the knowledge of several conditions given by the input data, the function is able to compute all the heat transfers previously described, combining them in order to obtain the new values of temperature of the components in the passenger compartment. Between all these outputs, the most important for the purpose of this study is, of course, the inside air temperature.

4.3 PI Controller

Heating and cooling of the cabin was made by acting on the HVAC load parameter (\dot{Q}_{HVAC}) in the inlet air enthalpy flux Equation (25). The right value of the thermal load was calculated through a PI controller, indeed able to compute the need of thermal power at each simulation time step. This need was mainly based on the difference between the objective temperature, set at 21 °C, and the current air temperature inside the cabin, computed through the *Cabin thermodynamic model* function.

A PI controller, where PI stands for Proportional-Integral, is a particular version of the more general PID, Proportional-Integral-Derivative, one. A PID controller is, in fact, a control loop feedback mechanism, widely used in many control systems applications.

A PID controller is of the form:

$$C(s) = K_P + \frac{K_I}{s} + K_D s \quad (39)$$

Where in this case s is the complex variable of the Laplace transform.

An example of application for the PID controller is represented by the following diagram (Figure 20):

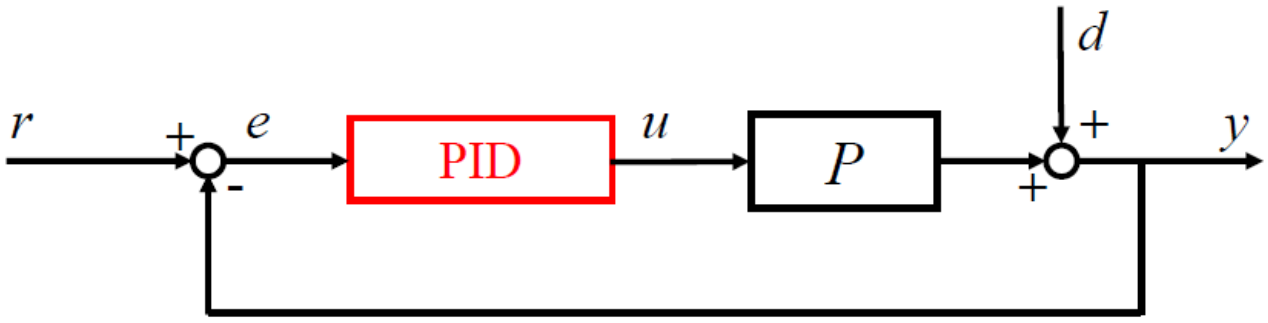


Figure 20. Example of application of the PID controller.

Where r is the reference value, e is the error, u is the input, d is the disturbance, y is the output and P is the plant considered.

As previously said, a controller of this type continuously calculates the error value as the difference between a desired value (desired temperature) and a measured variable (current cabin air temperature) and applies a correction based on proportional, integral and, but not in this case, derivative terms, as written in Equation (39). In this way it automatically applies accurate and responsive corrections to a control function. The decision of using a controller of this type was mainly due to its simplicity and, at the same time, effectiveness.

The equations describing the chosen PI controller are the following:

$$\text{Proportional action} = K_p(T_{objective} - T_{cabin}) + K_I K_a (T_{objective} - T_{cabin}) T_{sampling} k \quad (40)$$

$$\text{Integral action} = K_I \int (T_{objective} - T_{cabin}) dT_{sampling} \quad (41)$$

Where k is the simulation time step and $T_{sampling}$ is the simulation sampling time.

Proportional and integral coefficients of the created controller were tuned manually to obtain an acceptable response avoiding non-physical solutions. Eventually, the values of the coefficients were chosen as follows:

- $K_p = 1$ – proportional coefficient
- $K_I = 3$ – integral coefficient
- $K_A = 3$ – additional coefficient.

As it can be noticed, in the proportional action of the controller, an additional part was added, proportional to both the integral coefficient and to a new coefficient, K_A , introduced in order to reduce the large oscillations that were occurring due to the fact that the car, during a cycle, changes its velocity very quickly compared to the times related to the transfers of heat.

Moreover, together with the functioning of the A/C, a dehumidification operation was added, as described in Chapter 3.2.1.

The PI controller made in this way is able to control heating and cooling power of every technology taken into consideration. This fact is linked to the flexibility typical of this work, strongly present also in the cabin thermodynamic model.

Furthermore, an anti-windup part was introduced to limit the integral action of the controller to the set values of maximum achievable heating and cooling powers of the technologies considered: PTC heater and Air Conditioning system for BEV, waste heat (not consuming power) and Air Conditioning for ICEV, PTC or waste heat and Air Conditioning for PHEV. Integral windup, also known as integrator windup or reset windup, refers to the situation in a PID feedback controller where the integral term accumulates a significant error during the rise (windup), thus overshooting and continuing to increase as this accumulated error is continuously taken into account in further integrations. In order to avoid this problem, few lines of code were added so as to limit the value of the integrator to the maximum possible value:

```
int_max=Q_dot_ptc_max-prop;
int_min=Q_dot_ac_max-prop;
%antiwindup
if int > int_max
    int_sat=int_max;
elseif int < int_min
    int_sat=int_min;
else
    int_sat=int;
end
```

As written above, the maximum possible value for the integrator is equal to the maximum heating or cooling power available minus the value already computed by the proportional part of the controller.

It must be said that, as a first test, the anti-windup section was created as a function to be recalled when needed. After a time optimization study, analyzed in Chapter 4.4.2, the code related to the anti-windup was put directly in the working script.

4.4 Overall simulation

After the previously described phases, all the different blocks were put together to create a simulation environment able to analyze all powertrain concepts and all temperatures required during any desired cycle, even considering more than one cycle in the same simulation.

This was possible by creating four *for* loops. They were placed one inside the other, an operation called *nesting*, in order to loop over the following data and conditions:

- All the different concepts
- All the driving cycles, loaded one by one at each loop
- All the external temperatures considered
- The length of the current selected cycle.

Inside the code, the structure necessary to perform this activity is the following:

```
for j=1:length(concept)
    for kk = 1:length(driving_cycles_loading.mat)
        for i=1:length(T_ext)
            for k=1:N
                end
            end
        end
    end
end
```

Going more in detail, the first *for* loop, the most external, is related to the different powertrain concepts analyzed, which in this case were BEV, ICEV and PHEV. Therefore, every iteration, in this case, computes the energy demand for one concept at a time. The second loop, placed inside the first one, is related to the driving cycles that can be studied: every iteration corresponds to one concept over one cycle at a time. The third loop, placed inside the previous two, is related to the various external temperatures taken into account: the iterations compute the energy consumption of a certain concept, over a certain cycle, for every single temperature needed. Finally, the last *for* loop, the most internal, is linked to the secondary users calculations during the cycle currently under consideration. Here it is possible to find the PI controller for computing the thermal power needed step by step, its anti-windup section and the cabin thermodynamic model function, in which all relevant temperatures are evaluated at every simulation step. The time step in this loop is, in fact, the sampling time of the simulation, which is equal to 0.1 s.

Finally, at the end of a simulation of this type, it is possible to have a quite large set of results. In fact, the outputs of this operation, for each cycle, are:

- Temperature trends over time of cabin air and all cabin components (interiors, dashboard, external shell of doors and external shell of roof)
- Water mass and water mass fraction trends over time in the cabin air
- Heating and/or cooling power trends over time
- Secondary users' power requirement trends over time
- Energy requirement amount for each external temperature.

Also in this case, in the Appendix it is possible to find the complete MATLAB code related to the simulation.

4.4.1 Driving cycles

As a first step, in order to check the reliability of the model and to make the necessary tuning, the simulations have been tested on the most common type-approval driving cycles, listed and described here below:

- *WLTP* (Class 3 vehicle): *Worldwide harmonized Light vehicles Test Procedure*. Entered into force on September 1st, 2017 for new car models and on September 1st, 2018 for all vehicles. It defines a global harmonized standard for determining the levels of pollutants and CO₂ emissions, fuel or energy consumption, and electric range for light-duty vehicles. The WLTC driving cycle for a Class 3 vehicle (normal passenger car) is divided in four parts for Low, Medium, High, and Extra-High

speed; in case $V_{max} < 135$ km/h, the Extra-High speed part is replaced with the Low speed part. In Figure 21 the velocity trend over time is reported.

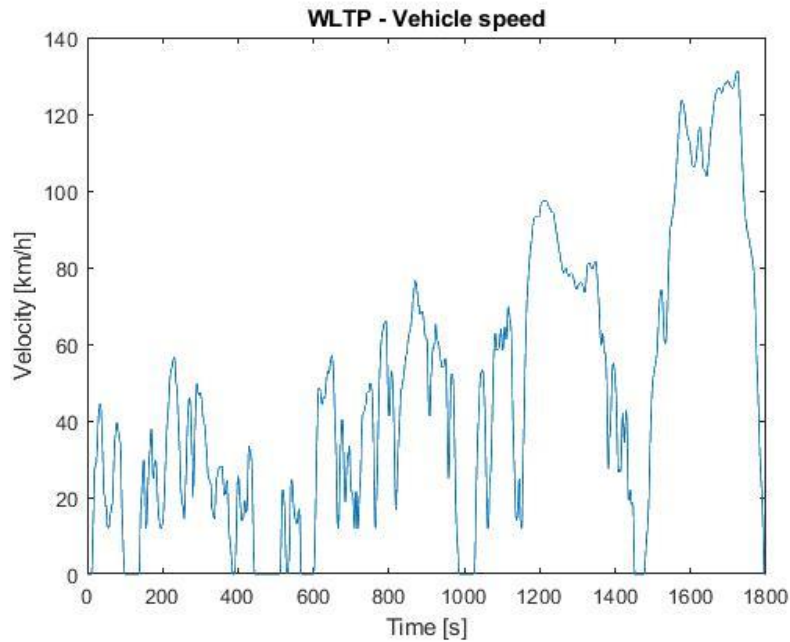


Figure 21. Velocity vs Time, WLTP cycle.

- *NEDC: New European Driving Cycle.* Type-approval cycle in use in the European Union before the advent of WLTP. It consists of four repeated ECE-15 urban driving cycles (UDC) and one Extra-Urban driving cycle (EUDC). It was supposed to represent the typical usage of a car in Europe, but it must be said that this cycle was very far from being representative of a real driving condition. In Figure 22 the velocity trend is plotted versus time and it is easy to understand the big difference with respect to the WLTP cycle.

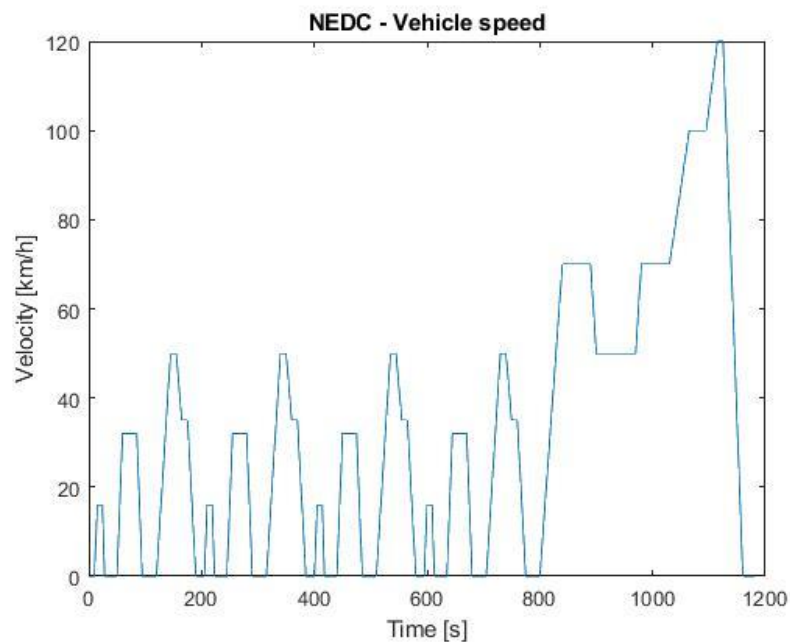


Figure 22. Velocity vs Time, NEDC cycle.

- *ECE-15*: called also *UDC, Urban Driving Cycle*. Designed to represent typical driving conditions of busy European cities. It is characterized by low engine load, low exhaust gas temperature, and a maximum speed of 50 km/h, as plotted in Figure 23.

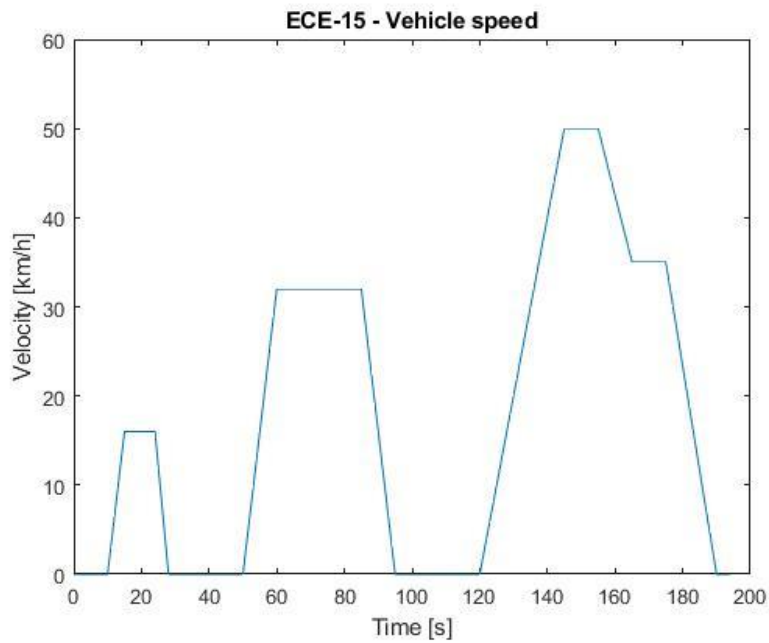


Figure 23: Velocity vs Time, ECE-15 cycle.

- *FTP-75*: also called *EPA Federal Test Procedure*. Type-approval driving cycle used in the USA. The cycle simulates a urban route with frequent stops and it consists of three phases, separated by stopping the engine for 10 minutes, as can be seen in Figure 24.

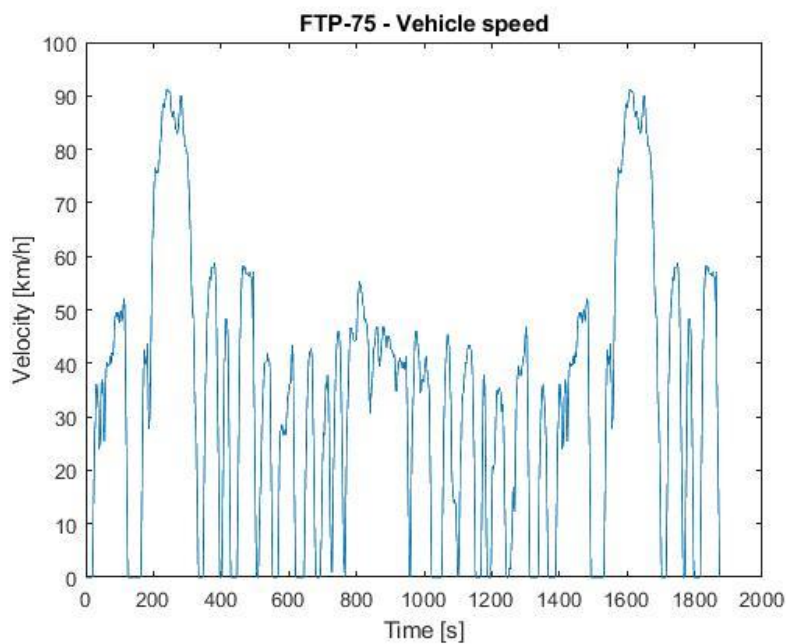


Figure 24. Velocity vs Time, FTP-75 cycle.

In Table 4 the main features of the previously described cycles are listed.

Table 4. Main features of the type-approval cycles considered.

| | Length [km] | Duration [s] | Max. speed [km/h] | Avg. speed [km/h] |
|--------|-------------|--------------|-------------------|-------------------|
| WLTP | 23.3 | 1800 | 131.3 | 46.5 |
| NEDC | 11.007 | 1180 | 120 | 33.6 |
| ECE-15 | 1.013 | 195 | 50 | 18.7 |
| FTP-75 | 17.8 | 1877 | 91.2 | 34.1 |

4.4.2 Time optimization study

Due to the fact that the analysis carried out for this thesis takes into consideration many different conditions at the same time, in terms of different powertrain concepts, different driving cycles and different ambient temperatures, the simulation time can reach quite high values. It has been then necessary to realize a deep study with the objective to minimize it in order to improve the overall performance and usability of the model. This task was carried out through the use of the MATLAB functionality called *Profiler*, able to track the execution time of each line of code, including the functions called inside the script.

As a first attempt, the computation time for all 3 concepts and for all 51 temperatures between -10 °C and +40 °C along the WLTP cycle resulted equal to what written in Figure 25. As can be seen, the most time consuming part was simply due to the function *interp1*, namely an interpolation needed to adapt the input velocity data to the simulation sampling time. This function was initially placed inside the most internal *for* loop, leading to a very high number of calls, as can be seen in the image. As a solution, this interpolation operation was simply moved as externally as possible to avoid useless calls: it was finally placed inside the most external loop, linked to the vehicle concepts, leading to a reduction of about 240 seconds. Another part on which it was possible to work was the *antiwindup* function: as previously mentioned, including the code directly inside the main script could reduce the overall time by around 4 seconds.

Profile Summary

Generated 05-Nov-2018 14:16:16 using performance time.

| <u>Function Name</u> | <u>Calls</u> | <u>Total Time</u> | <u>Self Time*</u> | Total Time Plot (dark band = self time) |
|--|--------------|-------------------|-------------------|---|
| Secondary_users_model | 1 | 450.180 s | 95.967 s |  |
| interp1 | 1854000 | 239.962 s | 219.825 s |  |
| Cabin_thermodynamic_model_FUNCTION | 1854000 | 109.715 s | 109.715 s |  |
| interp1>reshapeAndSortXandV | 1854000 | 14.442 s | 11.341 s |  |
| interp1>parseinputs | 1854000 | 5.694 s | 5.694 s |  |
| antiwindup | 1854000 | 4.498 s | 4.498 s |  |
| interp1>reshapeValuesV | 1854000 | 3.101 s | 3.101 s |  |
| run | 1 | 0.030 s | 0.019 s | |
| close | 1 | 0.008 s | 0.001 s | |
| close>safegetchildren | 1 | 0.007 s | 0.003 s | |
| strcat | 2 | 0.005 s | 0.004 s | |
| allchild | 1 | 0.004 s | 0.003 s | |
| Parameters | 1 | 0.003 s | 0.003 s | |

Figure 25. Profile summary – first attempt.

Finally, after few other small adjustments in the writing of the code, an acceptably low time for this simulation was found, obtaining the results shown in Figure 26. As it is possible to understand, the optimization study led to a very important time reduction, more the 4 times lower.

It has to be said, for sake of completeness, that a further reduction could be possible by choosing a higher order integration method for the discretization of the differential equations, solution not considered in this work.

Profile Summary

Generated 05-Nov-2018 13:36:27 using performance time.

| <u>Function Name</u> | <u>Calls</u> | <u>Total Time</u> | <u>Self Time*</u> | Total Time Plot (dark band = self time) |
|--|--------------|-------------------|-------------------|---|
| Secondary_users_model | 1 | 105.656 s | 9.892 s |  |
| Cabin_thermodynamic_model_FUNCTION | 1854000 | 95.677 s | 95.677 s |  |
| interp1 | 3 | 0.040 s | 0.039 s | |
| run | 1 | 0.034 s | 0.017 s | |
| close | 1 | 0.012 s | 0.001 s | |
| close>safegetchildren | 1 | 0.011 s | 0.005 s | |
| Parameters | 1 | 0.010 s | 0.008 s | |

Figure 26. Profile summary – final results.

4.4.3 Results

The results presented in this section, mainly in the form of plots, are related to the previously described cycles. Furthermore, the attention is mainly placed on BEVs, because in this first step, only secondary users' consumption is considered, independently from primary users' one, so in case of ICEVs and PHEVs the majority of results would be equal to BEVs outcome, if not explicitly mentioned. Moreover, due to the hybrid vehicles' intrinsic capability of switching between internal combustion engine and electric motor, it is more interesting to carry out a wider analysis considering also the drivetrain operation strategy, which can be found in Chapter 5. Finally, the energy consumption considered here for conventional vehicles, ICEVs, must be taken as is and independent from the effect that it could have on fuel consumption, since in this first step only the energy demand was calculated.

4.4.3.1 WLTP

In the following, all the results obtained for the WLTP cycle are presented.

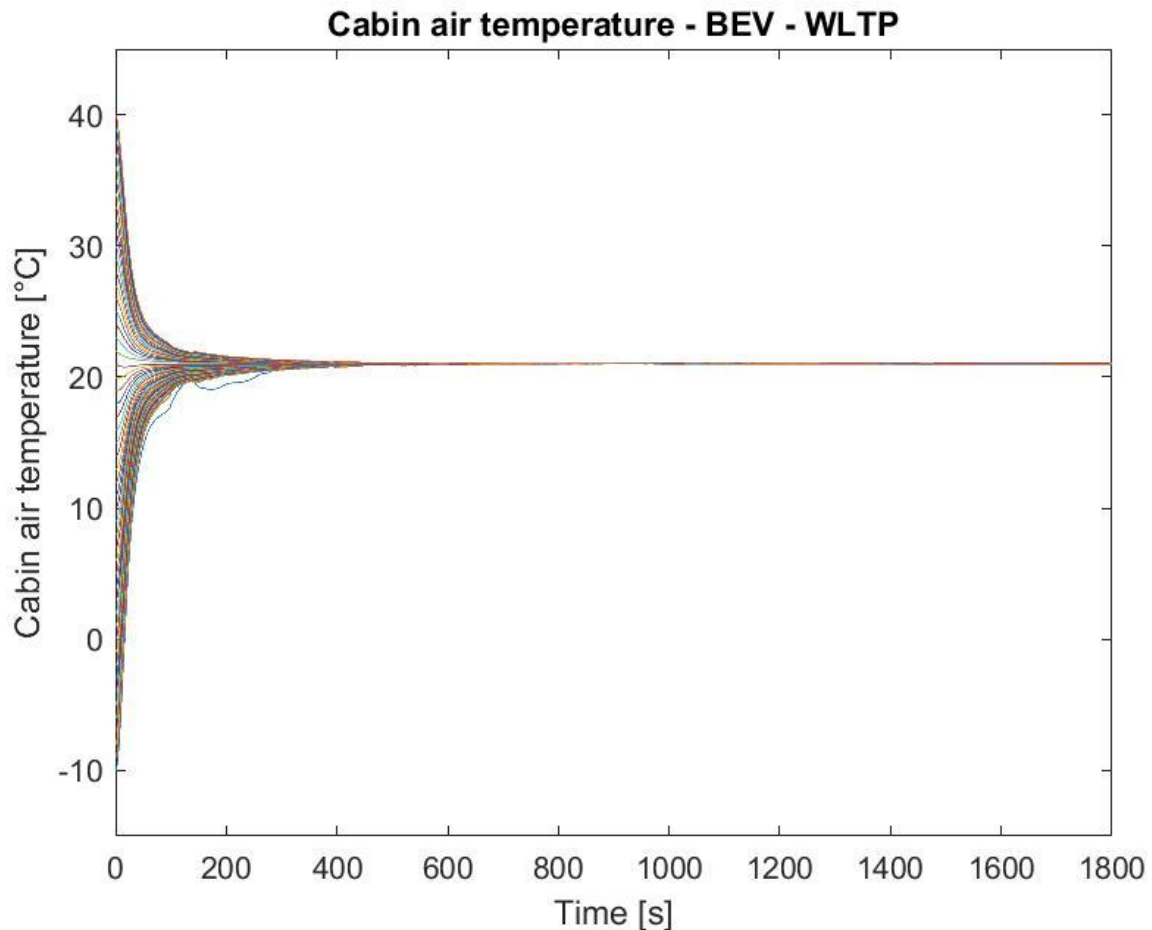


Figure 27. Cabin air temperature trends in case of a BEV in the WLTP cycle.

In Figure 27 it is possible to see the trend of air temperature inside the passenger compartment of a full electric vehicle, for every starting condition from $-10\text{ }^{\circ}\text{C}$ to $+40\text{ }^{\circ}\text{C}$. As already stated at the end of Chapter 4.1, in Equation (10), the initial value of the cabin temperature is equal to external one, at the beginning of every simulation. It can be noticed that a transient phase is present, in which the temperature changes quickly, since the power demand is close, or equal, to the maximum power available. Even in the most extreme conditions, the enthalpy flux entering the car can make the air reach the desired temperature of $21\text{ }^{\circ}\text{C}$ in less than 3 minutes. After the transient phase, it is possible to find a very stable steady-state condition in which the objective of the heating or cooling element is just to maintain the desired comfort conditions, consuming a lower amount of energy. Some small oscillations are present: this is due to the dynamic of the driving cycle. The HVAC system must follow the speed variations of the car, which change the heat transfer coefficients of windows, doors and roof, and which are faster than the heat transfer variations. Cooling and heating conditions are quite specular, even though the maximum power considered for PTC element and A/C system is different. This is due to the fact that not always the PI controller triggers the highest possible thermal power.

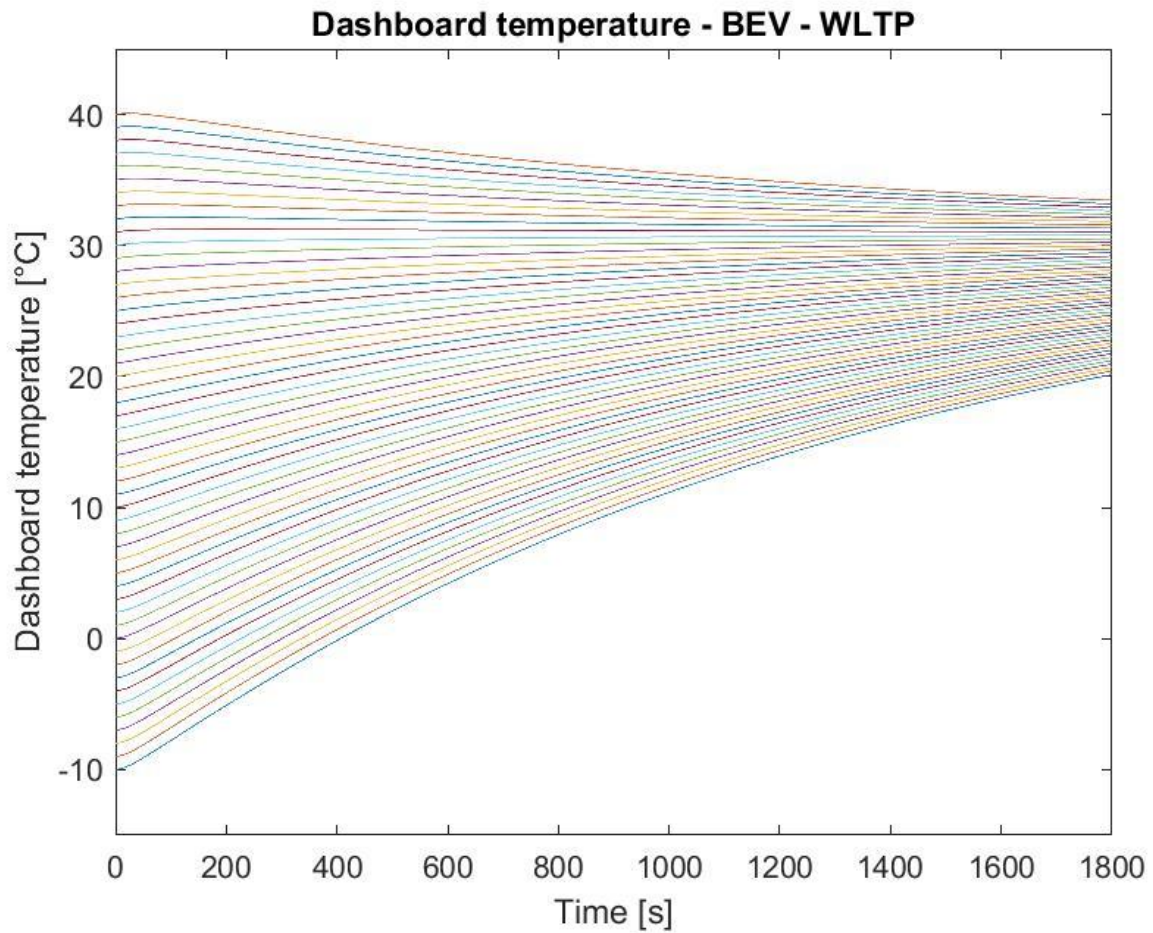


Figure 28. Dashboard temperature trends in case of a BEV in the WLTP cycle.

In Figure 28, all cases of dashboard temperature trend are plotted. As can be noticed, since the thermal mass is quite high, it needs quite a lot of time to change its temperature with respect to the air. When the A/C is on, its temperature decreases, but at an even lower pace. This is due to the considered solar radiation acting directly on the dashboard and so providing a continuous positive thermal power.

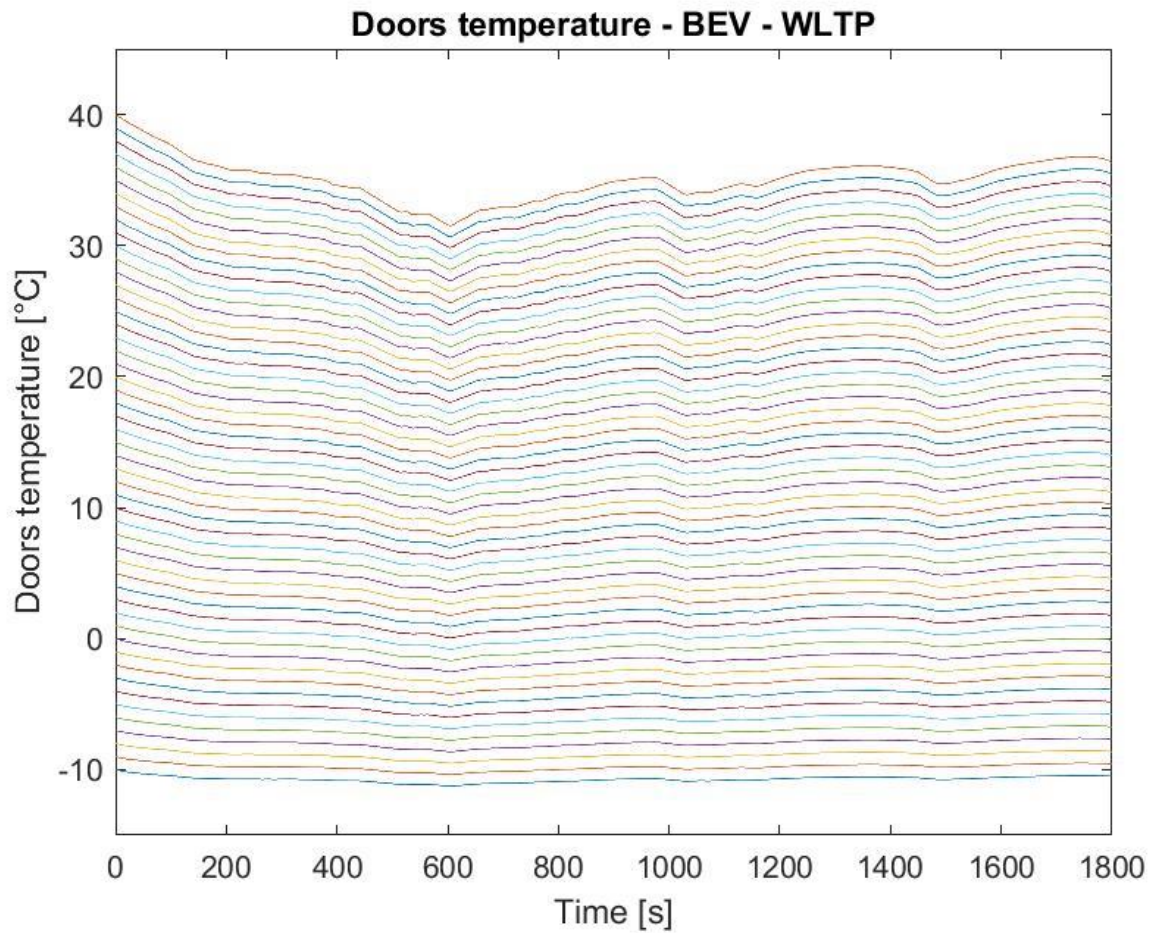


Figure 29. Doors temperature trends in case of a BEV in the WLTP cycle.

In Figure 29 it can be seen the temperature versus time of the external shell of the doors. As could be expected, it remains more or less constant when outside temperatures are low, while it decreases of almost 10 °C when the environment is hot. This is due to the fact that a lot of heat is removed by convection directly from the doors surface when the car is moving.

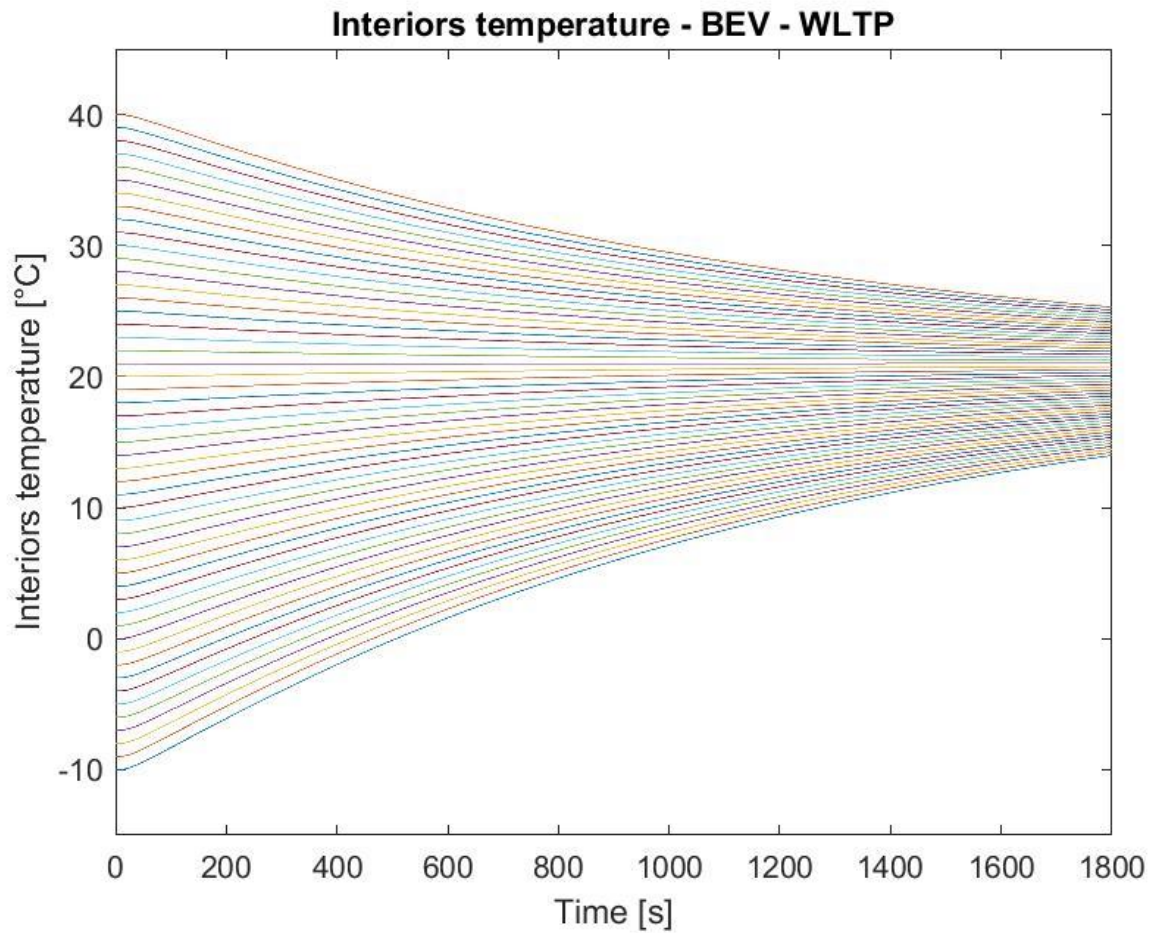


Figure 30. Interiors temperature trends in case of a BEV in the WLTP cycle.

In Figure 30 the temperature variations of car interiors are plotted. The interiors are represented mainly by the seats. Even though it is quite difficult to be really precise in estimating analytically the temperature for these components, the results obtained are reasonable, giving an idea of what can be expected to happen, considering that the thermal mass of the interiors can have quite high values and thus both heating and cooling phases need a lot of time to change their temperature.

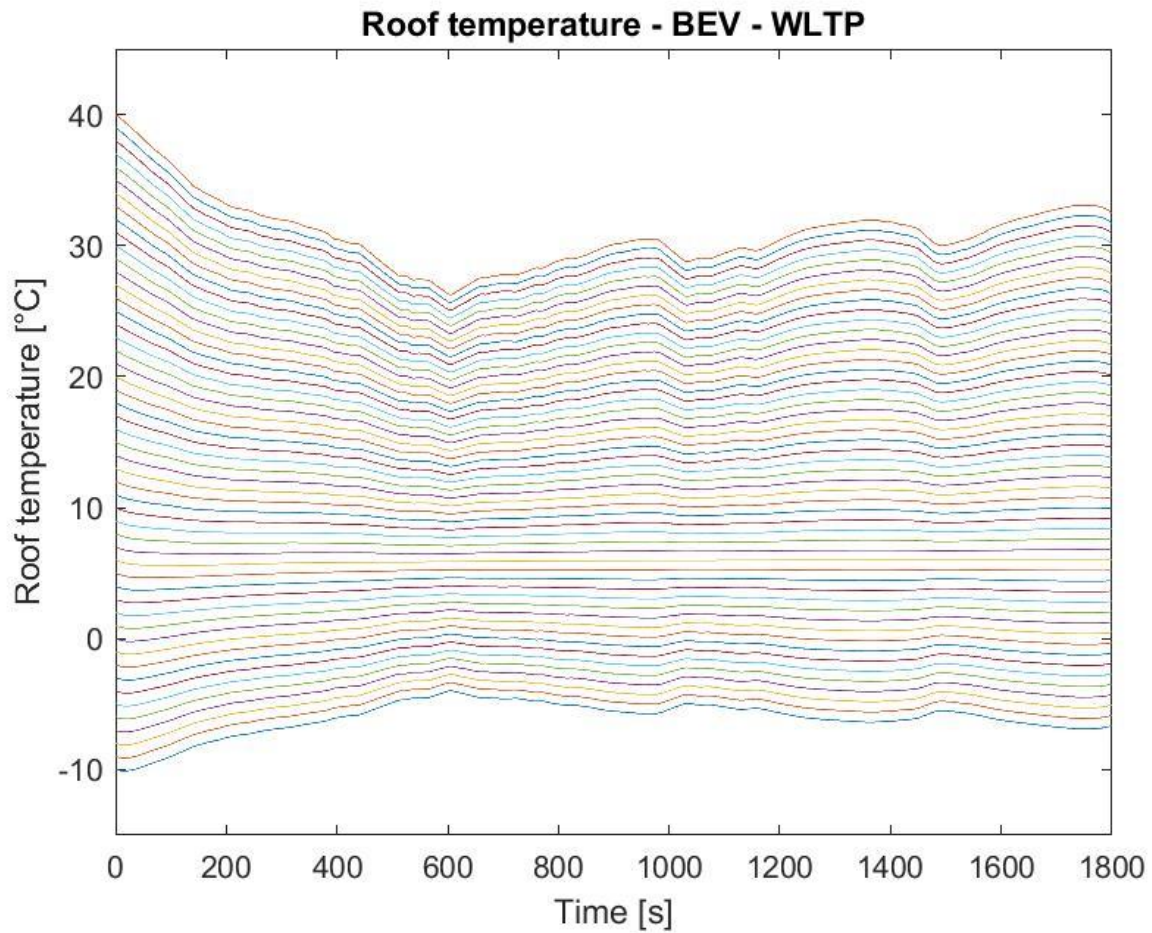


Figure 31. Roof temperature trends in case of a BEV in the WLTP cycle.

Figure 31 represents the temperature trends of the external shell of the roof. They are slightly similar to the doors' case, except for some greater temperature variations especially during cooling. These greater variations are due to the fact that less thermal resistances were considered with respect to the doors, thus this led to a higher heat exchange.

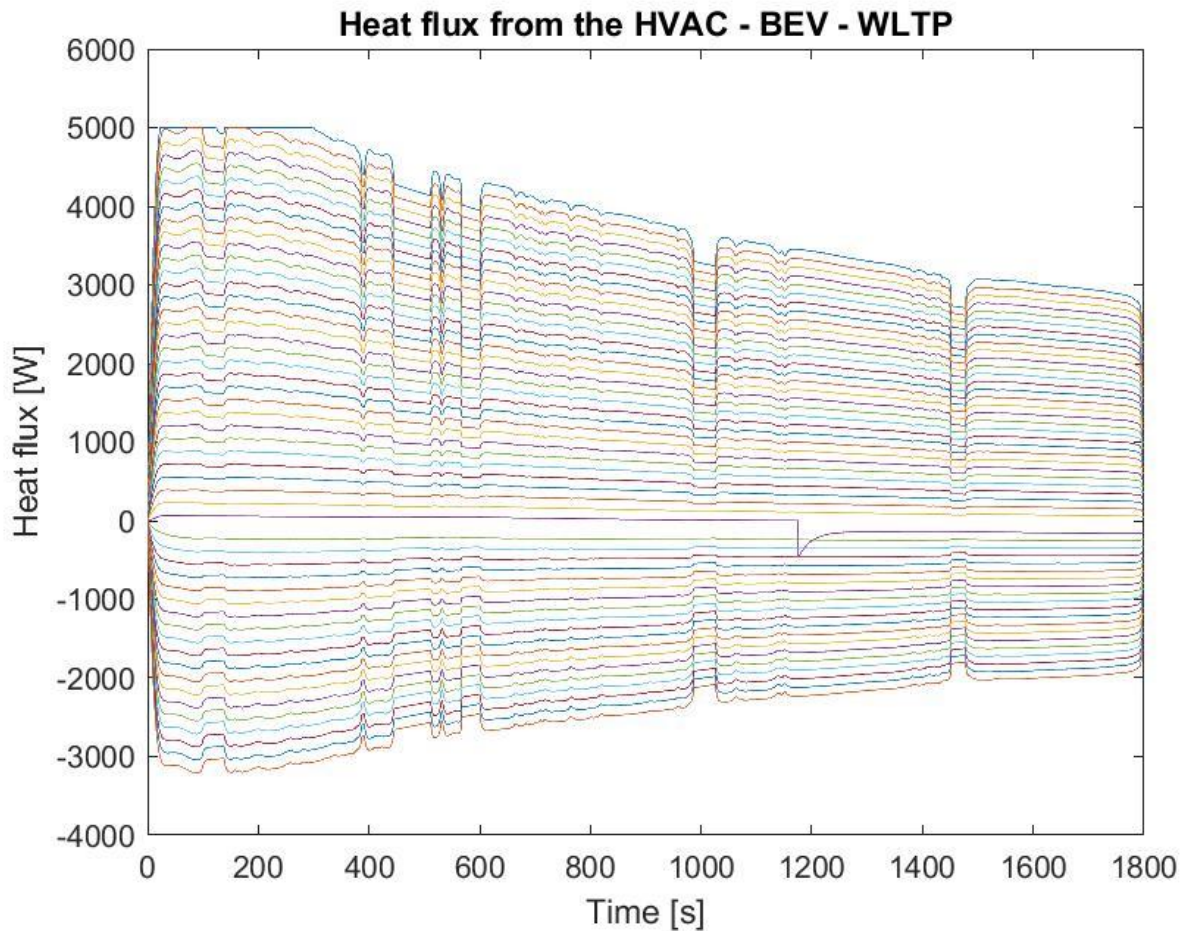


Figure 32. Heat fluxes along time in case of a BEV in the WLTP cycle.

The heat flux generated by the HVAC system is represented in Figure 32. It is clear the distinction between heating phases, with positive heat fluxes, and cooling phases, with negative heat fluxes. Moreover, it is clear also the initial phase where there is a peak in power demand, equal or close to the maximum power available, and the following phase, where the energy demand decreases. Due to the PI controller, every condition considered has an overall trend almost proportional to how much the desired temperature is far from the actual temperature present in the cabin. The quite important oscillations present are due to the car velocity variations during the driving cycle. It can be noticed also a sudden reversal of the heat flux sign in one specific condition, when the starting temperature is equal to the desired one. In this case both the solar radiation acting on the car and the humidity level are responsible for a very low power demand which in particular cases can make the inside temperature oscillate around the objective one and so causing the reversal of the heat flux, from positive to negative.

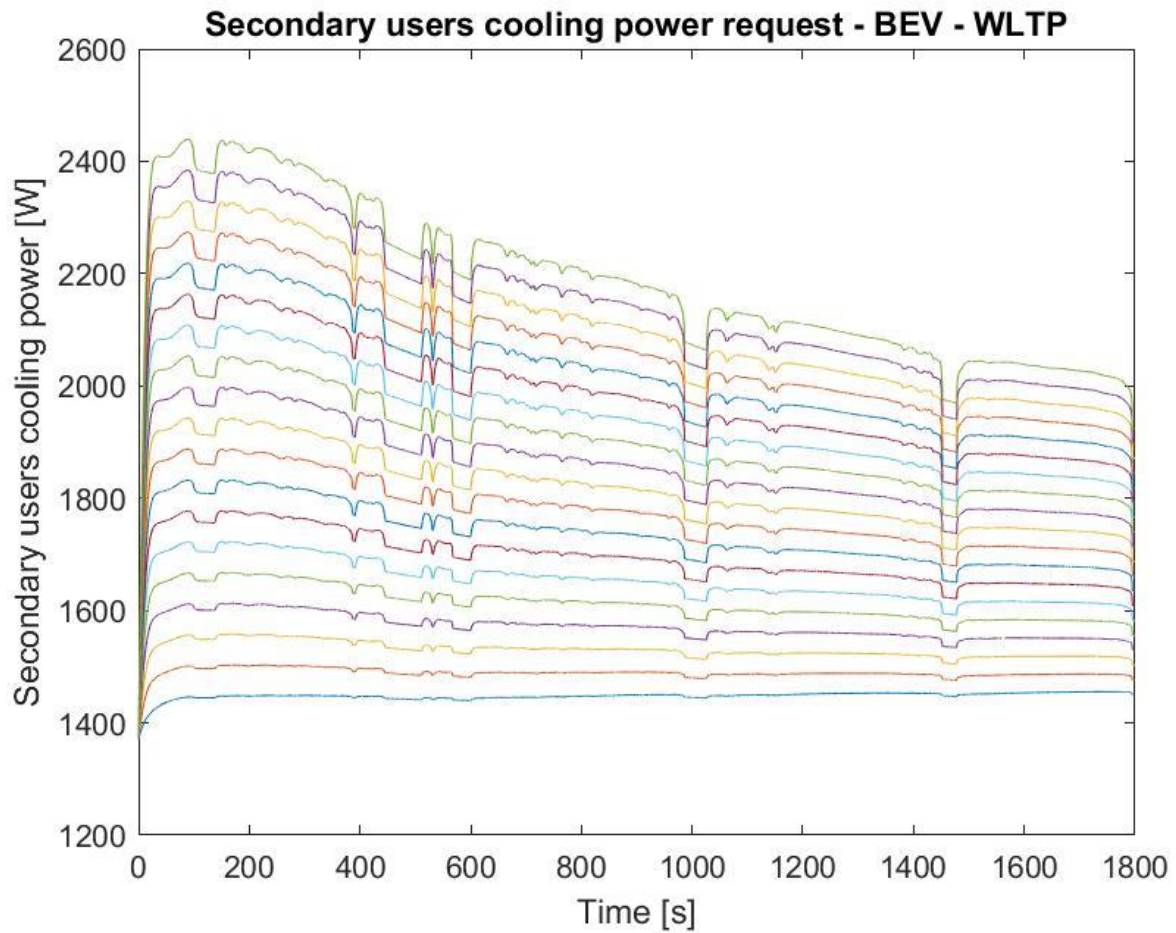


Figure 33. Secondary users electrical power demand for cooling, versus time in case of a BEV in the WLTP cycle.

In Figure 33 the electrical power demands for the A/C is plotted. The trend is equal and opposite to the heat fluxes case, while the values are lower, in absolute value, since to obtain the electrical power, the heat flux values were divided by a COP higher than 1.

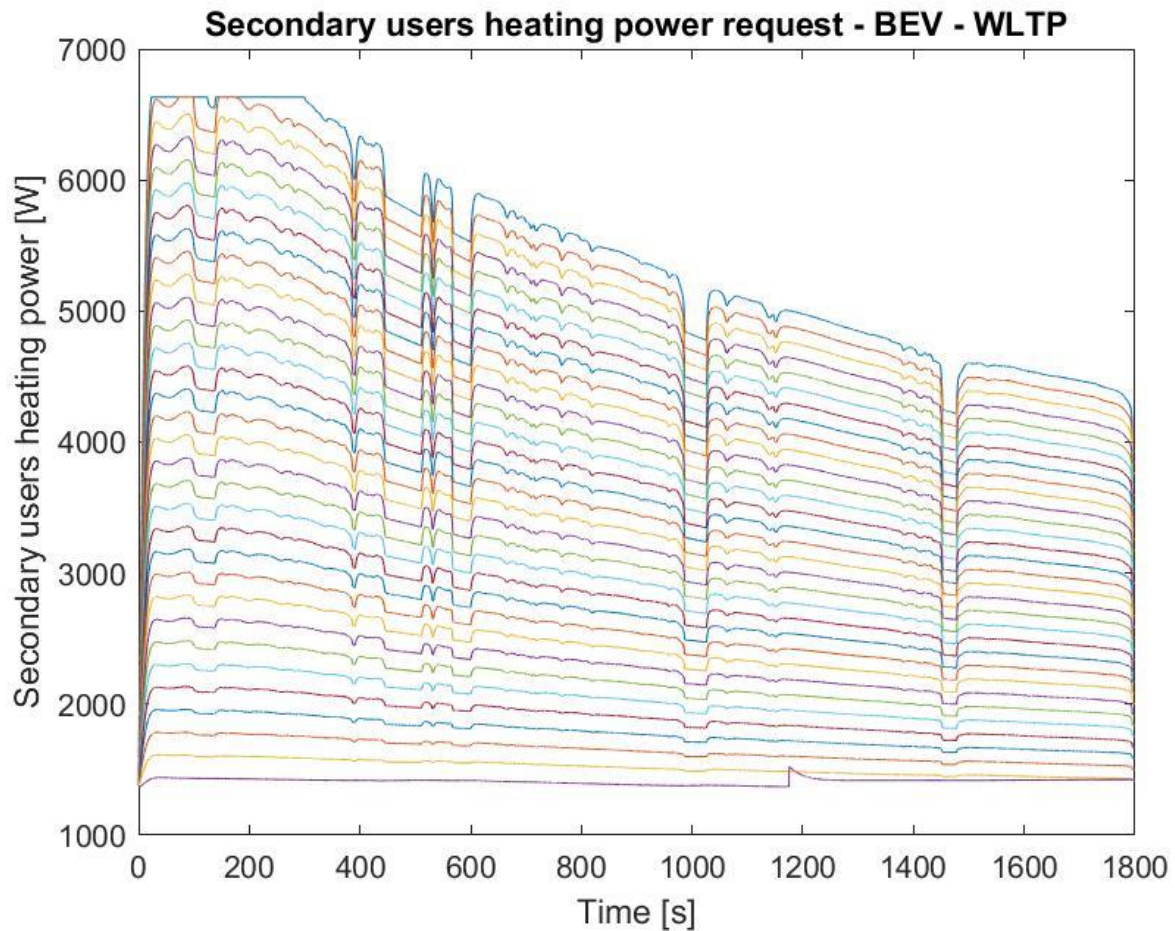


Figure 34. Secondary users electrical power demand for heating, versus time in case of a BEV in the WLTP cycle.

In Figure 34 the electrical power demands for the PTC element is plotted. The trend is equal to the heat fluxes case, while the values are higher, since to obtain the electrical power, the heat flux values were divided by an efficiency smaller than unity. It can be clearly seen the reaching of the limit condition in case of extreme temperature. It is important to remember that these results include not only the HVAC system, but also a certain number of constant loads, described in detail in Section 1.2. For what concerns, instead, the condition at 21 °C, it is possible to see a peak in electrical demand around 1200 s, corresponding to the reversal in the sign of the heat flux, as already discussed for Figure 32. This condition means a deactivation of the PTC element and an activation of the A/C.

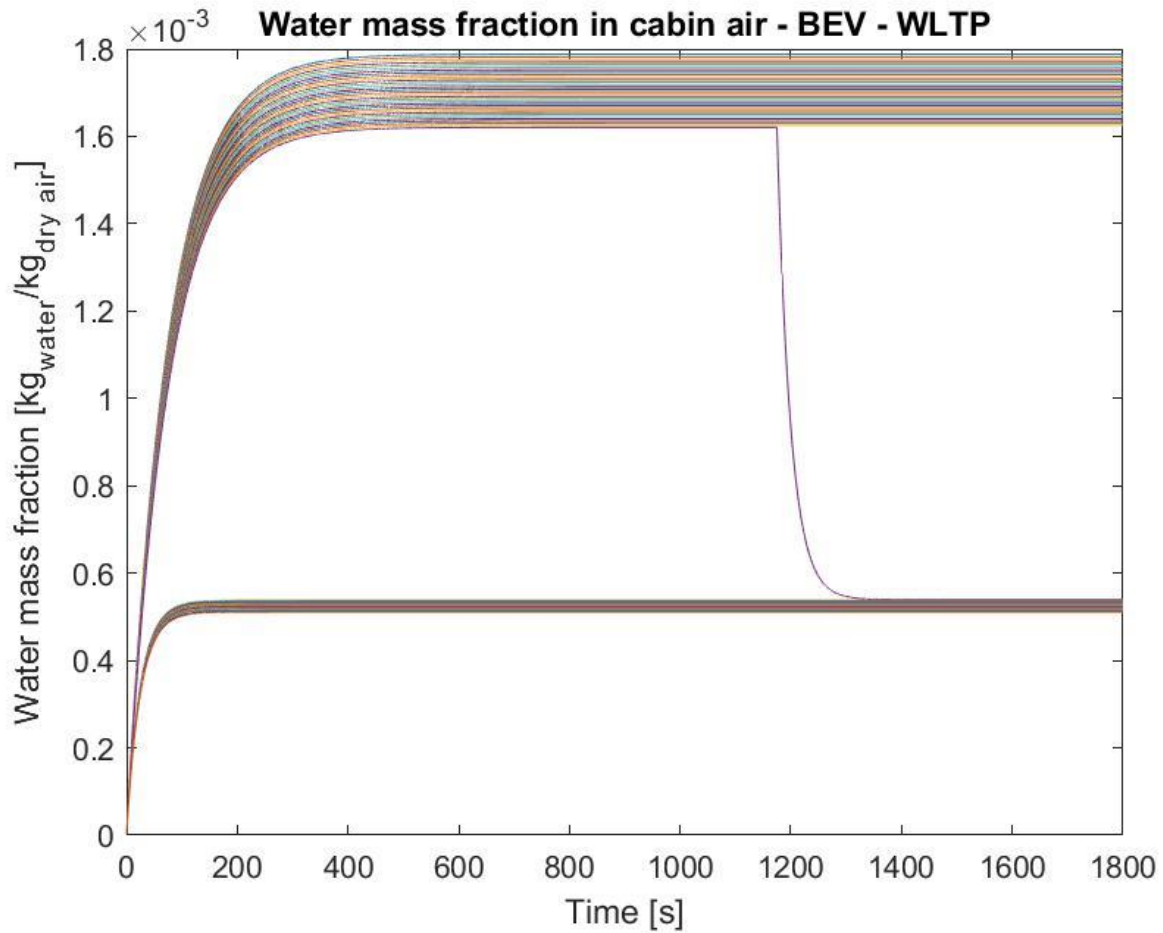


Figure 35. Water mass fraction trends in case of a BEV in the WLTP cycle.

The trends of the water mass fraction in air can be seen in Figure 35. The two clearly separated “groups” of lines represent the two phases: heating phase on top and cooling phase on bottom. This big difference is due to the dehumidification effect acting when A/C is on, hence lowering the moisture level by one order of magnitude. Anyway, in both cases, the values reach a steady-state condition after a null starting point. It is worth to remember that the humidity sources are just the external environment and the human being inside the car. Noteworthy is the sudden change occurring when the starting condition is equal to the desired temperature, situation already discussed earlier in this Chapter: after a certain period of time the HVAC system switches between PTC and A/C, thus activating the dehumidification, leading to a reduction of the moisture level in the cabin air.

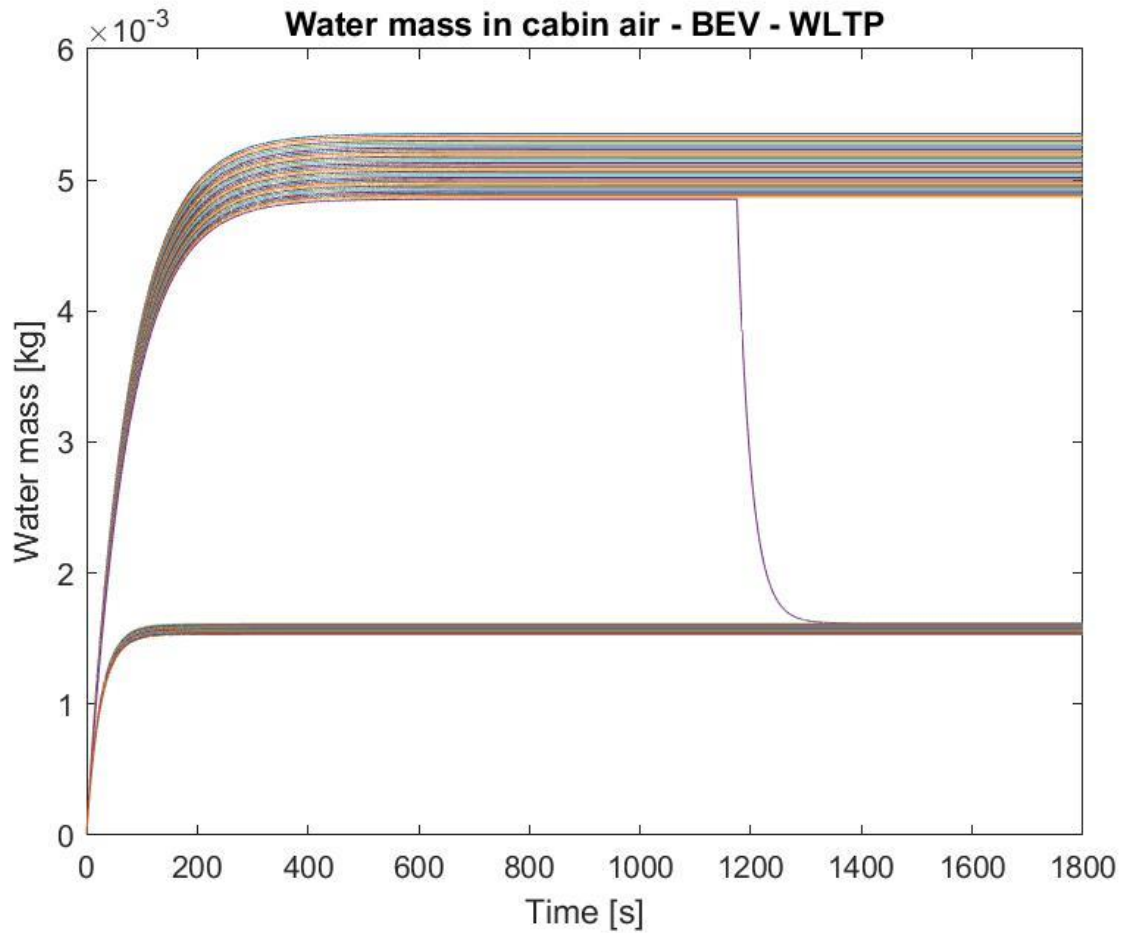


Figure 36. Water mass trends in case of a BEV in the WLTP cycle.

For sake of completeness, in Figure 36 the water mass in the air is represented. The trends are, of course, exactly equal to the water mass fraction ones, while the values are obviously different. It must be noticed that in this case the sultry limit of $13 \frac{g_{water}}{kg_{dry air}}$ is never reached.

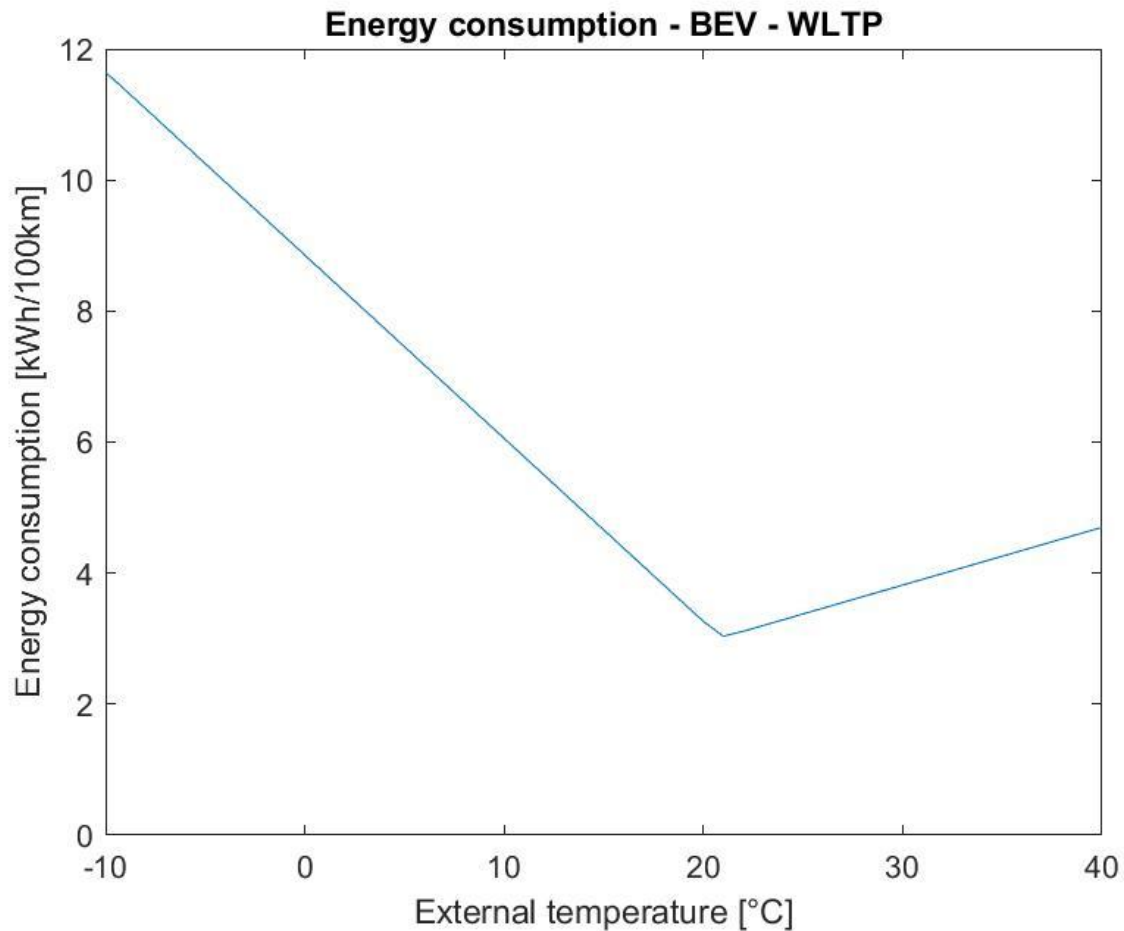


Figure 37. Energy consumption for only secondary users in case of a BEV in the WLTP cycle.

The most important outcome of this work is plotted in Figure 37. In fact, this image reports the energy consumption, in kWh/100km due to only secondary users acting in the vehicle, along the chosen cycle, the WLTC in this case. From this graph it is possible to get a certain number of information. First of all, the heating phase, comprising all conditions below the desired temperature of 21 °C, needs more energy with respect to the cooling phase. This can be understood just by looking at the different slopes between the parts. This difference in energy demand is mainly due to the different efficiencies of the two considered systems: PTC for heating has an efficiency of 0.95, while A/C for cooling has a COP equal to 3. It can then be noticed that the minimum of this curve is found at 21 °C, which is exactly the objective temperature. This should not be surprising, since the only energy demand in that case is the one necessary to maintain the same condition along the cycle. However, the minimum is not a fixed point, since there are parameters which can contribute to move it on the left or on the right of the x axis, such as solar radiation, external humidity and number of passengers. Finally, it can be seen from the plot in Figure 37 that the function is piecewise linear: strictly decreasing from -10 °C to 20 °C and strictly increasing from 21 °C to 40 °C. Between 20 °C and 21 °C, the function is again decreasing, but with a slightly less steep slope.

It should be noticed that this result is very similar to what presented in the literature review, in Section 1.1, especially in Figure 1 and Figure 2. This can be considered as a sort of validity proof, since no other experimental data are present.

In case of an Internal Combustion Engine Vehicle, here below the main variations with respect to the BEV are presented. As a matter of fact, since the values of maximum heating and cooling power are equal, the only differences are found in the field of energy consumption, as can be seen in Figure 38. As already anticipated, it must be said that the results reported here consider only a theoretical energy consumption in kWh/100km, without considering, in this case, the conversion in fuel consumption, more fitting to ICEVs.

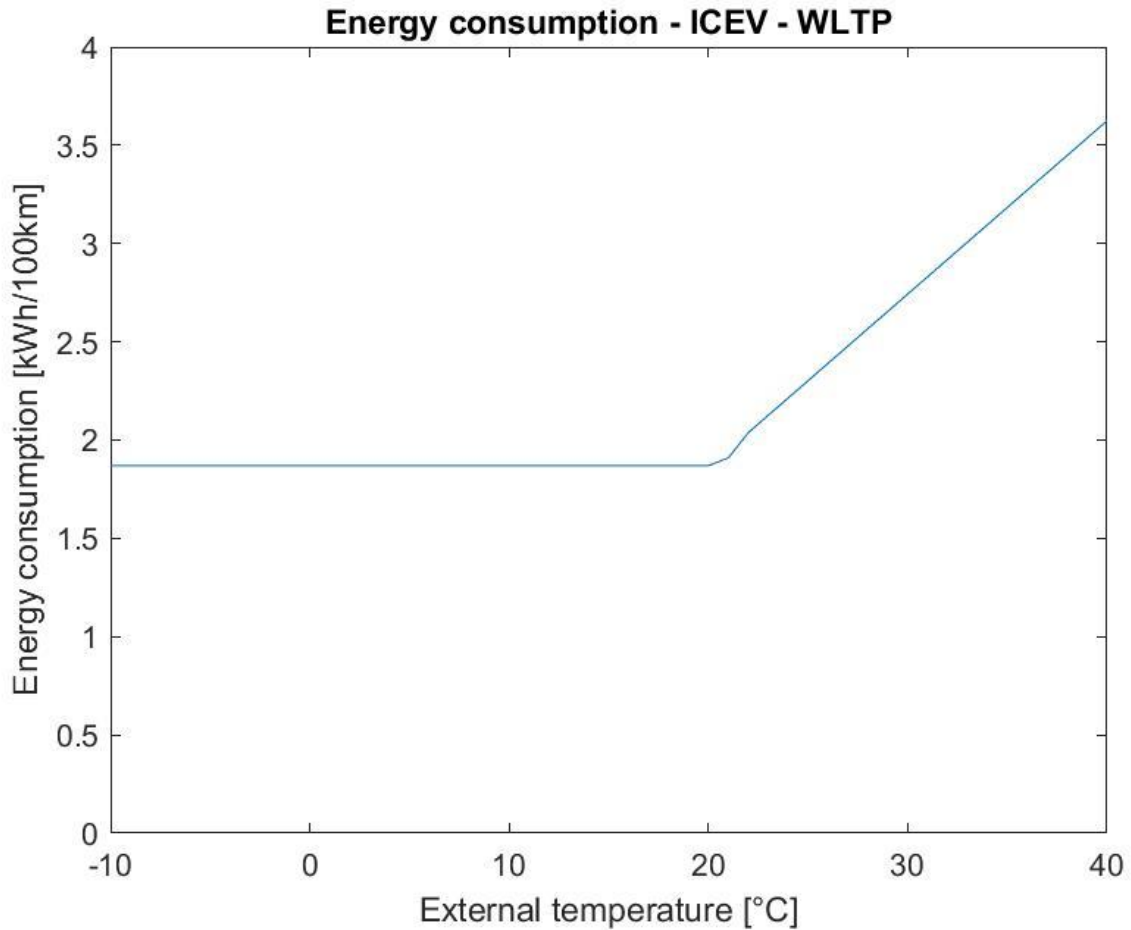


Figure 38. Energy consumption for only secondary users in case of an ICEV in the WLTP cycle.

Since the heating phase is performed by the engine waste heat, no energy is consumed apart from the previously described constant loads. Hence this part is described by constant values of energy consumption from -10 °C up to 20 °C. Cooling, instead, is performed by the A/C, so an increasing demand with increasing temperature is expected, as depicted in Figure. The reason why at 21 °C the demand is higher than the minimum is to be found in the influence of solar radiation and humidity level.

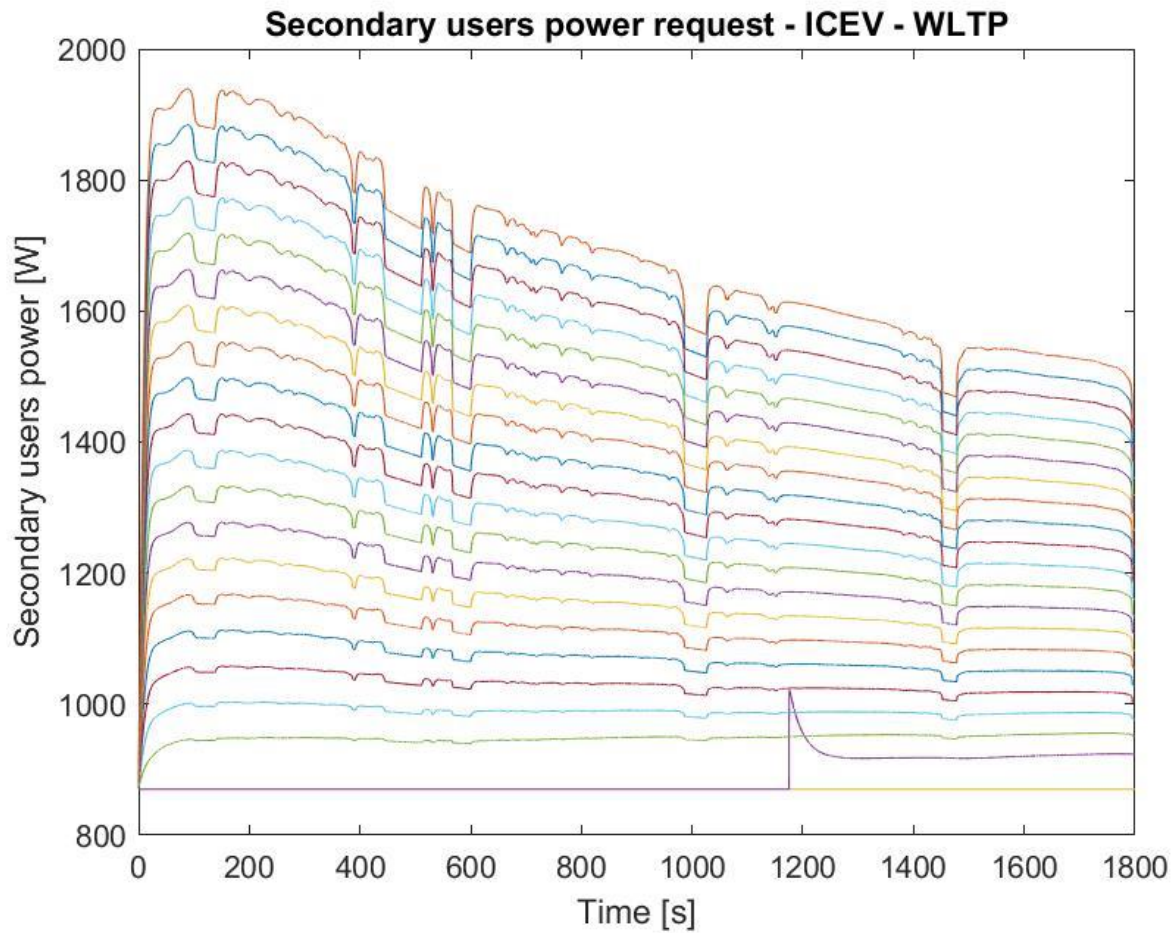


Figure 39. Secondary users electrical power demand versus time in case of an ICEV in the WLTP cycle.

In Figure 39, representing secondary users' power demand along the cycle, it can be noticed the straight lines at the bottom representing the heating phase, when only constant loads consume energy. Also in this case, it is possible to find a peak in power demand in case of starting temperature equal to desired one, due to the sudden activation of the HVAC system because of the influence of solar radiation and humidity.

4.4.3.2 NEDC

In this section only the most relevant results related to the New European Driving Cycle are presented, in order to have the possibility to make a comparison with the other cycles analyzed.

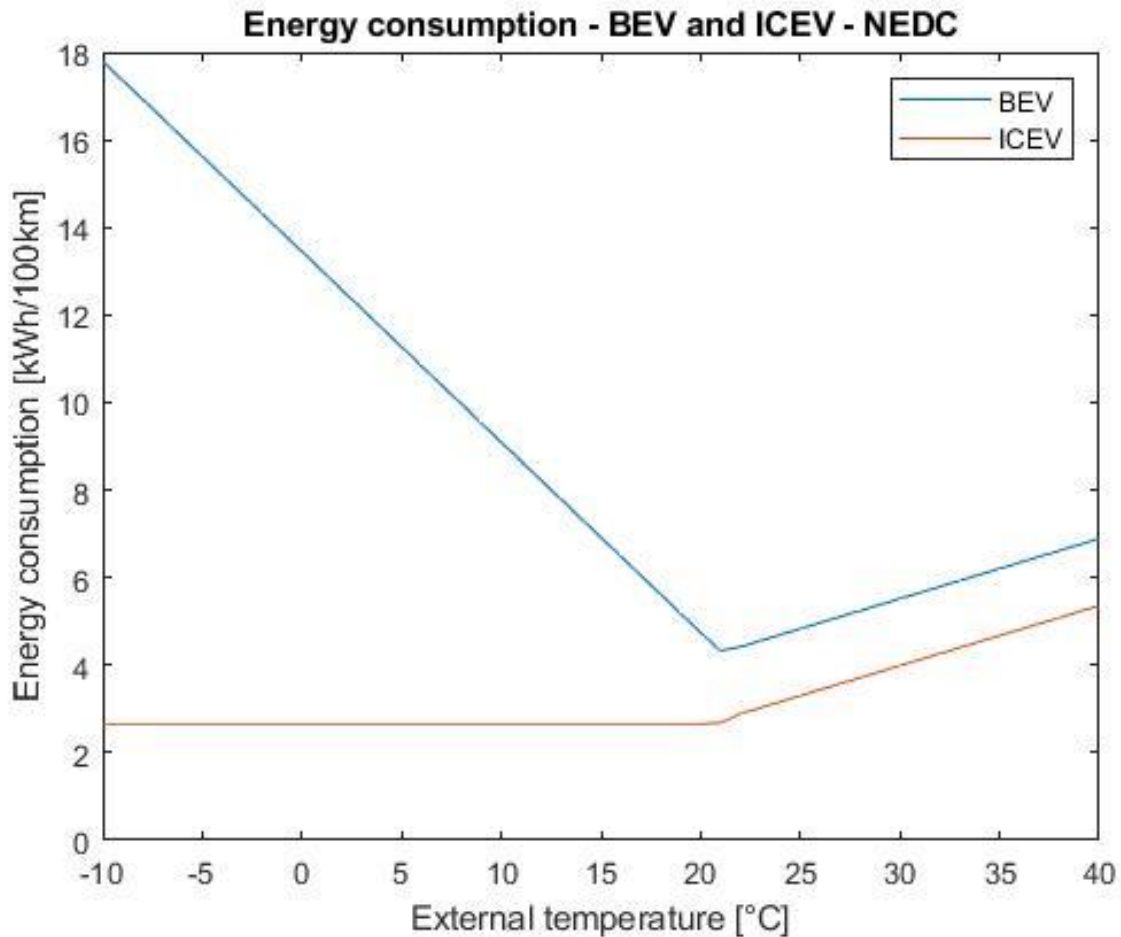


Figure 40. Energy consumption for only secondary users in case of BEV and ICEV in the NEDC cycle.

In Figure 40 the energy demand of secondary users is plotted for a BEV and an ICEV. About the former, with respect to the WLTP case, the final values are always higher, while the minimum is again at 21 °C. The fact that the energy consumption, expressed in kWh/100km, is higher is because the NEDC cycle is much shorter than the WLTP, while the HVAC system tends anyway to reach the objective temperature as soon as possible, often using the maximum power available at the beginning, when the temperature difference is higher. For this reason the final ratio between consumption and distance has higher values. A much smaller effect is played also by the different car velocities between the cycles.

For what concerns the ICEV, again the results are very similar to the WLTP case, but with higher values for the reason just explained.

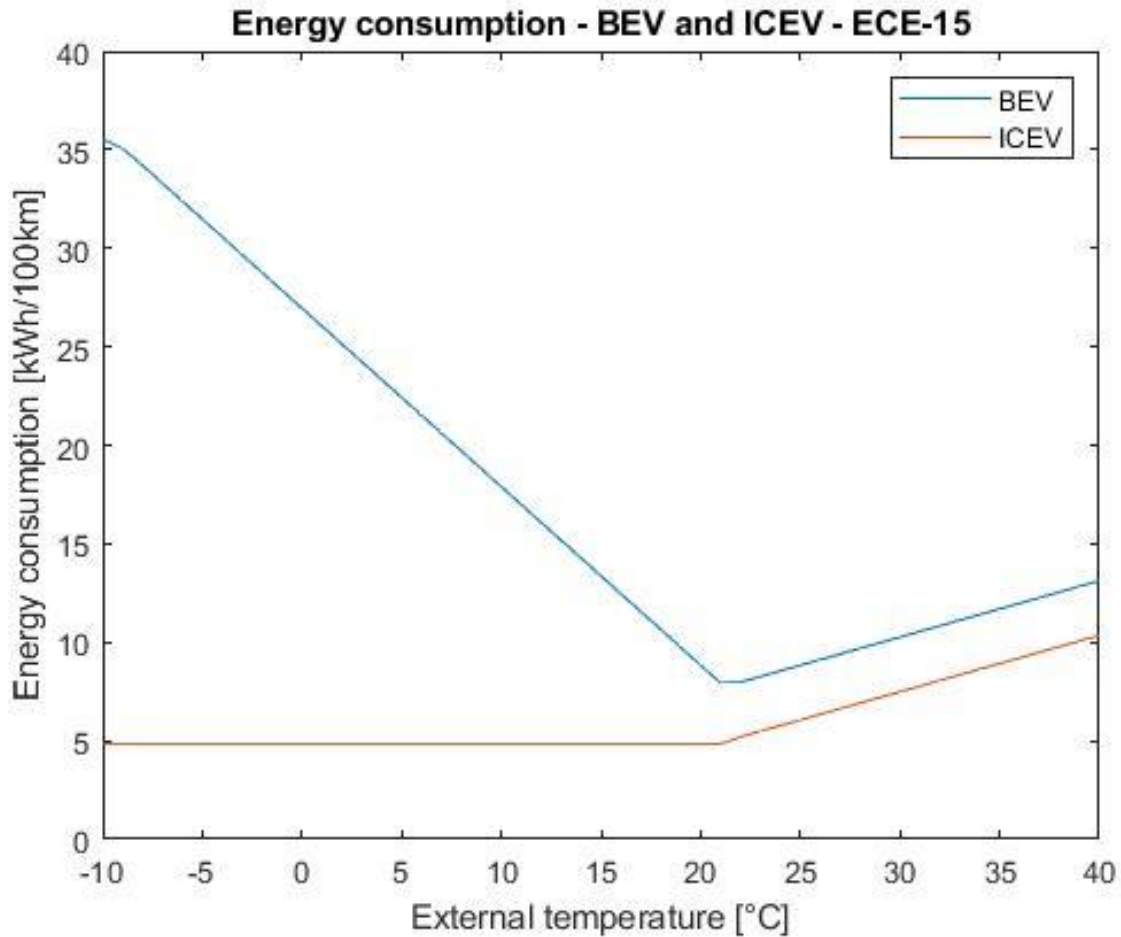


Figure 41. Energy consumption for only secondary users in case of BEV and ICEV in the ECE-15 cycle.

In case a much shorter cycle is considered, such as ECE-15, Figure 41, the results that can be found for BEV have again a trend similar to the ones related to the previous cycles, but with much higher values for the reasons explained in the case of the NEDC cycle. The minimum is, once more, found at 21 °C.

The same outcome applies also to ICEVs, on the same plot.

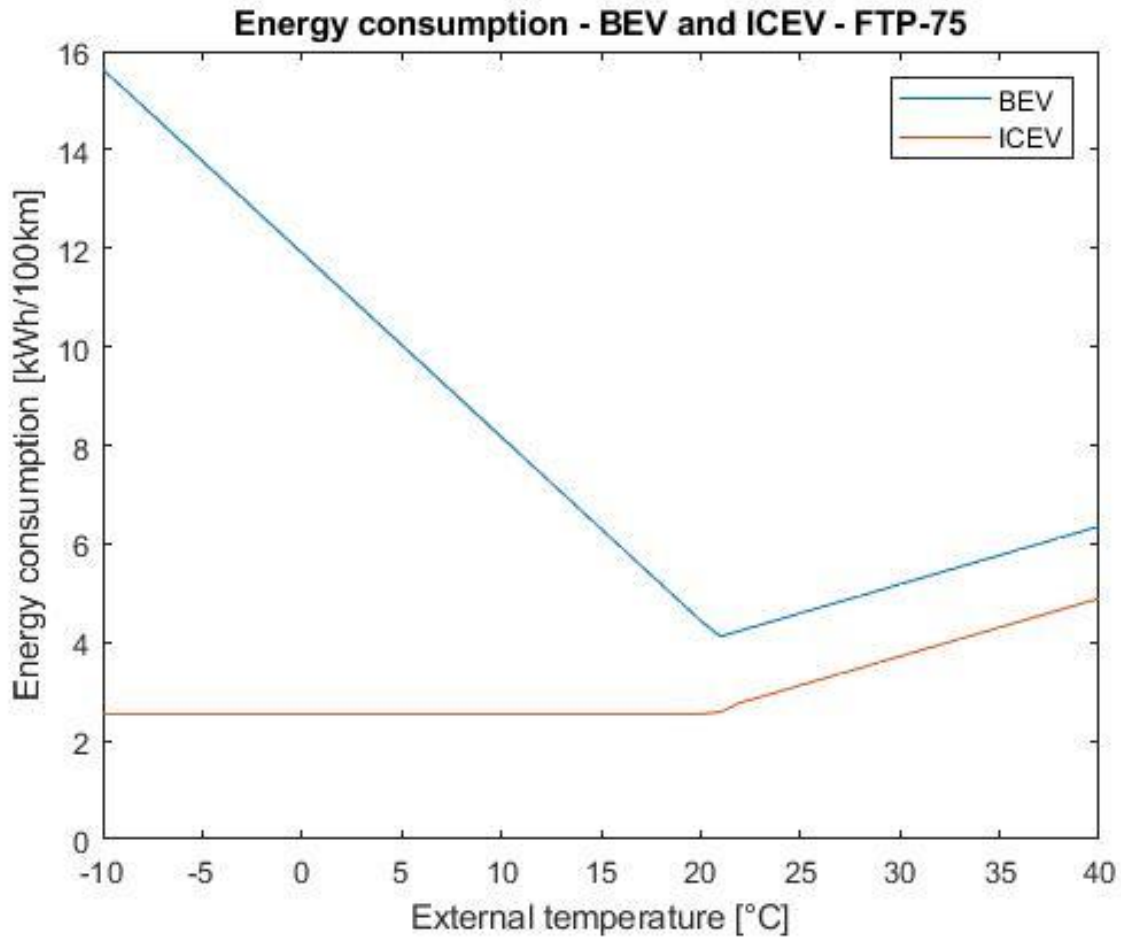


Figure 42. Energy consumption for only secondary users in case of BEV and ICEV in the FTP-75 cycle.

In case of the FTP-75 cycle, Figure 42, the outcome of the simulation for BEV is similar to the others but the results deserve a further investigation. This cycle, in fact, has a duration slightly higher than WLTP, but length, maximum speed and average speed are much lower. These differences lead to the conclusion that the energy consumed by secondary users, referred to a 100 km basis, is higher than the WLTP case, but still lower than NEDC and, of course, ECE-15.

The same reasoning just made applies also to the ICEV case, on the same figure.

5 Integration in the optimization environment

What has been described so far is able to perform computations on its own comprising all temperatures and all concepts considered, for every desired cycle given as input, even considering multiple cycles at a time. Nevertheless, since the final scope of this study was to compute the overall energy consumption of different concepts, so considering also the energy needed by primary users, which is the one necessary to move the vehicle, the model for secondary users consumption was integrated in an already present optimization environment able to calculate the electrical and petrochemical energies consumed by primary users over a whole driving cycle and, moreover, also able to find the minimum total CO₂ for the chosen concept and cycle for the whole life cycle of the car. Anyway, in this analysis, the focus was only on the energy consumption, without considering CO₂ emissions. In this way it was possible, within the same simulation, to loop over different powertrain concepts, different cycle lengths and different external air temperatures, in order to finally calculate the total energy demand for each case and thus to compare the different results obtained.

The integration of the secondary consumption model with the primary one was performed just by including inside the previously described *for* loops all the lines of code related to the primary users calculation. In this way primary and secondary energy consumption calculations are carried out simultaneously and interact with each other. In particular, in case of a PHEV, the secondary energy consumption depends on the operating strategy because a different heating technology is used when driving purely electric or with the combustion engine and it increases with increasing electrical driving percentage, since less waste heat is available. Thus, a higher demand in electric energy for heating results in a reduced electric range, which influences the primary energy consumption because of a different operating strategy.

It has to be said that, in order to simplify the calculations, it was decided to consider only the mean value of secondary users' power consumption over each cycle and not the whole trend over time, like it is possible to see in the previous results. Finally, it was chosen also to consider only a limited number of temperatures, since in many cases the trend of energy consumption has a linear behaviour, as shown in the previous results: -10 °C, 0 °C, 10 °C, 19 °C, 20 °C, 21 °C, 30 °C and 40 °C.

5.1 Description of the optimization environment

The optimization environment is a MATLAB model developed at the Institute for Mechatronic Systems in Mechanical Engineering at TU Darmstadt. It consists of a primary energy demand modelling based on a backwards approach for the longitudinal dynamics, which uses an equation for the driving resistance, including air drag, road slope resistance, rolling resistance and acceleration force, to compute the required torque and rotational speed at the wheels for each considered driving cycle and vehicle parameters. Moreover, in order to obtain an accurate estimation of the required energy demand and of the losses in the machines, as a function of torque and speed, the modelling of the drivetrains is based on efficiency maps: a Brake Specific Fuel Consumption (BSFC) map is used for the ICE while a an efficiency map is considered for the electric machine (EM). For the multiple speed transmissions (ICEV and PHEV) and the single speed transmission (BEV), constant efficiencies are defined and, in the same way, the battery is modelled with a

constant charging and discharging efficiency. This approach provides a good tradeoff between consumption estimation accuracy and computational performance.

The Equivalent Consumption Minimization Strategy (ECMS) is applied to determine the optimal operating points of the traction machine for every time step [18]. The ECMS is applicable for all drivetrain concepts in the same way, which further enhances the comparability of the results. The cost function J as shown in Equation (42) quantifies an equivalent fuel mass flow rate of petrochemical and electrical energy and is minimized at each time step of the simulation [19]. For that purpose, all possible combinations of ICE and EM power that satisfy the current traction demand of the driving cycle are calculated. The equivalent cost factor s is used to define a cost ratio between electrical energy and petrochemical energy. For the ICEV and BEV the cost function simplifies since they can only use one energy source. For the PHEV it is generally desired to maximize the use of electrical energy, which is done by tuning the equivalent cost factor s , such that the battery is depleted at the end of a trip.

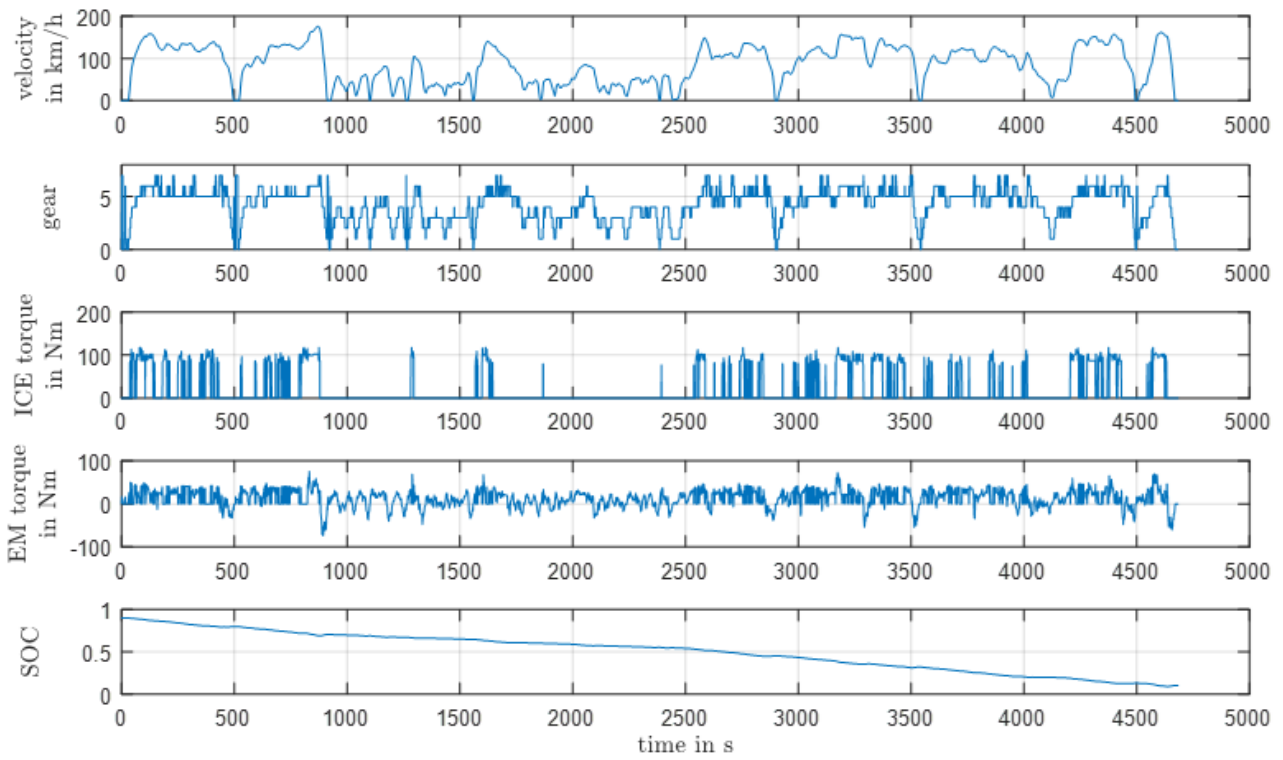
$$J = b_e P_{ICE} + s \frac{1}{LHV} \frac{1}{\eta_{EM} \eta_{batt}} P_{EM} \quad (42)$$

The choice of the gear is the only degree of freedom for the ICEV to adjust the operating point of the engine in order to minimize consumption. In the case of the PHEV, gear choice and torque split between ICE and EM have to be determined, increasing in this way the computational effort. The torque split choice offers advanced functionality like load point shifting to potentially increase the overall efficiency. The main characteristics of the considered drivetrain concepts are summarized here below in Table 5.

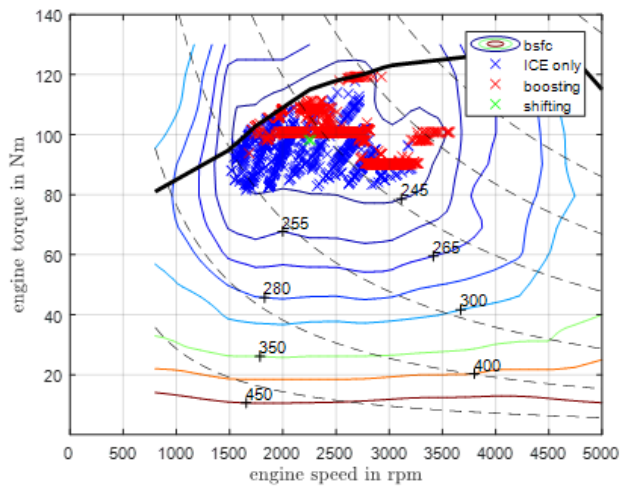
Table 5. Main parameters of the defined vehicle drivetrain concepts.

| | ICEV | BEV | PHEV |
|--------------------------------|-------------|------------|-------------|
| ICE power [kW] | 96 | - | 85 |
| EM power [kW] | - | 300 | 120 |
| Battery capacity [kWh] | - | 60 | 20 |
| Number of gears | 7 | 1 | 7 |
| Total mass [kg] | 1109 | 1635 | 1358 |
| Necessary starting torque [Nm] | 1656 | 2442 | 2028 |

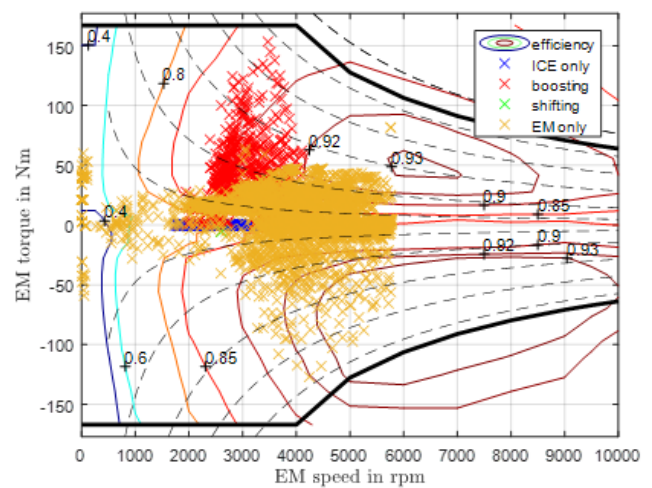
In Figure 43 it is possible to see the exemplary simulation results of the PHEV for one of the representative driving cycles described in the next Section. As stated in the previous Chapter, the gear choice and torque coordination is performed by the ECMS. The operating strategy chooses the operating points to maximize the use of electrical energy which can be seen in the state of charge (SOC) curve. The SOC drops from 0.9 to 0.1, which have been defined as the maximum and minimum SOC, respectively. The operating points are chosen such that the ICE is mainly used in an area around peak efficiency. For longer trips, the ECMS would decrease the use of electrical energy per km to distribute the same amount of electrical energy stored in the battery over a longer driving distance in order to completely deplete the battery. In case of short trips, an almost solely electric operating mode is chosen and the ICE is only started if the EM is not able to satisfy the driving power demand by itself. Additionally, the operation strategy of the vehicle includes the secondary energy demand for the choice of the operating points.



(a)



(b)



(c)

Figure 43. Exemplary outputs of the primary consumption model for the PHEV on a representative driving cycle with a trip distance of 100 km. In figure (a), the time-resolved graphs of vehicle velocity, gear, ICE and EM torques, SOC are shown. In figure (b) and (c), the chosen operating points of ICE and EM are shown in the BSFC and efficiency maps, respectively.

5.2 Driving cycles for the evaluation of vehicle's consumption

For this more complete analysis it was decided to not take into account the usual type-approval driving cycles considered before. This decision was due to the necessity of evaluating real life driving conditions and overcoming the limits imposed by the classical cycles. In fact, vehicles are always evaluated in predefined procedures with static driving cycles. This procedure contains fixed system boundaries and conditions under which the vehicles consumptions and emissions are determined. However, it is not suitable to describe the various conditions present in a real life driving, depicted in Figure 44 (a) and (b), so it cannot be considered an objective indicator for reducing car emissions. For this reason, since the scope of this work is a simulative analysis and comparison of different drivetrain concepts regarding the sensitivity of their consumption under varying operating conditions, a new set of cycles was created for this purpose.

As it is possible to understand analyzing the results in Chapter 4.4.3, the length of each driving cycle is of fundamental importance for the average consumption referred to the distance, since the cabin has to be heated up from the ambient temperature to the desired cabin temperature for each single trip.

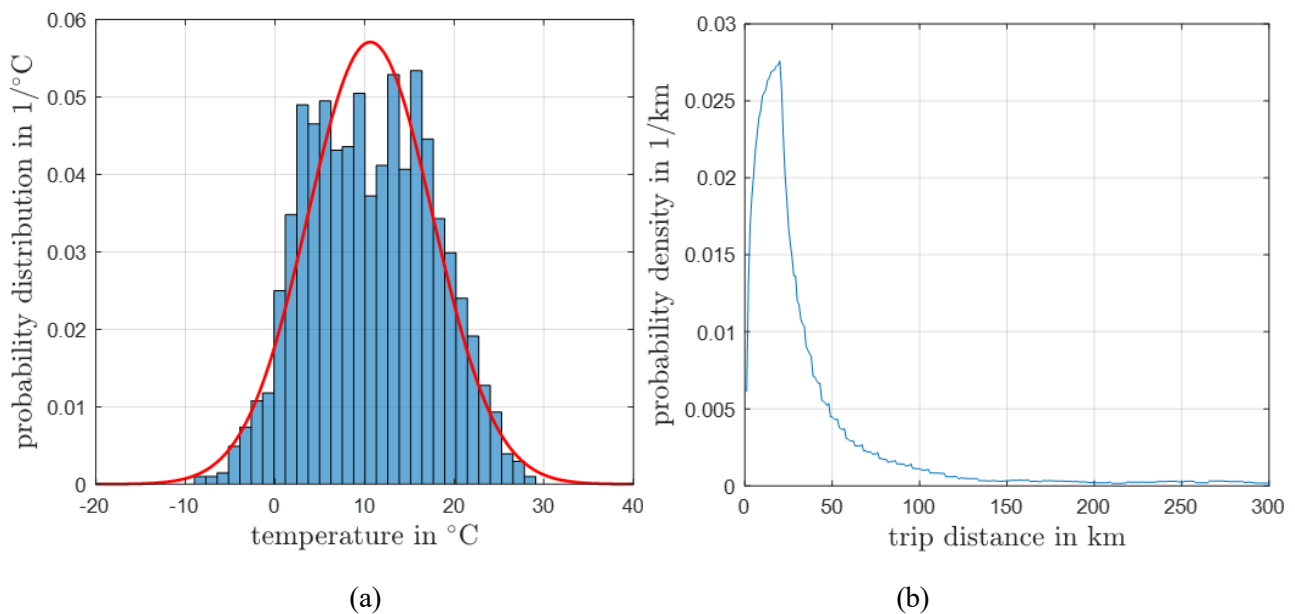


Figure 44. Distribution of the daily mean ambient temperatures measured in Darmstadt by “Deutscher Wetterdienst” during the period from January 2013 until January 2017 with a fitted normalized distribution in (a) and distribution of trip distances of passenger cars from a testing fleet within Germany in (b).

For this reason, to make a meaningful comparison between the computed energy demands as a function of trip distance, it is necessary to create a driving cycle which can be considered equivalent for each distance taken into account. Unfortunately, repeating multiple times a type-approval cycle like the WLTC in order to get a longer distance just limit the driving profile to integer multiples of the base cycle without being representative of a real driving situation. Hence, it is necessary to generate driving cycles with different trip distances that are representative for a given driving profile. Thus, the approach introduced in [20] is applied to synthesize driving cycles of different trip distances with the property that all cycles represent the respective overall driving profile.

To create a realistic real world driving profile, a database is built from GPS tracks provided by *OpenStreetMap* [21]. The region considered is a large area around the cities of Darmstadt and Frankfurt in

Germany, in order to represent a metropolitan area including urban, rural and highway driving. To enhance the quality of the generated database, all tracks are checked automatically and manually for physical plausibility and to guarantee that non-vehicle GPS tracks are omitted. During this process, only around 5% of the tracks were found to be of sufficient quality. Furthermore, a maximum velocity of 200 km/h is imposed to exclude extremely sportive driving from the investigation. An overview over the determined real-world driving profile is given in Figure 45. The driving profile is composed of 55 hours of driving and a total traveled distance of around 16000 km. The generated real-world driving profile predominantly consists of idling and cruising phases. As expected, the highest accelerations occur at lower velocities while the maximum acceleration decreases with raising velocities.

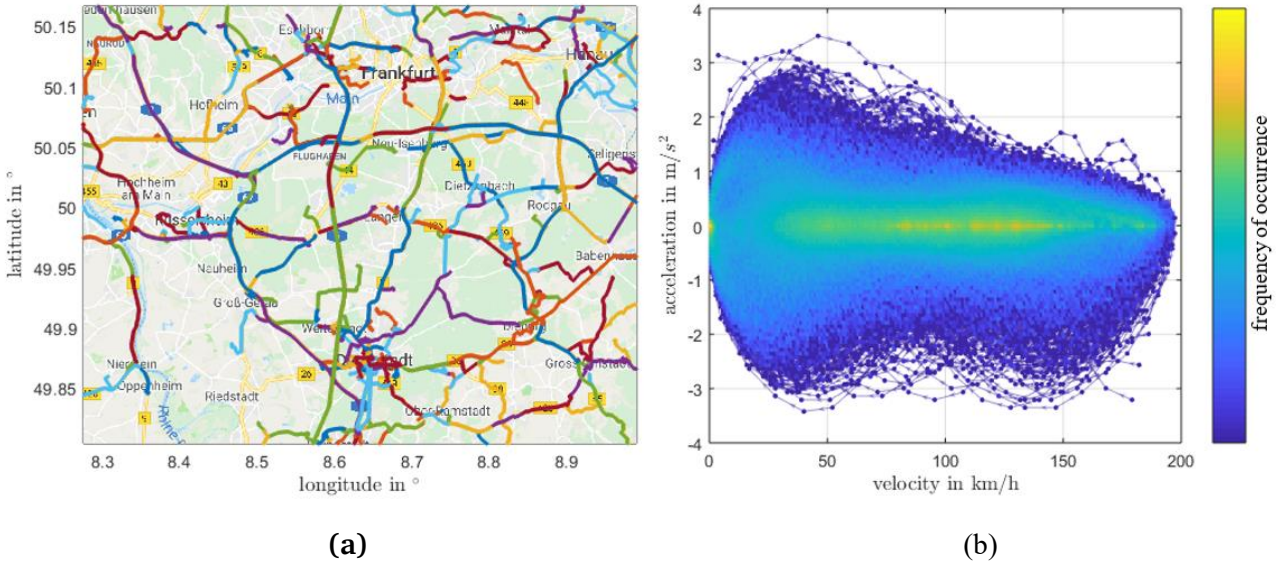


Figure 45. Database of driving data used for this study. In (a), the considered tracks from the region around the cities of Darmstadt and Frankfurt in Germany are illustrated. In (b), the occurrence frequency of driving states in the velocity-acceleration plane is plotted.

As discussed before, it is necessary to synthesize driving cycles with different trip distances under the requirement that all cycles are representative of the overall profile seen in Figure 45b. To quantify how well the cycles represent the overall driving profile, different criteria are defined to compare the characteristics of the cycles to those of the overall profile. From the state of the art, there is no consensus in literature which criteria should be used to guarantee a good estimation of the vehicle's energy demand. In general, it is recommended to first define a criteria set θ containing multiple single criteria θ_i to calculate the relative errors between the cycle and profile characteristics. Afterwards a mean error is determined that represents the quality of a single cycle. In this study a criteria set θ of six single criteria θ are applied which are:

- The mean velocity:

$$\theta_1 = \frac{1}{t_{end}} \int_0^{t_{end}} v(t) dt \quad (43)$$

- The variance of the velocity signal:

$$\theta_2 = \frac{1}{t_{end}} \int_0^{t_{end}} (v(t) - \theta_1)^2 dt \quad (44)$$

- The variance of the longitudinal acceleration:

$$\theta_3 = \frac{1}{t_{end}} \int_0^{t_{end}} (a(t) - \bar{a})^2 dt \quad (45)$$

- The normalized energy demand for the air drag over the evaluation time:

$$\theta_4 = \frac{1}{s_{tot}} \int_{t \in \tau_{acc}}^{t_{end}} v^3 dt \quad (46)$$

- The normalized energy demand for the rolling resistance over the evaluation time:

$$\theta_5 = \frac{1}{s_{tot}} \int_{t \in \tau_{acc}}^{t_{end}} v dt = \frac{s_{acc}}{s_{tot}} \quad (47)$$

- The normalized energy demand for the acceleration resistance over the evaluation time:

$$\theta_6 = \frac{1}{s_{tot}} \int_{t \in \tau_{acc}}^{t_{end}} \dot{v} v m dt \quad (48)$$

Table 6 shows the exemplary calculation of the overall error based on the six single criteria θ_i . Since the cycles are synthesized stochastically, results vary according to a certain probability distribution and can thus vary in their quality. Therefore, for each defined distance, 10000 cycles are synthesized and the best are chosen for further evaluation. This approach is shown in Figure 46. The best cycles for all distances have errors of less than 2 % when their properties are compared to the overall fleet profile with the criteria set θ .

Table 6. Exemplary calculation of the overall error of the best synthesized cycle at a trip distance of 80 km for all single criteria θ_i and the criteria set θ .

| Criteria | Profile | Single cycle | Error |
|------------|---------|--------------|--------|
| θ_1 | 23.067 | 22.987 | 0.3 % |
| θ_2 | 150.481 | 150.233 | 0.1 % |
| θ_3 | 0.2084 | 0.2105 | 1.0 % |
| θ_4 | 577.369 | 582.641 | 0.9 % |
| θ_5 | 0.584 | 0.587 | 0.5 % |
| θ_6 | 0.1223 | 0.1236 | 0.1 % |
| θ | | | 0.66 % |

Using the best cycles enables the comparison of different vehicle's consumptions as a function of trip distance since all the cycles are representative of the overall fleet profile. All the synthesized driving cycles

make almost equal demands on the vehicles concerning the velocity and acceleration distributions. Therefore, differences in the estimated consumption are almost exclusively caused by the power demand of secondary users that are dependent on ambient temperature and trip distance.

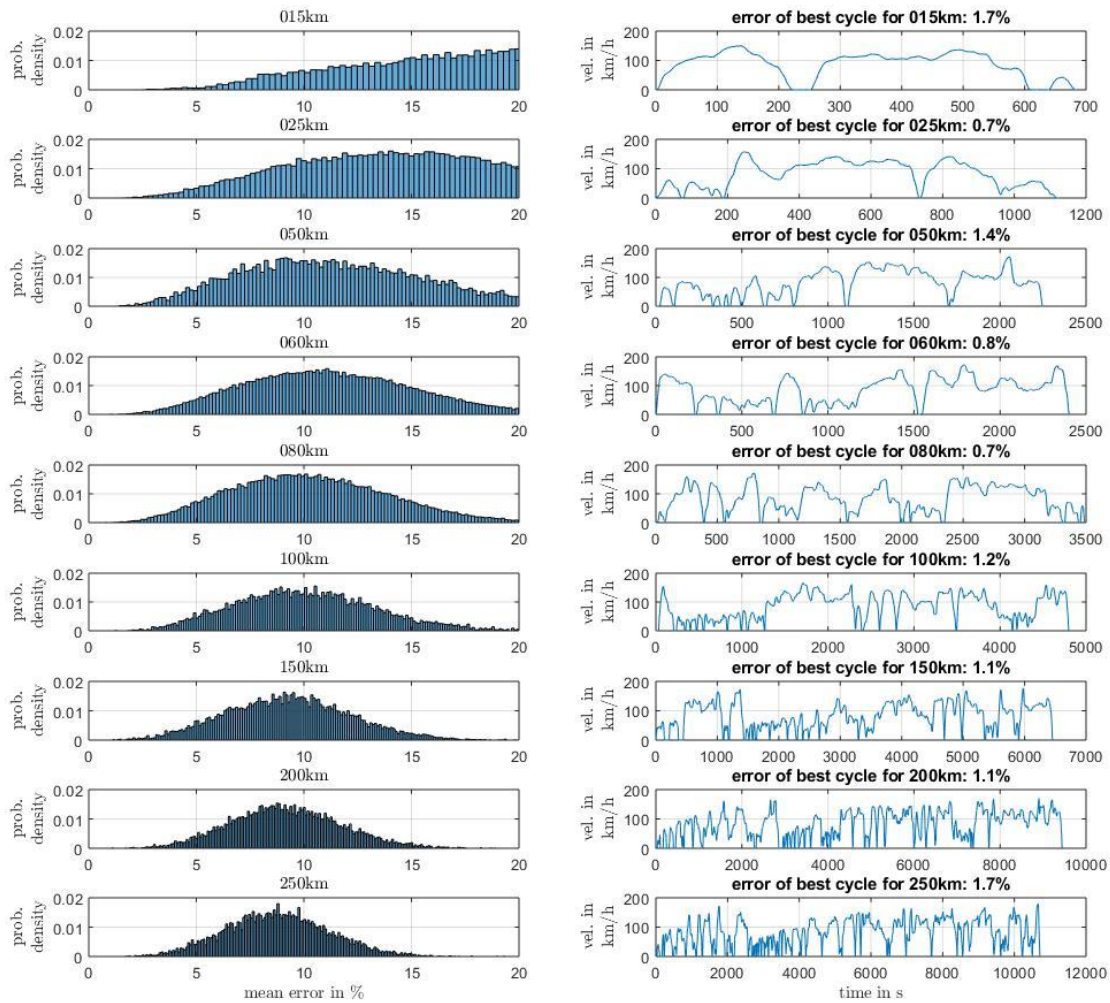


Figure 46. On the right, the best cycles and corresponding errors for each trip distance are displayed. On the left, the error distributions of synthesized cycles are shown. There is a bigger variation in cycle quality for shorter trips because it is more difficult to satisfy all evaluation criteria in this case.

5.3 Results

Thanks to this model it is finally possible to have a more complete and closer to reality picture of the actual consumptions, in various conditions, for different vehicle concepts. As already mentioned in the introduction, this is very important in order to better exploit the technologies for the mobility of the future and to have real objective data to use as a basis for further emissions reduction analysis.

5.3.1 Internal Combustion Engine Vehicle

As a first step, an ICEV is analyzed and in Figure 47 the results are plotted. In this case they are converted in l/100km, thanks to the intrinsic capability of the optimization environment. It is immediately clear the distinction between heating phase, below the desired temperature of 21 °C and cooling phase, above 21 °C. In the first region, the fuel consumption is not sensitive neither to outside temperature nor to trip distance because the waste heat coming from the engine is enough to heat up the cabin even in very cold ambient conditions. For what concerns the cooling phase, regarding external temperatures between 21 °C and 40 °C, the consumption increases, as already seen in the results in Chapter 4.4.3, because of the additional energy demand for the A/C operation. The impact is anyway quite low since the efficiency of the Air Conditioning system is relatively high and, differently from the case of a full electric vehicle, it takes energy directly from the crankshaft, increasing only slightly the load on the engine. Moreover, it can be noticed that short trip distances lead to increased fuel consumptions since the percentage of the overall energy demand required for climate control is bigger.

Finally, the maximum absolute and relative differences in determined consumptions for the analyzed range of trip distance and ambient temperature are 0.3 l/100km and 5.5 %, respectively. The maximum dependency only in trip distance, instead, is even lower: 1.9 %.

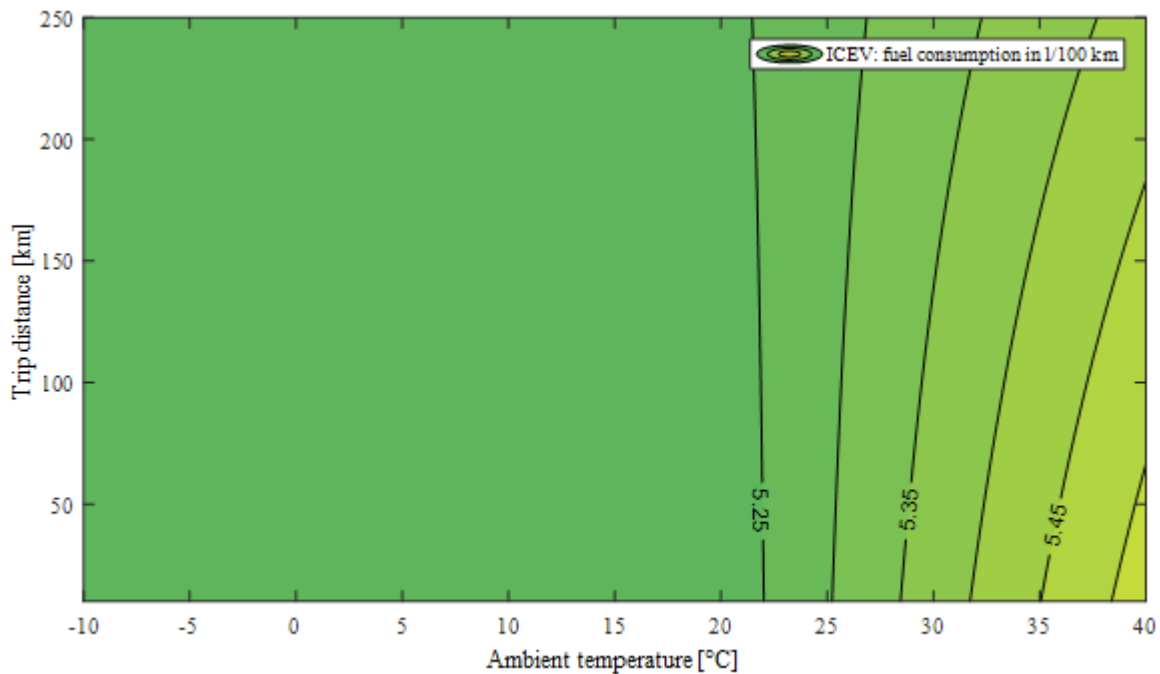


Figure 47. Fuel consumption in dependency of ambient temperature and trip distance for an ICEV.

5.3.2 Battery Electric Vehicle

For what concerns BEVs, the results are represented in Figure 48. It is evident the big difference with respect to the ICEV: the sensitivity in consumption, in this case, is much higher from the point of view of both trip distance and ambient temperature. The latter, in fact, has a strong influence in all operating conditions, differently from the ICEV case. The variation in consumption due to low external temperatures, on the left of

the graph, is higher than the outcomes of the cooling phase, right part of the plot. This difference in the additional energy demand is due to the PTC elements that have to provide the whole heating power since no engine waste heat is available in this case. For cooling, instead, the A/C system is used resulting in a less significant increase in energy consumption. For what concerns the influence of the trip distance, even in this case a much higher variation in consumption can be seen with respect to the results of the ICEV, especially for low ambient temperatures. When the vehicle has to be heated up to the desired cabin temperature from cold starting conditions during a very short trip, a high amount of power is required within a short time span leading to an increase in consumption per distance. For longer trips, the influence of the secondary energy demand on the consumption is lower since after heating up the cabin, the power required to maintain the stationary conditions is lower for the remaining part of the trip.

The maximum difference in consumption is 5.85 kWh/100km with a relative variation of 22.7 %.

Furthermore, the chosen battery capacity is not sufficient to finish all trips, as can be understood by looking at the blank region in Figure 48. That is because at higher consumptions the maximum possible vehicle range is reduced.

It shows that the overall dependency in trip distance is higher than in case of an ICEV at a maximum derivation of 11.0% while the dependency in ambient temperature is even higher at a maximum of 22.7%.

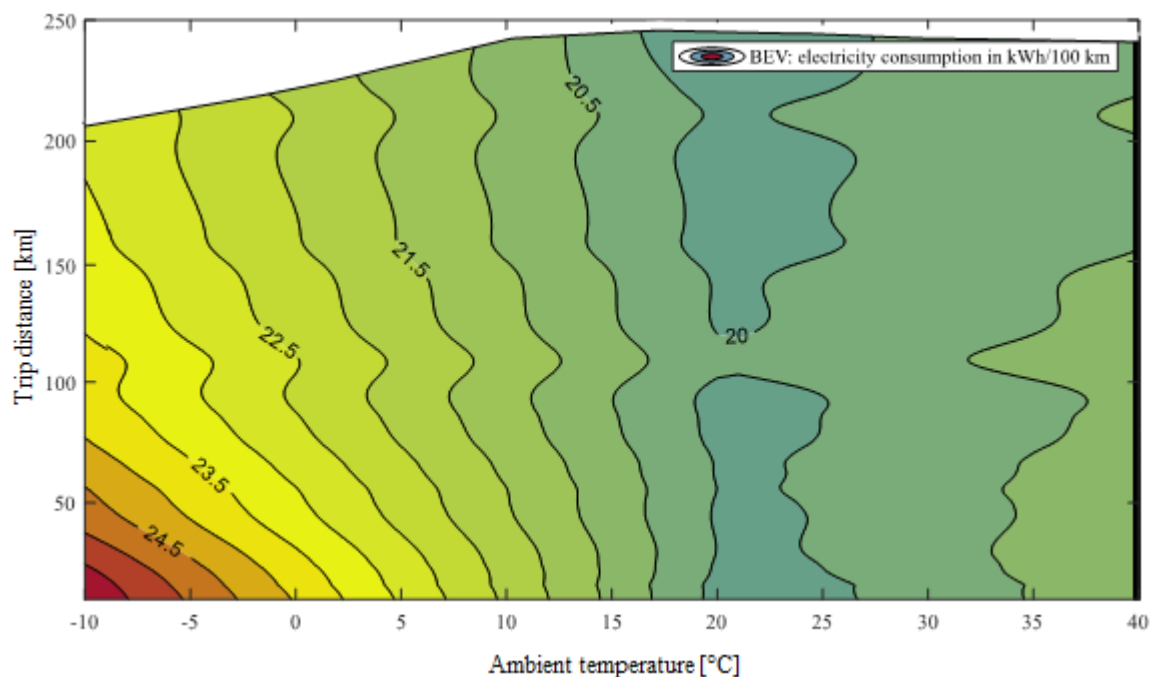


Figure 48. Electricity consumption in dependency of ambient temperature and trip distance for a BEV.

5.3.3 Plug-In Hybrid Electric Vehicle

Regarding the PHEV drivetrain concept, the situation is more complicated since the operating strategy plays a fundamental role. Two plots are derived in this case, one for fuel consumption and one for electricity consumption. As already described, the operating strategy does not operate in charge sustaining mode, but tries to fully deplete the battery for every trip distance. Therefore, the vehicle drives almost purely electrical at low trip distances.

The results, shown in Figure 49 and in Figure 50, show a complex behavior that can be analyzed as follows. It is assumed that the PHEV starts each trip with a fully charged battery. The electricity consumption map can be divided into two regions, separated by the electrical range of the vehicle. The electrical range as a function of ambient temperature can approximately be derived from the fuel consumption plot as it is close to the first contour line where the fuel consumption is greater than zero. In the region below the electrical range of the vehicle, the PHEV can drive almost purely electrically. Therefore, the fuel consumption is nearly zero. Very small values can occur though, since it is possible that the vehicle needs both ICE and EM power at the same time to fulfill the requested driving maneuver. Thus, in the region below the electrical range, the PHEV has a similar characteristic to the BEV. High and low ambient temperatures increase the electricity consumption for the climate control of the cabin, with colder ambient temperatures being more energy demanding. Therefore, as for the BEV, the electrical range is dependent on the ambient temperature due to the secondary demands. The trip distance is also very relevant in this region, since the vehicle has to be heated to stationary conditions with a high demand in power for HVAC. Hence, the energy required to heat the cabin accounts for a greater percentage of the total energy demand. Thus, the highest electrical consumption occurs at low trip distances and low ambient temperatures. The second region above the electrical range shows a completely different sensitivity to ambient temperature and trip distance. The electrical consumption is now independent from ambient temperatures because the battery is fully depleted during each trip and all ambient temperatures. This means that the electrical consumption can be directly derived when dividing the available battery capacity by the distance of the trip, thus forming a hyperbole function of trip distance. Higher overall energy demand is still required for low temperatures due to secondary demands which results in an increase in fuel consumption.

In general, the operating strategy can decide on factors like the percentage of purely electrical driving, boosting or load point shifting. The chosen operating strategy with the assumption that the battery, if possible, is always fully depleted after each trip, has a major influence on the results. This assumption leads to the abrupt change in sensitivity when exceeding the electrical range. Additionally, higher trip distances lead to a higher percentage of the ICE being turned on. Therefore, more waste heat is available that can be used to heat the cabin. The results show that colder ambient temperatures are more energy intensive than warmer conditions for medium trip distances (around 100-150 km), since the electrical driving percentage is still high, resulting in less available waste heat. For longer trip distances, the electrical driving percentage diminishes, and the vehicle can use the additional waste heat from the ICE in colder temperatures. Therefore, at around 250 km, the dependency of the energy demand on ambient temperature decreases. When even longer trip distances are considered, the PHEV further approaches the characteristics of the ICEV with very robust consumption behavior in colder environments. The determined electrical and fuel consumption are calculated under the assumptions that the vehicles start with a maximum state of charge and that the operational strategy tries to maximize the electrical driving percentage. It can therefore be considered as an optimal result in terms of potential CO₂ reduction.

The results show that the consumption characteristic of a PHEV is strongly dependent on the usage profile. According to the typical distribution of trip distances, shown in Figure 44b, short trips are the most relevant, hence the PHEV is often operated with a very high electrical driving percentage. For these short trips, it even has a lower electrical consumption than the long range BEV since it is, as shown in Table 5, much lighter because of the smaller battery. For longer trips, the PHEV takes advantage of the ICE to fulfill the trip requirements. Since the operation strategy tries to fully deplete the battery, the electrical energy consumption

is highly sensitive to trip distance. Below the electrical range of the vehicle, the electric consumption is much higher and shows a strong dependency on ambient temperature, similar to the BEV. Above the electrical range, the electric consumption is almost constant with respect to ambient temperature, but decreases with higher trip distances because of the increasing use of fuel.

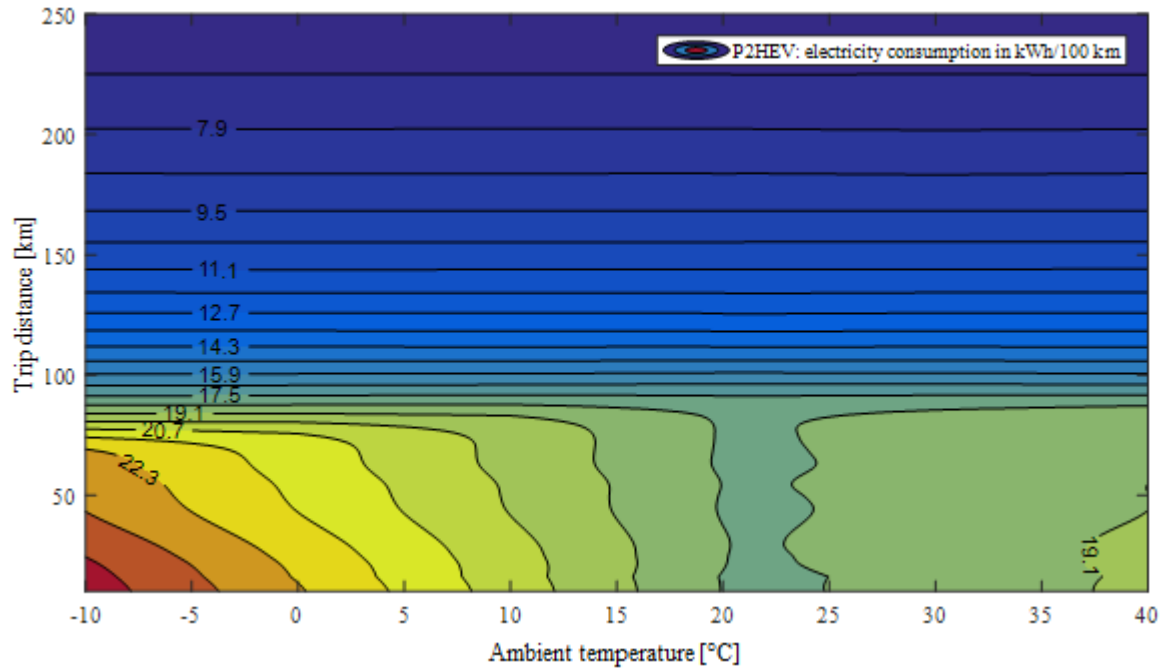


Figure 49. Electricity consumption as a function of ambient temperature and trip distance for the PHEV.

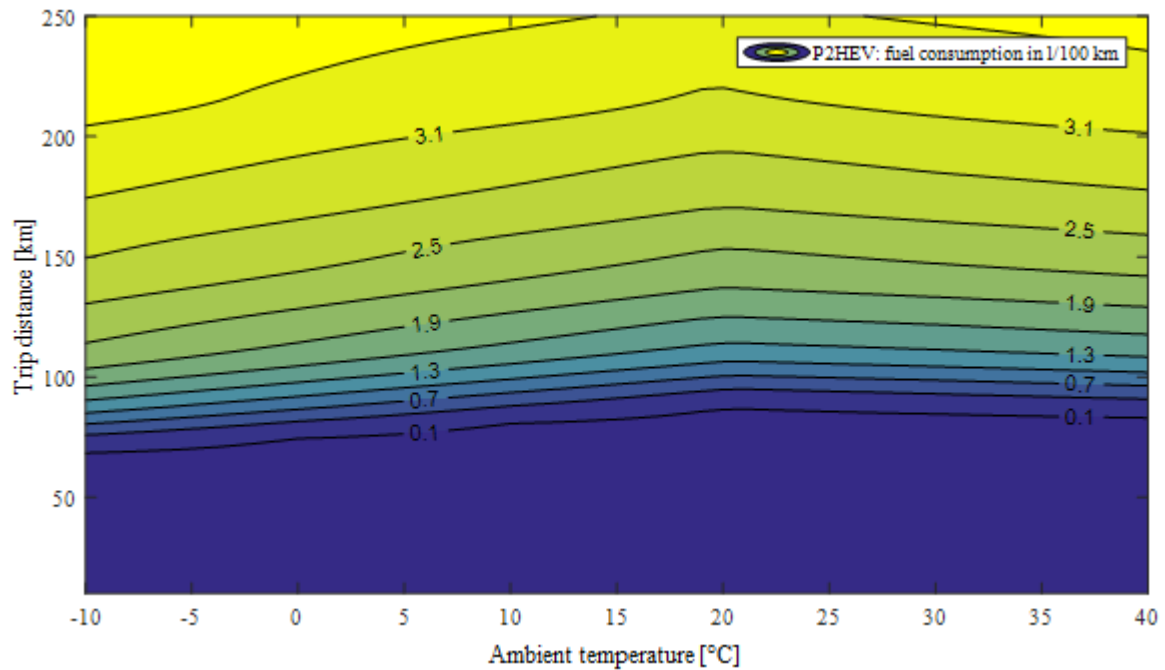


Figure 50. Fuel consumption as a function of ambient temperature and trip distance for the PHEV.

6 Conclusions and future developments

Through this work it was possible to understand the big influence that secondary users can have on the overall energy consumption of a vehicle, especially on electrified drivetrain concepts, during different environmental conditions. Regarding full electric vehicles, the results found showed a very high increase in energy demand, up to 22.7 %, to reach an acceptable comfort level for the passengers, during very low external temperatures. For this kind of vehicles, having only one source of energy, the battery, an increase in consumption has to be seen directly as an important reduction in range, which remains one the weakest point to overcome before an increase in market share for BEVs. As expected, instead, ICEVs did not suffer of a big increment of fuel consumption due to secondary users, being the internal combustion engine quite insensitive to auxiliary loads. For what concerns PHEVs, probably the most interesting drivetrain solution for the near future in terms of range and emissions, the results showed a behaviour equal to the BEV one in case of short trips, while for long trips it was equal to the ICEV outcomes. Thus demonstrating a high dependence on the operating strategy, which is one of the most important degrees of freedom of hybrid vehicles for reducing consumptions and, consequently, emissions.

Furthermore, the opportunity to simulate over driving cycles representing real world driving conditions led to the achievement of important results much closer to reality than with type-approval cycles. As a matter of fact, since the reduction of car emissions, both pollutants and greenhouse gas, through the electrification of drivetrains is the most important objective for future mobility solutions, it is of paramount importance to evaluate emissions by means of analyses with extended system boundaries able to depict the real world usage of a passenger vehicle.

Therefore, as a conclusion of this work it is necessary to say that future vehicle concepts have to be evaluated in more realistic operating conditions considering wider system borders. Until today, the development focused on ICEVs which do only show a small sensitivity to ride length and ambient temperatures. Therefore, neglecting these influences was tolerable. From now on, when developing new electrified vehicle drivetrain concepts to effectively reduce CO₂ emissions, fleet representative driving conditions including the real driving behavior and external operating conditions have to be considered. An approach to generate a more realistic norm for the consumption of different drivetrain concepts could be to investigate the energy demand of drivetrain concepts under all operating conditions, by means of simulations, and perform a weighting according the real occurrence frequency of these external conditions, which have been shown in Figure 44. In this way, the sensitivity of the drivetrain concepts would be incorporated and the adaption towards a specific testing procedure could be avoided.

Future developments for this work can be made by increasing the complexity of the model describing the car. In fact, a quite important contribution to energy demands is represented by the thermal management of the battery and its temperature dependent efficiency.

Finally, since this work was based only on a simulative approach, it would be necessary to validate the results found through experimental data, in order to make a more reliable comparison between simulations and real world.

7 Acknowledgements

The plots shown in Chapter 5 are the results of a combined work between the author of this thesis and the following people of the Institute for Mechatronic Systems in Mechanical Engineering of TU Darmstadt: Dr. Philippe Jardin, Dr. Arved Esser, Dr. Tobias Eichenlaub, Dr. Jean-Eric Schleiffer and Prof. Dr. Ing. Stephan Rinderknecht. These results will be included in a scientific paper published in the journal “Vehicles” in 2019. The authors of the paper gave the permission of publishing the outcomes of the analysis in advance in this thesis.

First of all I would like to thank Prof. Andrea Tonoli for giving me the possibility to write my thesis abroad, at a prestigious university like the TU Darmstadt and thus to have the wonderful experience of living in another country.

Thanks also to Philippe Jardin and Arved Eßer, Ph.D. candidates at the TU Darmstadt, for helping me and supervising my work with great patience and competence and for giving me the fantastic opportunity to write my first scientific paper. With the hope to be the first of a long series and that it can give a little help to the scientific research for a less polluted world.

A special thanks goes to the friends with whom I shared the unique experience of living in Germany: Annica, Caro, Lisa and Jannik. Thank you for everything you did for me from the first moment I arrived in Darmstadt. Thank you for helping me every time I needed, for speaking English for months, for teaching me the German culture and language and for spending your time with me. It has been great to meet you. With the hope of never losing contact and one day returning the favor in Italy.

Thanks also to all my family for letting me have all these fantastic experiences and supporting every decision I take, especially during my university years. Without you I could not have come this far.

Finally, last but not least, a big thank you goes to my girlfriend Cristina, always by my side during all my crazy adventures and always supporting my choices. Thanks for being patient and honest all the time. Thanks for pushing me to reach always new goals and for helping me to overcome obstacles I could not overcome alone. Without you I would never have achieved all these results.

Appendix – MATLAB Code

Parameters script:

```
%% PARAMETERS
```

```
T_obj=294.15; %[K] cabin objective temperature
```

```
T_ext=[-10+273.15 0+273.15 10+273.15 19+273.15 20+273.15 21+273.15 30+273.15 40+273.15];
```

```
air_param.ro_ext=1.2; %[kg/m^3] external air density at 21 °C
```

```
air_param.mu_ext=1.81*10^(-5); %[kg/(m*s)] external air dynamic viscosity at 21 °C
```

```
air_param.cp_ext=1006; %[J/kg*K] external dry air specific heat at constant pressure at 21 °C
```

```
air_param.cond_coeff_ext=0.026; %[W/m*K] external air thermal conductivity at 21 °C
```

```
air_param.ro_int=1.2; %[kg/m^3] internal air density at 21 °C
```

```
air_param.mu_int=1.81*10^(-5); %[kg/(m*s)] internal air dynamic viscosity at 21 °C
```

```
air_param.cp_int=1006; %[J/kg*K] internal air specific heat at constant pressure at 21 °C
```

```
air_param.cond_coeff_int=0.026; %[W/m*K] internal air thermal conductivity at 21 °C
```

```
air_param.cp_steam=1864; %[J/kg*K] steam specific heat at constant pressure at 27 °C
```

```
air_param.recirculation_factor=0.5; %[-] recirculation factor
```

```
air_param.m_dot=0.08; %[kg/s] air mass flow rate
```

```
air_param.p_saturation=286.57; %[Pa] saturation pressure of the air
```

```
air_param.R=287.05; %[J/kg*K] dry air
```

```
air_param.rel_humidity_ext=0.8; %[-] relative humidity of the environment
```

```
air_param.sultry_limit=13*10^-3; %[kg_water/kg_dry_air]
```

```
water_param.delta_h_vap=2451200; %[J/kg] enthalpy of vaporization of water at 21 °C
```

```
water_param.cp=4186; %[J/kg*K] water specific heat at constant pressure
```

```
hvac_velocity=2; %[m/s] air speed from HVAC for internal convection
```

```
car_param.cabin_volume=2.5; %[m^3]
```

```
car_param.glass.area_windshield=1.1; %[m^2]
```

```
car_param.glass.area_laterals=1.2; %[m^2]
```

```
car_param.glass.area_rear=0.5; %[m^2]
```

```
car_param.glass.cond_coeff=0.8; %[W/m*K]
```

```
car_param.glass.thickness=0.006; %[m]
```

```
car_param.glass.L_char=0.5; %[m] characteristic length
```

```
car_param.glass.transmittance=0.90; %[-]
```

```
car_param.roof.area=1.7; %[m^2]
```

```
car_param.roof.plastic_thickness=0.002; %[m]
```

```
car_param.roof.plastic_cond_coeff=0.22; %[W/m*K] polypropylene
```

```
car_param.roof.air_thickness=0.002; %[m]
```

```
car_param.roof.metal_thickness=0.001; %[m]
```

```
car_param.roof.L_char=0.8; %[m] characteristic length
```

```
car_param.roof.absorbance=0.20; %[-]
```

```
car_param.roof.epsilon=0.5; %[-]
```

```
car_param.roof.m=13; %[kg]
```

```
car_param.roof.cp=500; %[J/kg*K]
```

```
car_param.metal_cond_coeff=16; %[W/m*K] stainless steel
```

```
car_param.door.area=3; %[m^2]
```

```
car_param.door.plastic_thickness=0.002; %[m]
```

```
car_param.door.plastic_cond_coeff=0.22; %[W/m*K] polypropylene
```

```
car_param.door.L_char=0.8; %[m] characteristic length
```

```

car_param.door.air_1_thickness=0.002; %[m]
car_param.door.metal_1_thickness=0.001; %[m]
car_param.door.air_2_thickness=0.05; %[m]
car_param.door.metal_2_thickness=0.001; %[m]
car_param.door.cp=502; %[J/kg*K]
car_param.door.absorbance=0.20; %[-]
car_param.door.epsilon=0.5; %[-]
car_param.door.m=16; %[kg]
car_param.door.cp=500; %[J/kg*K]
car_param.interiors.area=7.3; %[m^2]
car_param.interiors.cond_coeff=0.8; %[W/m*K]
car_param.interiors.thickness=0.020; %[m]
car_param.interiors.L_char=0.4; %[m] characteristic length
car_param.interiors.m=100; %[kg]
car_param.interiors.cp=1250; %[J/kg*K]
car_param.interiors.absorbance=0.70; %[-]
car_param.dash.area=1; %[m^2]
car_param.dash.epsilon=0.97; %[-] emissivity coefficient for polypropilene
car_param.dash.m=10; %[kg]
car_param.dash.cp=1920; %[J/kg*K]
car_param.dash.absorbance=0.80; %[-]

human_param.body_mean_surface=1.8; %[m^2]
human_param.metabolic_rate=58; %[W/m^2]
human_param.n_passengers=0; %[-] number of passengers except the driver, >=0
human_param.m_dot_water=(human_param.n_passengers+1)*8.3*10^-6; %[kg/s] humidity production of
the passengers

sigma=5.670*10^(-8); %[W/(m^2*K^4)] Stefan-Boltzmann constant

I_tot_solar=200; %[W/m^2] solar radiation

simulation_sampling = 0.1; %[s] sampling time of the simulation

%% DERIVED PARAMETERS

air_param.m_dot_recirculating=air_param.recirculation_factor*air_param.m_dot; %[kg/s]
air_param.m_dot_fresh=(1-air_param.recirculation_factor)*air_param.m_dot; %[kg/s]
air_param.cabin_mass=air_param.ro_int*car_param.cabin_volume; %[kg] air mass in the cabin
air_param.p_vapor=air_param.rel_humidity_ext*air_param.p_saturation; %[Pa]

%% PTC parameters

Q_dot_ptc_max=5000; %[W] maximum PTC heating power
eta_ptc=0.95; %[-]
P_ptc=0; %initial condition

%% AC parameters

Q_dot_ac_max=-3500; %[W] maximum AC cooling power
cop_ac=3; %[-] Coefficient Of Performance
P_ac_beve=0; %initial condition
P_ac_icev=0; %initial condition
P_ac_hev=0; %initial condition

```

%% Heat Pump parameters

Q_dot_hp_max=3500; %[W] maximum HP cooling power
cop_hp=cop_ac+1; %[-] Coefficient Of Performance
P_hp=0; %initial condition

%% Additional secondary users parameters

P_blower=200; %[W] blower power requirement
P_lights=150; %[W]
P_infotainment=20; %[W]
P_power_steering=500; %[W] electric

P_add_sec_users=P_blower+P_lights+P_infotainment+P_power_steering; %[W]

P_battery_tms=500; %[W] mean power for battery thermal management

%% Engine waste heat

Q_dot_waste=5000; %[W] heat to the HVAC due to engine waste heat

Cabin thermodynamic model:

```
function [ Temperatures ] = Cabin_thermodynamic_model_FUNCTION( i, air_param, car_param,  
human_param, I_tot_solar, m_water_cabin, Q_dot_hvac, sigma, simulation_sampling, T_ext, T_cabin,  
T_dash, T_doors, T_interiors, T_roof, v_current, hvac_velocity, water_param, X_cabin, X_environment,  
spec_enthalpy_fresh_air, ac_dehum, m_water_cabin_pre )
```

```
%CABIN THERMODYNAMIC MODEL
```

```
% This model gives the variation of cabin air temperature as function of  
% external air temperature and heat transfers
```

```
%% GLASSES
```

```
% External convective coefficient
```

```
Re_glass_ext=v_current*car_param.glass.L_char*air_param.ro_ext/air_param.mu_ext; %Reynolds number  
Pr_glass_ext=air_param.cp_ext*air_param.mu_ext/air_param.cond_coeff_ext; %Prandtl number  
Nu_glass_ext=2*0.332*Re_glass_ext^(1/2)*Pr_glass_ext^(1/3); %average Nusselt number for laminar flow  
on a flat plate  
conv_ext_glass=Nu_glass_ext*air_param.cond_coeff_ext/car_param.glass.L_char; %[W/m^2*K]  
convective coefficient on external side of the glass
```

```
% Internal convective coefficient
```

```
Re_glass_int=hvac_velocity*car_param.glass.L_char*air_param.ro_int/air_param.mu_int; %Reynolds  
number  
Pr_glass_int=air_param.cp_int*air_param.mu_int/air_param.cond_coeff_int; %Prandtl number  
Nu_glass_int=2*0.332*Re_glass_int^(1/2)*Pr_glass_int^(1/3); %average Nusselt number for laminar flow  
on a flat plate  
conv_int_glass=Nu_glass_int*air_param.cond_coeff_int/car_param.glass.L_char; %[W/m^2*K] convective  
coefficient on external side of the glass
```

```
% Global heat transfer through the glasses (conduction and convection)
```

```
glass_heat_tr_coeff=((1/conv_ext_glass)+(car_param.glass.thickness/car_param.glass.cond_coeff)+(1/conv_  
int_glass))^(-1); %[W/m^2*K] global heat transfer coefficient through windshield and lateral windows  
glass_heat_tr_coeff_rear=((car_param.glass.thickness/car_param.glass.cond_coeff)+(1/conv_int_glass))^(-  
1); %[W/m^2*K] global heat transfer coefficient through rear window
```

```
%% DOOR
```

```
% External convective coefficient
```

```
Re_door_ext=v_current*car_param.door.L_char*air_param.ro_ext/air_param.mu_ext; %Reynolds number  
Pr_door_ext=air_param.cp_ext*air_param.mu_ext/air_param.cond_coeff_ext; %Prandtl number  
Nu_door_ext=2*0.332*Re_door_ext^(1/2)*Pr_door_ext^(1/3); %average Nusselt number for laminar flow  
on a flat plate  
conv_ext_doors=Nu_door_ext*air_param.cond_coeff_ext/car_param.door.L_char; %[W/m^2*K] convective  
coefficient on external side of the glass
```

```
% Internal convective coefficient
```

```
Re_door_int=hvac_velocity*car_param.door.L_char*air_param.ro_int/air_param.mu_int; %Reynolds  
number  
Pr_door_int=air_param.cp_int*air_param.mu_int/air_param.cond_coeff_int; %Prandtl number
```

```
Nu_door_int=2*0.332*Re_door_int^(1/2)*Pr_door_int^(1/3); %average Nusselt number for laminar flow on a flat plate
conv_int_doors=Nu_door_int*air_param.cond_coeff_int/car_param.door.L_char; %[W/m^2*K] convective coefficient on external side of the glass
```

%% DASHBOARD & INTERIORS

```
Q_dot_solar_dash=I_tot_solar*car_param.dash. absorbance*car_param.glass.transmittance*car_param.dash.area; %[W] thermal load on the dashboard
```

% Seat convective coefficient

```
Re_interiors=hvac_velocity*car_param.interiors.L_char*air_param.ro_int/air_param.mu_int; %Reynolds number
Pr_interiors=air_param.cp_int*air_param.mu_int/air_param.cond_coeff_int; %Prandtl number
Nu_interiors=2*0.332*Re_interiors^(1/2)*Pr_interiors^(1/3); %average Nusselt number for laminar flow on a flat plate
conv_interiors=Nu_interiors*air_param.cond_coeff_int/car_param.interiors.L_char; %[W/m^2*K] convective coefficient
interiors_heat_tr_coeff=2*((car_param.interiors.thickness/car_param.interiors.cond_coeff)+(1/conv_interiors))^(-1); %[W/m^2*K] global heat transfer coefficient through the glass
```

```
dash_heat_tr_coeff=interiors_heat_tr_coeff;
```

%% ROOF

% External convective coefficient

```
Re_roof_ext=v_current*car_param.roof.L_char*air_param.ro_ext/air_param.mu_ext; %Reynolds number
Pr_roof_ext=air_param.cp_ext*air_param.mu_ext/air_param.cond_coeff_ext; %Prandtl number
Nu_roof_ext=2*0.332*Re_roof_ext^(1/2)*Pr_roof_ext^(1/3); %average Nusselt number for laminar flow on a flat plate
conv_ext_roof=Nu_roof_ext*air_param.cond_coeff_ext/car_param.roof.L_char; %[W/m^2*K] convective coefficient on external side of the glass
```

% Internal convective coefficient

```
Re_roof_int=hvac_velocity*car_param.roof.L_char*air_param.ro_int/air_param.mu_int; %Reynolds number
Pr_roof_int=air_param.cp_int*air_param.mu_int/air_param.cond_coeff_int; %Prandtl number
Nu_roof_int=2*0.332*Re_roof_int^(1/2)*Pr_roof_int^(1/3); %average Nusselt number for laminar flow on a flat plate
conv_int_roof=Nu_roof_int*air_param.cond_coeff_int/car_param.roof.L_char; %[W/m^2*K] convective coefficient on external side of the glass
```

%% HUMANS

% Passengers thermal load production due to metabolism

```
Q_dot_passengers=human_param.n_passengers*human_param.metabolic_rate*human_param.body_mean_surface; %[W] non driving passengers
```

```
Q_dot_driver=human_param.metabolic_rate*human_param.body_mean_surface*1.4; %[W] driver
```

```
Q_dot_humans=Q_dot_driver+Q_dot_passengers;
```

%% HUMIDITY

spec_humidity=m_water_cabin/(air_param.cabin_mass-m_water_cabin); %[kg_water_vapour/kg_dry_air]
specific humidity of the air in the cabin

```
if X_cabin >= air_param.sultry_limit
    ac_dehum = 1;
end
```

%% CABIN - GLOBAL

```
H_dot_supply=air_param.m_dot_recirculating*(T_cabin*air_param.cp_int+X_cabin*(air_param.cp_steam*
T_cabin+water_param.delta_h_vap))+air_param.m_dot_fresh*spec_enthalpy_fresh_air+Q_dot_hvac;
H_dot_exhaust=air_param.m_dot*T_cabin*(air_param.cp_int+X_cabin*air_param.cp_steam)+air_param.m
_dot*X_cabin*water_param.delta_h_vap;
H_dot_total=H_dot_supply-H_dot_exhaust;
```

```
m_water_cabin=m_water_cabin+simulation_sampling*((air_param.m_dot_recirculating-
air_param.m_dot)*m_water_cabin/air_param.cabin_mass+X_environment*air_param.m_dot_fresh+human_
param.m_dot_water-ac_dehum*air_param.m_dot*spec_humidity);
X_cabin=m_water_cabin/(air_param.cabin_mass-m_water_cabin);
```

```
Q_dot_roof_ext=I_tot_solar*car_param.roof. absorbance*car_param.roof.area-
car_param.roof.epsilon*sigma*T_roof^4-conv_ext_roof*car_param.roof.area*(T_roof-T_ext(i));
Q_dot_roof_int=((1/conv_int_roof)+(car_param.roof.plastic_thickness/car_param.roof.plastic_cond_coeff)+
(car_param.roof.air_thickness/air_param.cond_coeff_int)+(car_param.roof.metal_thickness/car_param.metal
_cond_coeff))^(1)*car_param.roof.area*(T_roof-T_cabin);
```

```
T_roof=T_roof+simulation_sampling*(Q_dot_roof_ext-
Q_dot_roof_int)/(car_param.roof.m*car_param.roof.cp);
```

```
Q_dot_doors_ext=0.5*I_tot_solar*car_param.door. absorbance*car_param.door.area-
car_param.door.epsilon*sigma*T_doors^4-conv_ext_doors*car_param.door.area*(T_doors-T_ext(i)); % 0.5
reducing factor
```

```
Q_dot_doors_int=((1/conv_int_doors)+(car_param.door.plastic_thickness/car_param.door.plastic_cond_coef
f)+(car_param.door.air_1_thickness/air_param.cond_coeff_int)+(car_param.door.metal_1_thickness/car_par
am.metal_cond_coeff)+(car_param.door.air_2_thickness/air_param.cond_coeff_int)+(car_param.door.metal
_2_thickness/car_param.metal_cond_coeff))^(1)*car_param.door.area*(T_doors-T_cabin);
```

```
T_doors=T_doors+simulation_sampling*(Q_dot_doors_ext-
Q_dot_doors_int)/(car_param.door.m*car_param.door.cp);
```

```
Q_dot_interiors=interiors_heat_tr_coeff*car_param.interiors.area*(T_interiors-T_cabin);
```

```
Q_dot_glasses=glass_heat_tr_coeff*car_param.glass.area_windshield*(T_ext(i)-
T_cabin)+glass_heat_tr_coeff*car_param.glass.area_laterals*(T_ext(i)-
T_cabin)+glass_heat_tr_coeff_rear*car_param.glass.area_rear*(T_ext(i)-T_cabin);
```

```
Q_dot_dash=dash_heat_tr_coeff*car_param.dash.area*(T_dash-T_cabin);
```

```
T_dash=T_dash+simulation_sampling*(Q_dot_solar_dash-
Q_dot_dash)/(car_param.dash.m*car_param.dash.cp);
```

```
T_cabin=T_cabin+(simulation_sampling*(Q_dot_glasses+Q_dot_doors_int+Q_dot_dash+Q_dot_interiors+
Q_dot_roof_int+Q_dot_humans+H_dot_total)-((m_water_cabin-
```

```
m_water_cabin_pre)*(T_cabin*water_param.cp+water_param.delta_h_vap)))/(air_param.cabin_mass*air_param.cp_int+m_water_cabin*water_param.cp);
```

```
T_interiors=T_interiors-simulation_sampling*(Q_dot_interiors)/(car_param.interiors.m*car_param.interiors.cp);
```

```
Temperatures(1)=T_cabin;
```

```
Temperatures(2)=T_dash;
```

```
Temperatures(3)=T_interiors;
```

```
Temperatures(4)=T_doors;
```

```
Temperatures(5)=T_roof;
```

```
Temperatures(6)=X_cabin;
```

```
Temperatures(7)=m_water_cabin;
```

```
Temperatures(8)=m_water_cabin; %needed for T_cabin calculation
```

```
Temperatures(9)=spec_humidity;
```

```
end
```

Secondary users power consumption calculation:

```
clear all
close all
```

```
concept={'BEV','ICEV','P2HEV'};
```

```
driving_cycles_loading=what('Cycles');
```

```
run Parameters.m;
```

```
for j=1:length(concept)
```

```
    P_sec_users=0;
```

```
    for kk = 1:length(driving_cycles_loading.mat)
```

```
        filename = driving_cycles_loading.mat{kk};
        current_cycle = load(['Cycles', '/', filename]);
        datafilename = char(fieldnames(current_cycle));
        driving_data = current_cycle.(datafilename);
        N=driving_data.time(end)/simulation_sampling;
        v_interp =
```

```
interp1(driving_data.time,driving_data.velocity,simulation_sampling:simulation_sampling:driving_data.time
(end));
```

```
        distance(kk)=sum(v_interp)*simulation_sampling/1000; %[km] distance travelled in the cycle
```

```
        concept_current=concept(j);
```

```
        for i=1:length(T_ext)
```

```
            % variables computation and reset
```

```
            T_cabin = T_ext(i); % cold start
```

```
            T_dash = T_cabin;
```

```
            T_interiors= T_cabin;
```

```
            T_doors = T_ext(i);
```

```
            T_roof = T_ext(i);
```

```
            m_water_cabin=0;
```

```
            X_cabin=m_water_cabin/air_param.cabin_mass;
```

```
            m_water_cabin_pre=m_water_cabin;
```

```
            T_cabin_int=0;
```

```
            deltaT=0;
```

```
            Q_dot=0;
```

```
            P_ptc=0;
```

```
            P_ptc_hev=0;
```

```
            P_ac_bev=0;
```

```
            P_ac_icev=0;
```

```
            P_ac_hev=0;
```

```
            P_hp=0;
```

```
            spec_enthalpy_fresh_air=air_param.cp_ext*T_ext(i); %[J/kg]
```

```
            p_total=air_param.R*T_ext(i)*air_param.ro_ext; %[Pa]
```

```
            X_environment=0.622*air_param.p_vapor/(p_total-air_param.p_vapor);
```

```
            int=0;
```

```
            Kp=1;
```

```

Ki=3;
Ka=3;

for k=1:N

    t_current=k*simulation_sampling;
    v_current=v_interp(k);
    if v_current < 0
        v_current = 0;
    end
    T_cabin_int(k)=T_cabin;
    deltaT(k)=T_obj-T_cabin_int(k);

    prop=Kp*(T_obj-T_cabin)+Ki*Ka*(T_obj-T_cabin)*simulation_sampling*k; %proportional part
of the PI controller

    if k == 50000
        Ki = 1;
    end

    int=int+Ki*deltaT(k)*simulation_sampling; %integral part of the PI controller

    %          int=int+Ki*deltaT(k)*simulation_sampling;

    if strcmp(concept_current,'BEV')

        int_max=Q_dot_ptc_max-prop;
        int_min=Q_dot_ac_max-prop;
        %int_sat=antiwindup(int, int_max, int_min);

        %antiwindup
        if int > int_max
            int_sat=int_max;
        elseif int < int_min
            int_sat=int_min;
        else
            int_sat=int;
        end

        Q_dot(k)=prop+int_sat; %PI controller [W]

        if Q_dot(k) >= 0
            P_ptc(k)=Q_dot(k)/eta_ptc; %[W] PTC electrical power consumed
            P_ac_bev(k)=0;
            ac_dehum=0;

        elseif Q_dot(k) < 0
            P_ptc(k)=0;
            P_ac_bev(k)=abs(Q_dot(k))/cop_ac; %[W] AC electrical power consumed
            ac_dehum=1;
        end

    elseif strcmp(concept_current,'ICEV')

        int_max=Q_dot_waste-prop;

```

```
int_min=Q_dot_ac_max-prop;
%antiwindup(int, int_max, int_min);
```

```
%antiwindup
if int > int_max
    int_sat=int_max;
elseif int < int_min
    int_sat=int_min;
else
    int_sat=int;
end
```

```
Q_dot(k)=prop+int_sat; %[W] PI controller
```

```
if Q_dot(k) < 0
    P_ac_icev(k)=abs(Q_dot(k))/cop_ac; %[W] AC electrical power consumed
    ac_dehum=1;
else
    P_ac_icev(k)=0;
    ac_dehum=0;
end
```

```
elseif strcmp(concept_current,'HEV') || strcmp(concept_current,'P2HEV')
```

```
int_max=Q_dot_hp_max-prop;
int_min=Q_dot_ac_max-prop;
```

```
%antiwindup
if int > int_max
    int_sat=int_max;
elseif int < int_min
    int_sat=int_min;
else
    int_sat=int;
end
```

```
Q_dot(k)=prop+int_sat; %PI controller [W]
```

```
if Q_dot(k) >= 0
    P_ptc_hev(k)=Q_dot(k)/eta_ptc; %[W] PTC electrical power consumed
    P_ac_hev(k)=0;
    ac_dehum=0;
elseif Q_dot(k) < 0
    P_ac_hev(k)=abs(Q_dot(k))/cop_ac; %[W] AC electrical power consumed
    P_ptc_hev(k)=0;
    ac_dehum=1;
end
```

```
end
```

```
Q_dot_hvac=Q_dot(k); %[W]
```

```
T(k,:) = Cabin_thermodynamic_model_FUNCTION( i, air_param, car_param, human_param,
I_tot_solar, m_water_cabin, Q_dot_hvac, sigma, simulation_sampling, T_ext, T_cabin, T_dash, T_doors,
```

```

T_interiors, T_roof, v_current, hvac_velocity, water_param, X_cabin, X_environment,
spec_enthalpy_fresh_air, ac_dehum, m_water_cabin_pre );
    T_cabin = T(k,1); %[K]
    T_dash= T(k,2); %[K]
    T_interiors= T(k,3); %[K]
    T_doors = T(k,4); %[K]
    T_roof = T(k,5); %[K]
    X_cabin = T(k,6); %[-]
    m_water_cabin = T(k,7); %[kg]
    m_water_cabin_pre= T(k,8); %[kg]

end

T_cabin_history(:,i,kk)=T(:,1); %[K]
T_dash_history(:,i,kk)=T(:,2);
T_interiors_history(:,i,kk)=T(:,3);
T_doors_history(:,i,kk)=T(:,4);
T_roof_history(:,i,kk)=T(:,5);
X_cabin_history(:,i,kk)=T(:,6);
m_water_cabin_history(:,i,kk)=T(:,7); %[kg]
Q_dot_history(:,i,kk)=Q_dot; %[W]

if strcmp(concept_current,'BEV')
    P_sec_users=P_ptc+P_ac_bev+P_add_sec_users+P_battery_tms; %[W]
elseif strcmp(concept_current,'ICEV')
    P_sec_users=P_ac_icev+P_add_sec_users; %[W]
elseif strcmp(concept_current,'P2HEV')
P_sec_users(kk,i)=P_ptc_hev+P_ac_hev+P_add_sec_users+P_battery_tms; %[W]
end

P_sec_users_history(:,i,kk)=P_sec_users;
E_sec_users(:,i,kk)=sum(P_sec_users_history(:,i,kk)/1000)*simulation_sampling/3600; %[kWh]

end
end
end

time=linspace(driving_data.time(1),driving_data.time(end),driving_data.time(end)/simulation_sampling);

fuel_economy=E_sec_users/distance*100; % [kWh/100km] fuel economy for each T_ext

figure(1)
plot(time,T_cabin_history-273.15)
xlabel('Time [s]')
ylabel('Cabin air temperature [°C]')
title('Cabin air temperature - BEV - ECE-15')
saveas(figure(1),'Cabin air temperature','fig')
saveas(figure(1),'Cabin air temperature','jpg')

figure(2)
plot(time,T_dash_history-273.15)
xlabel('Time [s]')
ylabel('Dashboard temperature [°C]')
title('Dashboard temperature - BEV - ECE-15')
saveas(figure(2),'Dashboard temperature','fig')

```

```

saveas(figure(2),'Dashboard temperature','jpg')

figure(3)
plot(time,T_interiors_history-273.15)
xlabel('Time [s]')
ylabel('Interiors temperature [°C]')
title('Interiors temperature - BEV - ECE-15')
saveas(figure(3),'Interiors temperature','fig')
saveas(figure(3),'Interiors temperature','jpg')

figure(4)
plot(time,T_doors_history-273.15)
xlabel('Time [s]')
ylabel('Doors temperature [°C]')
title('Doors temperature - BEV - ECE-15')
saveas(figure(4),'Doors temperature','fig')
saveas(figure(4),'Doors temperature','jpg')

figure(5)
plot(time,T_roof_history-273.15)
xlabel('Time [s]')
ylabel('Roof temperature [°C]')
title('Roof temperature - BEV - ECE-15')
saveas(figure(5),'Roof temperature','fig')
saveas(figure(5),'Roof temperature','jpg')

figure(6)
plot(time,X_cabin_history)
xlabel('Time [s]')
ylabel('Water mass fraction [kg_w_a_t_e_r/kg_d_r_y_a_i_r]')
title('Water mass fraction in cabin air - BEV - ECE-15')
saveas(figure(6),'Water mass fraction in cabin air','fig')
saveas(figure(6),'Water mass fraction in cabin air','jpg')

figure(7)
plot(time,m_water_cabin_history)
xlabel('Time [s]')
ylabel('Water mass [kg]')
title('Water mass in cabin air - BEV - ECE-15')
saveas(figure(7),'Water mass in cabin air','fig')
saveas(figure(7),'Water mass in cabin air','jpg')

figure(8)
plot(time,Q_dot_history)
xlabel('Time [s]')
ylabel('Heat flux [W]')
title('Heat flux from the HVAC - BEV - ECE-15')
saveas(figure(8),'Heat flux from the HVAC','fig')
saveas(figure(8),'Heat flux from the HVAC','jpg')

figure(9)
plot(time,P_sec_users_history)
xlabel('Time [s]')
ylabel('Secondary users power [W]')
title('Secondary users power request - BEV - ECE-15')

```

```
saveas(figure(9),'Secondary users power request','fig')
saveas(figure(9),'Secondary users power request','jpg')

figure(10)
plot(time,P_sec_users_history(:,(1:32))) %heating power
xlabel('Time [s]')
ylabel('Secondary users heating power [W]')
title('Secondary users heating power request - BEV - ECE-15')
saveas(figure(10),'Secondary users heating power request','fig')
saveas(figure(10),'Secondary users heating power request','jpg')

figure(11)
plot(time,P_sec_users_history(:,(33:51))) %cooling power
xlabel('Time [s]')
ylabel('Secondary users cooling power [W]')
title('Secondary users cooling power request - BEV - ECE-15')
saveas(figure(11),'Secondary users cooling power request','fig')
saveas(figure(11),'Secondary users cooling power request','jpg')

figure(12)
plot(T_ext-273.15,fuel_economy)
xlabel('External temperature [°C]')
ylabel('Energy consumption [kWh/100km]')
title('Energy consumption - BEV - ECE-15')
saveas(figure(12),'Energy consumption','fig')
saveas(figure(12),'Energy consumption','jpg')
```

References

- [1] European Commission, Reducing CO₂ emissions from passenger cars https://ec.europa.eu/clima/policies/transport/vehicles/cars_en.
- [2] Liu, K.; Wang, J.; Yamamoto, T.; Morikawa, T. *Exploring the interactive effects of ambient temperature and vehicle auxiliary loads on electric vehicle energy consumption*. Applied Energy 2017, doi:10.1016/j.apenergy.2017.08.074.
- [3] Fiori, C.; Ahn, K.; Rakha, H.A. *Power-based electric vehicle energy consumption model: Model development and validation*. Applied Energy 2016, 168, 257–268, doi:10.1016/j.apenergy.2016.01.097.
- [4] Yuksel, T.; Michalek, J.J. *Effects of regional temperature on electric vehicle efficiency, range, and emissions in the United States*. Environmental science & technology 2015, 49, 3974–3980, doi:10.1021/es505621s.
- [5] Huang, D.; Wallis, M.; Oker, E.; Lepper, S. *Design of Vehicle Air Conditioning Systems Using Heat Load Analysis*. In SAE Technical Paper Series. SAE World Congress & Exhibition, APR. 16, 2007; SAE International 400 Commonwealth Drive, Warrendale, PA, United States, 2007.
- [6] Titov, G.; Lustbader, J.A. *Modeling Control Strategies and Range Impacts for Electric Vehicle Integrated Thermal Management Systems with MATLAB/Simulink*. In WCX™ 17: SAE World Congress Experience, APR. 04, 2017; SAE International 400 Commonwealth Drive, Warrendale, PA, United States, 2017.
- [7] Katharina Lange *Energiebilanzierung von Komfortverbrauchern batterieelektrischer Fahrzeuge*, Bachelor thesis, Darmstadt, April 2018.
- [8] Musat R., Helerea E. *Characteristics of the PTC Heater Used in Automotive HVAC Systems*. In: Camarinha-Matos L.M., Pereira P., Ribeiro L. (eds) Emerging Trends in Technological Innovation. DoCEIS 2010. IFIP Advances in Information and Communication Technology, vol 314. Springer, Berlin, Heidelberg, 2010.
- [9] F. Schüppel, *Optimierung des Heiz- und Klimakonzepts zur Reduktion der Wärme- und Kälteleistung im Fahrzeug*, 1st ed. Göttingen: Cuvillier Verlag, 2015.
- [10] H. Großmann, *Pkw-Klimatisierung: Physikalische Grundlagen und technische Umsetzung*, Berlin, Heidelberg: Springer-Verlag Berlin Heidelberg, 2010.
- [11] J. Nerling, F. Schaller, and O. Arnhold *Vorkonditionierung von Elektrofahrzeugen zur Reichweiterehöhung*, ATZ Automobiltech Z, vol. 118, no. 7-8, pp. 42–47, 2016.
- [12] G. Brauner, B. Geringer, and M. Schrödl *Forschungsbedarf für das Elektrofahrzeug der Zukunft*, Elektrotech. Inftech., vol. 129, no. 3, pp. 110–117, 2012.
- [13] FAT Forschungsvereinigung Automobiltechnik e.V., Ed. *Rechnerische und probandengestützte Untersuchung des Einflusses des Kontaktwärmeübertragung in Fahrzeugsitzen auf die thermische Behaglichkeit*, Berlin, 2013.

-
- [14] C. Cap and C. Hainzmaier *Schichttheizer für Elektrofahrzeuge*, ATZ Automobiltech Z, vol. 115, no. 6, pp. 486–489, 2013.
- [15] G. Suck and C. Spengler *Lösungen für das Wärmemanagement von Batteriefahrzeugen*, ATZ Automobiltech Z, vol. 116, no. 7-8, pp. 12–19, 2014.
- [16] M. Wehowski, J. Grünwald, D. Neumeister, and A. Wiebelt *Batterietemperierung mittels Thermoelektrik*, ATZ Automobiltech Z, vol. 117, no. 7-8, pp. 36–39, 2015.
- [17] <https://weather-and-climate.com/average-monthly-Humidity-perc,darmstadt-hessen-de,Germany>
- [18] Paganelli, G.; Delprat, S.; Guerra, T.M.; Rimaux, J.; Santin, J.J. *Equivalent Consumption Minimization Strategy For Parallel Hybrid Powertrains*, IEEE Vehicular Technology Conference 2002.
- [19] Serrao, L.; Onori, S.; Rizzoni, G. *ECMS as a realization of Pontryagin's minimum principle for HEV control*, IEEE American Control Conference 2009.
- [20] Esser, A.; Zeller, M.; Foulard, S.; Rinderknecht, S. *Stochastic Synthesis of Representative and Multidimensional Driving Cycles*, Eds. WCX World Congress Experience, Detroit, APR. 10, 2018; SAE International, 2018.
- [21] OpenStreetMap. www.openstreetmap.org.